


Copyright
by
Kyle David Wilson
2017


The Dissertation Committee for Kyle David Wilson Certifies that this is the approved version of the following dissertation:

Hyperinflammatory Experimental Cerebral Malaria: Coagulation and Glial Cell Activation in *Plasmodium chabaudi* Infection of IL-10-deficient Mice

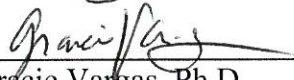
Committee:




Robin Stephens, Ph.D., Supervisor



Kathryn A. Cunningham, Ph.D.




Gracie Vargas, Ph.D.




Sara M. Dann, Ph.D.



A. Clinton White, Jr., M.D.



Johanna P. Daily, M.D.



David W. Niesel, Ph.D., Dean, Graduate School

**Hyperinflammatory Experimental Cerebral Malaria:
Coagulation and Glial Cell Activation in *Plasmodium chabaudi* Infection
of IL-10-deficient Mice**

by

Kyle David Wilson, B.S.

Dissertation

Presented to the Faculty of the Graduate School of

The University of Texas Medical Branch

in Partial Fulfillment

of the Requirements

for the Degree of

Doctor of Philosophy

The University of Texas Medical Branch

August, 2017

Dedication

I dedicate this dissertation to my family: my mother Sherry Wilson, and my father David

Wilson, who were my steadfast supporters and instilled in me the drive to pursue excellence in all my endeavors. Also, to my sister Jodie, my brother-in-law Matt, my niece Abby, and my nephew Austin, for always providing me a home to visit and a reminder of the values that I cherish most. Finally, to all my friends, near and far, that were a constant source of encouragement and inspiration.

“When Heaven is about to confer a great responsibility on any man, it will exercise his mind with suffering, subject his sinews and bones to hard work, expose his body to hunger, put him to poverty, place obstacles in the paths of his deeds, so as to stimulate his mind, harden his nature, and improve wherever he is incompetent”.

-Mencius

Acknowledgements

I would like to thank my supervisor, Dr. Robin Stephens, for all the support and direction given during my graduate career and for the opportunity to work on a challenging new project in her laboratory. I am grateful to my supervisory committee members, Dr. Kathryn Cunningham, Dr. Gracie Vargas, Dr. Sara Dann, Dr. A. Clinton White, Jr., and Dr. Johanna Daily for their constructive feedback and encouragement throughout the life of this project. I thank my current MD-PhD Combined Degree Program Director Dr. José Barral and the current Microbiology and Immunology Graduate Program Director Dr. Lynn Soong for their advocacy and guidance. I cannot adequately express the respect and admiration I have for Dr. Michael Opata, Dr. Samad Ibitokou, Victor Carpio, Edrous Alamer, Karis Marshall, and Gabriela Kaus as my companions and mentors in the Stephens Lab. I would like to recognize Dr. Gracie Vargas, Lorenzo Ochoa, Olivia Solomon, Sonja Stutz, Tiffany Dunn, Dr. Yongquan Jiang, Dr. Petra Cravens, Dr. Gustavo Valbuena, Dr. Kelly Dineley, Dr. Philip Keiser, Dr. Andrew Mendiola, Dr. Sandra Cardona, and Dr. Astrid Cardona, for their training experience, advice, and collaboration. Finally, I am thankful to my family and friends for their everlasting support, without which none of this would have been possible.

**Hyperinflammatory Experimental Cerebral Malaria:
Coagulation and Glial Cell Activation in *Plasmodium chabaudi* Infection
of IL-10-deficient Mice**

Publication No. _____

Kyle David Wilson, Ph.D.

The University of Texas Medical Branch, 2017

Supervisor: Robin Stephens, Ph.D.

Cerebral malaria is one of the most severe complications of *Plasmodium falciparum* infection and occurs mostly in young African children. This syndrome results from a combination of high levels of parasitemia and inflammation. While mutations in inflammatory cytokine genes and the levels of cytokines found in serum and cerebrospinal fluid are correlated with the severity of human malaria infection, very little cellular infiltrate is identified on autopsy in fatal cerebral malaria cases, suggesting a novel mechanism of local inflammation drives this syndrome. Vascular congestion is a prominent feature of all malaria parasites, although some species promote a primarily leukocytic congestion while others promote parasite sequestration. The role coagulation plays in congestion is becoming an active area of research. Although parasite sequestration in the brain vasculature is a feature of the human malaria parasite *P. falciparum*, sequestering strains do not uniformly cause severe disease, suggesting interplay with other factors. Infection of mice with *Plasmodium chabaudi*, a rodent malaria parasite, leads to mild illness in wildtype animals. However, IL-10 KO mice

respond to the parasite with increased levels of the pro-inflammatory cytokines IFN- γ and TNF. While *P. chabaudi* sequesters during the schizont stage, as all malaria parasites do, this parasite does not accumulate in the brain vasculature. Nevertheless, these mice exhibit some cerebral symptoms similar to human cerebral malaria, including gross cerebral edema and hemorrhage, allowing study of these critical features of disease without the influence of brain-sequestered parasite.

In these studies, IL-10 KO mice were found to suffer significant declines in behavioral and physical measures during infection compared to wildtype mice, suggesting that brain pathology contributes to the systemic consequences of infection. Elevated inflammatory monocyte and resident macrophage populations were identified in the IL-10 KO brain post-infection, and the activation state of monocytes and microglia was increased. CD4⁺ T cells making IFN- γ were also identified in the brain, but remained localized within the vasculature and did not enter the brain parenchyma. These T cells were also found to be contained within fibrinous thrombi.

In order to understand the mechanisms of cerebral leukocyte accumulation in *P. chabaudi* infection, we investigated the relationship of vascular congestion with leukocytes and fibrinogen to astrocyte activation. As coagulation is known to cause localized ischemia and hypoxia that can lead to brain tissue damage, we investigated hypoxia within the brain, and found scattered hypoxic neurons in infected IL-10 KO mice. In order to determine the driving mechanisms of inflammation and congestion, we also investigated the roles of TNF, and the anti-coagulants heparin and low-molecular-weight heparin, on vascular coagulopathy and astrocyte activation in order to identify drivers of pathology in the brain parenchyma. Neutralization of TNF reduced mortality as

previously reported, but also eliminated behavioral deficits, and significantly reduced both thrombus formation and astrocyte activation. Strikingly, anticoagulant treatment with low-molecular-weight heparin (LMWH) also rescued IL-10 KO mice from acute mortality, suggesting a role for coagulation in the lethal pathology. Glial cell activation near vessels in the brain was also partially-dependent on coagulation, as it was reduced with LMWH treatment.

These studies demonstrate that neuroinflammation, driven by TNF and characterized by accumulation of leukocytes in the vasculature, is concurrent with the development of behavioral symptoms and glial cell activation in *P. chabaudi* infection of IL-10 KO mice. Our data also demonstrate that congestion of the vasculature is driven by coagulation and promotes lethal pathology. These findings support the contribution of cytokines, coagulation, and leukocytes within the brain vasculature, to neuropathology in malaria infection. In addition, localization of inflammatory leukocytes within intravascular clots suggests a mechanism by which cytokines can drive local inflammation without considerable cellular infiltration into the brain parenchyma.

TABLE OF CONTENTS

List of Tables	x
List of Figures.....	xi
List of Abbreviations	xiii
INTRODUCTION.....	1
Chapter 1: History, infection with <i>Plasmodium</i> , and cerebral malaria.....	1
1.1 Malaria life cycle and pathogenesis.....	4
1.2 Clinical diagnosis.....	6
1.3 Treatment strategies	10
Chapter 2: Experimental insights into cerebral malaria pathogenesis.....	12
2.1 Human cerebral malaria pathophysiology	12
2.2 Sequestration hypothesis	13
2.3 Inflammatory/cytokine hypothesis	15
Chapter 3: Role of coagulation and inflammation in cerebral malaria.....	18
3.1 Coagulation activity in cerebral malaria.....	18
3.2 Hyperinflammatory experimental cerebral malaria	20
RESULTS	23
Chapter 4: Behavioral defects and cellular neuroinflammation in hyperinflammatory experimental cerebral malaria	23
Introduction.....	23
Materials and Methods.....	25
Results.....	32
4.1 IL-10 KO animals exhibit significant behavioral deficits	32
4.2 Increased cerebral CD11b+ immune cells and microglia activation	37
4.3 IFN- γ -producing T cells in the brain	40
4.4 CD4+ T cells exhibit intravascular localization.....	40
Discussion and Conclusions	45

Chapter 5: Thrombosis and astrocyte activation ameliorated by TNF and anticoagulation therapy in hyperinflammatory experimental cerebral malaria	49
Introduction.....	49
Materials and Methods.....	51
Results.....	56
5.1 Residual fibrinogen deposition	56
5.2 Leukocyte congestion of brain vasculature.....	58
5.3 Increased astrocyte activation	60
5.4 Astrocyte activation clusters with fibrinogen staining.....	61
5.5 Anti-TNF treatment prevents clotting and astrocyte activation.....	62
5.6 Hypoxic brain cells	66
5.7 Enoxaparin treatment of IL-10 KO mice	67
Discussion and Conclusions	70
REFERENCES.....	76
Vita	105

List of Tables

Table 1: <i>P. chabaudi</i> -infected IL-10 KO mice show impaired performance in the SHIRPA assessment.	34
---	----

List of Figures

Figure 1:	Female IL-10 KO animals succumb to <i>P. chabaudi</i> infection and exhibit increased malaria-related pathology	33
Figure 2:	IL-10 KO mice exhibit impaired general health, neurological reflexes and baseline behavioral measures during <i>P. chabaudi</i> infection.....	36
Figure 3:	Motor learning, balance, and motor coordination decreased in IL-10 KO mice during the recovery phase of infection.....	38
Figure 4:	mini-SHIRPA screen predicts worse outcomes in <i>P. chabaudi</i> -infected IL-10 KO mice.....	38
Figure 5:	Brains from IL-10 KO animals show increased CD11b ⁺ immune cell trafficking and MHC-II upregulation during <i>P. chabaudi</i> infection	39
Figure 6:	Brains from IL-10 KO animals show increased microglia activation during <i>P. chabaudi</i> infection.....	41
Figure 7:	Mice have IFN- γ -producing T cells in the brain during <i>P. chabaudi</i> infection.	42
Figure 8:	CD4 ⁺ T cells exhibit intravascular localization in IL-10 KO animals infected with <i>P. chabaudi</i>	43
Figure 9:	IL-10 KO mice do not die of multi-organ failure.	44

Figure 10: IL-10 KO mice have residual fibrin(ogen) deposition in and around brain vasculature, and increased liver fibrinogen	57
Figure 11: Vascular congestion in IL-10 KO mice with malaria includes thrombi containing monocytes and T cells.....	59
Figure 12: Increased astrocyte activation in IL-10 KO mice during <i>P. chabaudi</i> infection	62
Figure 13: Activated astrocytes cluster along thrombus-containing brain vasculature.	63
Figure 14: Anti-TNF antibody treatment improves survival of IL-10 KO mice infected with <i>P. chabaudi</i> , despite similar temperature and weight loss.	64
Figure 15: Anti-TNF antibody treatment prevents astrocyte activation and mortality in IL-10 KO mice during <i>P. chabaudi</i> infection.....	65
Figure 16: IL-10 KO mice infected with <i>P. chabaudi</i> have few, but significantly increased numbers of hypoxic cells in the brain.....	67
Figure 17: IL-10 KO mice are not rescued from fatal neurologic disease with unfractionated heparin treatment.	68
Figure 18: IL-10 KO mice are rescued from fatal neurologic disease with LMWH treatment.	69
Figure 19: Model of thrombus-associated lymphoid cluster (TALC)-mediated inflammation amplification.....	74

List of Abbreviations

3D	Three-dimensional
ANOVA	Analysis of variance
BBB	Blood-brain barrier
CM	Cerebral malaria
CNS	Central nervous system
CXCR3	C-X chemokine receptor 3
DIC	Disseminated intravascular coagulation
ECM	Experimental cerebral malaria
EPCR	Endothelial protein C receptor
FBS	Fetal bovine serum
GFAP	Glial fibrillary acidic protein
GPI	Glycophosphoinositol
ICAM-1	Intracellular adhesion molecule-1
IFN- γ	Interferon gamma
IL	Interleukin
i.p.	Intraperitoneal
iRBCs	Infected red blood cells
KO	Knockout
MHC-II	Major histocompatibility complex class II
MRI	Magnetic resonance imaging
PbA	<i>Plasmodium berghei</i> (ANKA)
PBS	Phosphate-buffered saline

PCR	Polymerase chain reaction
PMA	Phorbol 12-myristate 13-acetate
PRR	Pattern recognition receptor
RDT	Rapid diagnostic test
SD	Standard deviation
SEM	Standard error of the mean
SHIRPA	SmithKline Beecham, Harwell, Imperial College, Royal London Hospital, phenotype assessment
TALC	Thrombus-associated lymphoid cluster
TF	Tissue factor
TNF	Tumor necrosis factor
WHO	World Health Organization
WT	Wild-type, C57BL/6J

INTRODUCTION

Chapter 1: History, infection with *Plasmodium*, and cerebral malaria

With written documents describing malaria symptoms dated as early as 2700 BCE in the Chinese *Nei Ching* [1], the influence of malaria on the evolution of modern medicine cannot be understated. The name itself comes from the medieval Italian *malaria*, meaning “bad air”, in reference to its association with swampy marshlands and their often foul-smelling stench [2]. Indeed, the association of malaria with swamps and its potential transmission via insect vectors was first hypothesized by the Roman writers Varro and Columella in their descriptions of patients falling ill after being attacked by swarms [3]. Malaria was the first disease recognized as a repeatable collection of symptoms, as it was a widely known ailment to the Greek city-states in the 5th century BCE and was well-documented by the ancient medical scholar Hippocrates during this time [3]. In 1638, the curative properties of the quinine-producing *Cinchona* trees was discovered after Countess del Chinchon, the wife to the Viceroy of Peru, was cured from an intermittent fever after being treated with a tincture made from *Cinchona* bark [3]. However, the effectiveness of *Artemisia annua* in treating febrile illness was well-known by traditional Chinese physicians for almost 2,000 years before the eventual isolation and purification of artemisinin by Nobel laureate Tu Youyou and colleagues in 1972 [4].

The true etiology of malaria did not become apparent until philosophical advances in cell theory and technological innovations that allowed for more powerful microscopic lenses were realized in the mid-19th century. Observations by the French physician and Nobel laureate Charles Louis Alphonse Laveran in 1880 led to the discovery of

Plasmodium parasites within red blood cells of febrile patients, and his subsequent proposal of malaria disease being mediated by a protozoal infection [3]. This seminal discovery was followed by a proposal in 1894 from Sir Patrick Manson, recognized as the “Father of Tropical Medicine”, suggesting mosquitos as a potential vector for malaria after his similar findings in filariasis. Empiric evidence for the transmissibility of malaria parasite via *Anopheles* mosquitos followed quickly, and a complete life-cycle of the malaria parasite was established by Nobel laureate Sir Ronald Ross in 1897 [1, 3]. Despite humanity’s extensive history with malaria infection, true strides in controlling this debilitating disease were not evident until the last century.

Insights into the true nature and pathogenesis of malaria disease had an almost immediate impact on the lives of those affected. Construction of the Panama Canal was initiated by the French in the late 19th century, but was hindered indefinitely by engineering limitations and the heavy toll taken by tropical infectious diseases, primarily yellow fever and malaria. Estimations at the beginning of construction in 1884 placed the worker mortality rate at over 200 per month [5]. However, due to vector control interventions implemented after the United States of America’s acquisition of the canal, the hospitalization rates of workers dropped from 81% in 1906, to 11% in 1912. As a result, construction on the canal was quickly completed, leading to its opening in 1914, and providing an example of the effectiveness of vector control efforts on ameliorating the burden of mosquito-borne diseases.

Further advancements in malaria control continued to decrease the burden of disease with the discovery of chloroquine by Hans Andersag in 1934, and the introduction of residual insecticide spraying using DDT in the late 1940s [6]. Despite the

eventual recognition of the harmful effects of broad outdoor-spraying of DDT on wildlife and its eventual discontinuation as an insecticide in United States in the 1960s [7], endemic malaria transmission was eradicated from the North American continent largely as a result of stringent vector control efforts. Modern malaria control strategies continue to utilize vector management methods including indoor residual spraying, which is less harmful to the environment, and insecticide-treated bed nets. In the last decade, these methods have led to major reductions in the disease burden within sub-Saharan Africa and Southern Asia [8-10], the major regions still affected by endemic malaria transmission. However, many obstacles remain towards achieving complete parasite eradication in these regions: namely, the increases in incidence of insecticide-resistant mosquitos, and artemisinin-resistant infections. Secondary to these obstacles, are the paucity of effective therapeutic strategies with which to treat severe malaria cases, such as the most severe neurological complication of *P. falciparum* infection, cerebral malaria (CM), and persistent infections with *P. vivax* hypnozoites, which become dormant in the liver. Currently, there are no effective drugs to treat CM, and primaquine has been the only intervention to date shown to adequately prevent relapse of *P. vivax* infection [11].

Malaria infection remains a highly debilitating disease with elevated levels of morbidity in endemic regions. As a result, the most effective method adopted by scientific, medical, and humanitarian communities tasked with malaria control and prevention is to adopt a multifaceted approach, involving vector control strategies and continued research into novel and effective anti-malarial therapeutics and vaccines. Through the study of malaria pathogenesis and mechanisms of severe disease, new

insights with which the parasite can be combated are predicted to increase the chances of successful eradication of this devastating disease within the next few decades.

CHAPTER 1.1: MALARIA LIFE CYCLE AND PATHOGENESIS

The genus that includes the malaria parasite, *Plasmodium*, appears to have co-evolved alongside animals for millions of years, as there have been over 200 *Plasmodium* species identified to date, with individual species specifically infecting birds, reptiles, rodents, and primates. There are five *Plasmodium* species known to infect humans: *Plasmodium falciparum*, *P. vivax*, *P. malariae*, *P. ovale*, and *P. knowlesi*. Two of these species, *P. falciparum* and *P. vivax*, account for the majority of human infections, with *P. falciparum* responsible for the vast majority of severe disease and death [10]. Malaria infection is caused by transmission of the *Plasmodium* parasite from the mosquito vector, genus *Anopheles*, into a susceptible vertebrate host. This is accomplished via the inoculation of 20-200 *Plasmodium* sporozoites into the skin by a female *Anopheles* mosquito during the acquisition of a blood meal [12]. The sporozoites are injected into the dermis alongside mosquito salivary proteins that exhibit multiple local regulatory functions that facilitate quick entry into the bloodstream, such as anti-coagulation proteins, vasodilators, anti-histamines, and immunomodulators [13, 14]. This allows for a few infectious sporozoites to hematogenously spread quickly to the liver and infect hepatocytes within 1-3 hours of inoculation [15, 16]. Upon invasion of the liver, which initiates the complex intrahepatic stage of the parasite life cycle, the *Plasmodium* sporozoite enters into a process of replication which results in multinucleated schizonts being produced, each of which can generate thousands of merozoites that are released

upon hepatocyte rupture 5-15 days post-infection [17, 18]. It is estimated that up to 90,000 merozoites are generated and released during this stage [19]. The intrahepatic stage of malaria disease is largely “silent”, in that the parasite is successful in evading the host immune system via the downregulation of MHC proteins on hepatocytes [20], resulting in a lack of clinical symptoms.

Merozoite release into the bloodstream after hepatocyte rupture initiates the intraerythrocytic stage of the parasite life cycle, in which the *Plasmodium* parasite quickly invades circulating red blood cells (RBCs). Within the erythrocyte, the parasite undergoes a cyclical replication process that generates both sexual gametocytes and more infectious merozoites capable of infecting new RBCs upon erythrocyte rupture. Depending on the *Plasmodium* species, this cyclical invasion and lysis of red blood cells occurs every 24 hours (*P. knowlesi*, *P. chabaudi*), 48 hours (*P. falciparum*, *P. ovale*, *P. vivax*), or 72 hours (*P. malariae*), driven by host circadian regulation. Parasite-driven RBC rupture also promotes the paroxysmal fevers characteristic of malaria infection due to the massive release of parasite proteins and the upregulation of pro-inflammatory cytokines by innate immune cells [21]. These repeated rupture/invasion cycles occur with regular periodicity, and are characterized as either highly synchronous, in which most of the infected RBCs lyse together (as in *P. falciparum* and the rodent parasite *P. chabaudi*), or asynchronous, in which RBC lysis occurs when a given parasite independently reaches the mature schizont stage. These unique characteristics of parasite growth and propagation have distinct effects on the resultant parasitemia [22] and immune response [23].

The sexual gametocyte forms of the parasite circulate within the bloodstream until such a time that they can be acquired by an *Anopheles* mosquito taking a blood meal from an infected host. This initiates the mosquito, or sexual, stage of the parasite life cycle, which involves the fusion of male and female gametocytes to form zygotes that mature into motile ookinetes, which invade mosquito midgut epithelial cells and form oocysts. When the oocysts rupture, they release newly infectious asexual sporozoites that make their way to the mosquito salivary gland, thus completing the *Plasmodium* life cycle [18]. The sexual stage is an essential step in the *Plasmodium* life cycle that ensures continued transmission of the parasite. Therefore, many of the most effective and economical strategies to prevent malaria infection involve either limiting exposure to parasite-carrying mosquitos (bed nets, insect repellent sprays) or decreasing the parasite burden altogether (insecticides). Ingenious strategies to reduce the mosquito population by engineering “infectious sterility” and introducing *Plasmodium*-lethal proteins and microbionts are also currently being developed [24].

CHAPTER 1.2: CLINICAL DIAGNOSIS

Due to the eradication of endemic malaria on the North American and European continents, malarial disease is rarely observed within the United States. Occasional cases continue to be diagnosed in travelers returning from malaria-endemic regions, with over 1,700 cases reported in the United States by the Centers for Disease Control and Prevention in 2014 [25]. However, these infection rates pale in comparison to those in malaria-endemic countries, and malaria continues to be a major burden in many regions of the world. With 212 million new cases and 429,000 estimated deaths in 2015, malaria

is one of the most culturally and economically impactful infectious diseases worldwide [26]. As a result, while malaria disease is only suspected in travelers in the United States, it is a diagnosis of exclusion in South America, sub-Saharan Africa, and Southern Asia, where it makes up the majority of clinical cases of intermittent fever.

Upon infection with malaria, the first symptoms to arise are most often fever, chills, headaches, nausea/vomiting, and muscle pains. These symptoms coincide with the initiation of RBC lysis during the erythrocytic stage of the parasite life cycle about one week after infection. This is due to the massive release of parasite proteins that are capable of inducing a robust immune response [21] and the production of pyrogenic, pro-inflammatory cytokines, such as interleukin (IL)-1 β , IL-6, and tumor necrosis factor (TNF) [27]. As these symptoms are not specific and mimic those of other febrile illnesses, malaria is often diagnosed using various methods.

The first and simplest form of diagnosis is by examination of a thick blood smear and microscopic identification of the *Plasmodium* parasite located within RBCs. This can be accomplished using Giemsa stain and a light microscope. Due to the relative low-cost and simplicity of the reagents and equipment necessary to perform a Giemsa stain on a patient's blood, it remains the gold standard in malaria diagnosis with an estimated 203 million patients tested by microscopic examination in 2014. However, limitations can exist based on the quality of the reagents, the availability of a microscope, or the training of technicians. Symptoms of malaria can also be caused by many other disease and metabolic processes, particularly in severe cases, and the resultant parasitemia could be incidental and not related to the presenting illness. A 2004 study in Malawi found that 23% of children that met the criteria for CM, the most severe neurological complication

of *P. falciparum* infection, had died from alternative causes [28]. As a result, a suspected case of malaria is often confirmed with a second laboratory test.

Antigenic detection of *Plasmodium* proteins is often the most appropriate secondary diagnostic test to confirm a suspected malaria case. This is rapidly becoming more available with the introduction of rapid diagnostic tests (RDTs), which involve the use of *Plasmodium*-specific antibodies that are often engineered onto paper chromatographic strips that require little volume of blood from the patient and can be processed and read within 15 minutes. RDTs offer an alternative method for malaria diagnosis in settings where microscopic capabilities are lacking. The World Health Organization (WHO) reported that over 300 million RDT products were sold in 2014, with 62% of these being specific for detection of *P. falciparum* [26]. Parasite nucleic acids can also be detected using molecular methods, such as polymerase chain reaction (PCR). However, the need for laboratory space and technological expertise is often a limiting factor in this method as an effective diagnostic tool. Molecular techniques are further hindered by the time it takes to replicate the nucleic acid material to sufficient quantities for detection, hindering its feasibility for the treatment of acutely ill patients.

In cases of severe malaria, which includes severe anemia and CM, clinical findings suggestive of anemia (decreased hematocrit) or neurological dysfunction (coma, seizures, confusion) greatly increases the suspicion for malaria. As a result, the healthcare provider often includes a thorough neurological exam and panel of laboratory and metabolic tests capable of detecting features of severe malaria, including anemia, hypoglycemia, multiple-organ failure, or lactic acidosis.

Patients with CM often present with the typical fever/chills, headache, and vomiting characteristic of malaria infection, but also demonstrate signs of neurological dysfunction ranging from altered sensorium and irritability, to seizures and coma [29, 30]. CM is defined by the WHO as unarousable coma in patients demonstrating parasitemia positive for *P. falciparum*, while excluding other common causes of coma (viral encephalopathy, toxic syndromes, metabolic etiologies). Within the last decade, fundoscopic examination of the retina has become an important tool in the diagnosis of CM. Retinal findings suggestive of CM include macular whitening, vascular discoloration, and the presence of retinal hemorrhage, which were superior in differentiating CM from non-malarial coma when compared to laboratory tests [31], and was positively-correlated with coma length and disease severity [32]. The clinical suspicion of CM rises when combined with neuroimaging studies demonstrating cerebral edema and cortical infarcts [33-35], however imaging alone is neither specific to a CM diagnosis, nor widely available at many facilities with the highest burden of malaria patients. The presentation of CM also differs between children, who make up the majority of fatal cases in Africa, and adults, who make up the majority of fatal cases in Asia and among travelers [10]. Coma usually develops rapidly in children, with the majority of cases involving seizures (62%) [36]. The speed of onset contrasts sharply with adults, who exhibit a much more gradual decline in consciousness, and demonstrate a lower incidence of seizures (17%) [37]. Psychiatric manifestations can also be present, including delusions, hallucinations, and psychoses. However, these symptoms can also be a side-effect of treatment with the anti-malarial drug mefloquine, which is commonly used for prophylaxis.

CHAPTER 1.3: TREATMENT STRATEGIES

The standard treatment for uncomplicated malaria infections are oral anti-malarial medications, which are only active against the disease-causing, blood-stage *Plasmodium* parasite forms. Anti-malarial drugs are the only intervention that has been proven to reduce mortality in patients. The most common medications are those originally derived from the *Cinchona* tree (quinine, quinidine, chloroquine, mefloquine, primaquine) and the sweet wormwood, *Artemisia annua* (artesunate, artemether), which are now synthesized chemically. Each is known to exhibit potent anti-malarial effects. However, the recent increase in drug resistance, particularly against the more powerful artemisinins in Southeast Asia, is a cause for concern [38]. In response, combination therapy with artemisinins (artemether-lumefantrine) is recommended to combat resistance, and to shorten the duration of therapy and prevent toxicity (particularly with the cinchoids).

A small percentage of *P. falciparum* infections result in severe malarial disease. However, a significant proportion of severe malaria infections include CM, which is a leading cause of death in sub-Saharan African children and represents a major burden worldwide [39, 40]. CM accounts for over 500,000 cases per year, and correlates with high parasitemic burden, severe inflammation, and cerebral edema [40]. In cases of suspected CM, immediate action and timely anti-malarial treatment is essential for improving outcome. CM patients are transferred to the best health care facilities to receive supportive care focused on the recognition and prevention of common complications, including hypoglycemia, electrolyte imbalances, acidosis, and organ impairment. Lack of such facilities in areas with high malaria burden is a major factor contributing to the high mortality associated with CM cases [41]. However, even timely treatment with parenteral anti-malarial medication results in a mortality rate of 20% in children presenting with CM [42]. In addition, 10-25% of children that survive CM develop long-term neurological sequelae and cognitive dysfunction [43-46].

Since anti-malarial agents take at least 12-18 hours to become effective at eliminating the parasite in the blood, and given the rapid decline in many CM patients, adjunctive therapies administered early are being explored in hopes to reduce mortality and prevent future neurological sequelae in survivors. As of yet, despite many promising trials in animals, no adjunctive therapies have proven efficacious in reducing CM mortality [47]. Therefore, a better understanding of the mechanisms of disease is important for identifying new targets for treatment.

Chapter 2: Experimental insights into cerebral malaria pathogenesis

CHAPTER 2.1: HUMAN CEREBRAL MALARIA PATHOPHYSIOLOGY

Effective anti-malarial drugs often result in cure during uncomplicated malaria infection. However, as many as 10% of *Plasmodium falciparum* infections worldwide result in severe malaria disease, including severe anemia, pregnancy-associated malaria and CM [39, 40]. CM correlates with high levels of parasitemia, inflammation, and severe cerebral edema [40]. There is little evidence that specific strains of *P. falciparum* are linked to this syndrome, although parasite adhesion in the brain and retina is associated with death [28]. Adding to the complex etiology of CM, inflammation also promotes parasite sequestration, as demonstrated in murine models of experimental cerebral malaria (ECM) [39]. As a result, it is possible that inflammation is the primary precipitating cause of *P. falciparum* sequestration in the human brain and other organs.

Histopathological studies from fatal CM cases have provided insight into the pathologic events that correlate with fatal disease [48-50]. Recent striking studies linked evidence of severe cerebral edema with death [40]. Cytokines such as TNF can cause vascular leakage and edema; however, the causal mechanisms leading to blood-brain barrier (BBB) breakdown and brain swelling in human CM cases are not clear. While sequestration is cited as a cause of vascular blockage and edema [51], this has not been sufficiently demonstrated to date.

Several host genetic factors have been implicated in pathology. For example, mutations in the promoters of the inflammatory cytokine TNF, which drives the anti-malaria response of phagocytes, and the regulatory cytokine IL-10, which protects the host from excessive immunopathology, have been correlated with severe disease [52-54]. However, inflammatory cytokines also promote parasite sequestration by increasing expression of adhesion molecules on the vascular endothelium [39].

Causal mechanisms leading to brain pathology in human CM cases are multifactorial [55, 56]. Despite our incomplete understanding of the mechanisms of malaria pathogenesis, it is clear that the immune response causes much of the pathology associated with malaria infection [57]. Due to overlapping and synergistic mechanisms driving CM pathogenesis, determining the independent contributions of each pathway involved presents an ongoing challenge to investigators. The impact of parasite-specific factors, such as cerebral sequestration, have been studied in animal models of CM [58-60]. However, the interplay of inflammation with parasite-dependent factors makes it difficult to isolate the effects of organ-specific immune responses and their contribution to CM pathogenesis. This has been a historical struggle between investigators since the proposal of 2 competing hypotheses over 20 years ago concerning the mechanism of neuropathology in CM: the sequestration hypothesis, and the inflammatory/cytokine hypothesis.

CHAPTER 2.2: SEQUESTRATION HYPOTHESIS

The “sequestration hypothesis” inherited its name from the unique ability of *Plasmodium*-infected RBCs (iRBCs) to adhere to brain endothelial cells within the microvasculature and to uninfected RBCs, termed sequestration and rosetting, respectively [61]. This sequestration event was believed to be an essential mechanism that drives all downstream neuropathology, and was first postulated by Marchiafava and Ginami in 1894 [62]. It was thought these adhesive interactions would lead to the accumulation of iRBC and RBC aggregates inside the lumen of the blood vessel, obstructing blood flow, leading to localized tissue hypoxia and the buildup of toxic waste products, thus contributing to neural dysfunction and coma [42, 63]. Sequestration is the result of the expression of parasite proteins, *P. falciparum* erythrocyte membrane protein 1 (PfEMP-1) in particular, on the surface of iRBCs, which bind host cell-adhesion

molecules such as intercellular adhesion molecule 1 (ICAM-1) present on the surface of vascular endothelial cells [64, 65]. Some human studies support this idea, as infection with specific *P. falciparum* clones exhibiting brain-sequestering phenotypes correlate with a higher incidence of CM compared to non-sequestering *P. falciparum* clones [66, 67]. Parasites within the vasculature can promote local cytokine production and coagulation. However, the accumulation of lactic acid is often cited as evidence of local tissue hypoxia secondary to anaerobic respiration [68]. Available evidence suggests that cerebral pathology is in fact not linked to anaerobic glycolysis, but rather to other factors, such as decreased oxygen delivery secondary to anemia [69]. The possibility that decreased deformability of iRBCs compared to uninfected RBCs leads to increased susceptibility for vascular adhesion and plugging has been proposed as well, supported by evidence correlating deformability with poorer outcomes and similar effects observed in ECM [63]. Finally, several classic studies have shown an association with the density of vascular packing with CM disease [70, 71].

Despite this evidence, however, some questions remain that have yet to be answered by this hypothesis. The logical conclusion following the sequestration hypothesis suggests that an increase in the parasite load would increase vascular adhesion and blockage, thus, promoting downstream neuropathology. However, although severe malaria disease is associated with a higher parasitemia than mild malaria, there is little quantitative correlation between parasitemia and mortality in CM cases [72]. Also, the assumption that vessel blockage promotes brain pathology secondary to hypoxia is not supported by the observation that CM patients recovering from coma lack the same degree of permanent sequelae when compared to other ischemic and hypoxic brain conditions [73]. Though rare, there have also been reports of neurological symptoms in cases of *P. vivax* infection, which is not believed to exhibit vascular sequestration in the brain [74, 75]. Finally, *P. falciparum* is known to sequester in the microvasculature of other organs, such as the lungs, intestines, and heart, without causing apparent pathology

[61]. While compelling, the sequestration phenomenon alone lacks the capacity to completely explain the entire pathology observed in cases of CM.

CHAPTER 2.3: INFLAMMATORY/CYTOKINE HYPOTHESIS

The “inflammatory/cytokine hypothesis” was developed in 1948 by Maegraith and suggested that parasites generate a pro-inflammatory environment during infection that can elicit organ failure through coagulopathy, endothelial dysfunction, leukocyte accumulation, and edema [76, 77]. These changes would lead to microglia activation, and astrocyte/neuronal dysfunction, eventually inducing coma in the affected patient. Cytokine production was proposed to be initiated through the actions of parasite-derived toxins, particularly glycosphosphoinositol (GPI) and hemozoin, which we now know interact with pattern recognition receptors (PRRs) on innate immune cells to induce pro-inflammatory cytokines IL-1 β , IL-6, TNF, and nitric oxide (NO) [78, 79]. These pro-inflammatory cytokines would be toxic at the high levels produced during malaria infection and directly cause the neuropathological syndrome via immunopathology. The role of the parasite was primarily to induce the initial cytokine burst, which would be beneficial at promoting parasite killing, but would eventually lead to propagation and exacerbation of organ-specific immunopathology in the absence of sufficient regulation.

Increased production of the pro-inflammatory cytokines TNF and interferon (IFN)- γ , leads to upregulation of ICAM-1 on vascular endothelial cells during ECM [80, 81]. Serum levels of TNF and IFN- γ correlate with CM in humans [80], and there is strong evidence in ECM that IFN- γ and lymphotoxin (LT) are required for upregulation of ICAM-1 on brain endothelial cells and development of severe disease [82, 83]. Furthermore, studies in knockout mice support the role of the inflammatory response on the development of severe malarial disease [84].

Additionally, NO is suspected to play an important role in CM pathogenesis via its multiple roles in modulating sequestration, inflammation, and coagulation [85, 86]. NO is thought to be produced in high amounts during malaria infection and may contribute to parasite elimination [87], with the unintended effect of inducing neuronal dysfunction in the brain [73]. As a result, NO adjuvants have been proposed in the treatment of severe malaria. However, so far there is little evidence of a role for NO in *Plasmodium* killing [88], and there is conflicting data on its benefit, with one report even showing a positive correlation between levels of NO found in patient cerebrospinal fluid (CSF) with death [89].

However, a key missing piece of the structure supporting the inflammatory hypothesis is the source of cytokines behind the BBB in the brain parenchyma. As few leukocytes enter the parenchyma, there is little support for their role in brain-specific pathology. As a result, the current inflammatory/cytokine hypothesis, much like the sequestration hypothesis, cannot completely account for the pathology observed in CM. For example, high levels of systemic pro-inflammatory cytokines can be measured in non-lethal malaria infections, such as *P. vivax* [90], arguing against the sufficient role of systemic inflammation as the sole driver for the development of CM. Furthermore, immunomodulatory therapeutics aimed at controlling the excessive inflammatory response, so far including corticosteroids and anti-TNF/LT antibodies, have failed to yield a benefit in treating CM patients [91-93]. However, one study in adult CM patients using adjunctive pentoxifylline therapy, which inhibits TNF synthesis, did show improvement in coma resolution time and mortality [94]. There are two possible explanations as to why monoclonal antibodies to TNF did not prove curative: 1) some of the anti-TNF reagents may actually prolong the bioavailability of the cytokine by maintaining TNF in circulation, allowing for prolonged systemic effects [91], or 2) the amplification of inflammation may be too advanced at the time of presentation of CM patients compared to the early stages available for treatment in animal models. The latter

is a significant issue for most of the treatment regimens which have proven effective in small animal models [95]. Nonetheless, proponents of the inflammatory/cytokine hypothesis maintain that it is complementary to the sequestration hypothesis. For example, schizogony of parasites adherent in the blood vessels could induce elevated local concentrations of pro-inflammatory cytokines, although the exact mechanisms are not clear given the paucity of data on local leukocytes. Localized cytokine production would lead to downstream detrimental effects on the vasculature, and potentially the brain parenchyma, which would not necessarily be measurable in the serum [77]. This could be one explanation why some severely-ill patients with *P. falciparum* CM have much lower levels of systemic cytokines compared to uncomplicated *P. vivax* malaria, which does not sequester in the brain.

Excessive inflammation, promoted by genetic and environmental factors, is likely to predispose a malaria patient to neuropathology (and thus development of CM), but is likely not the sole cause. Mechanisms of local cytokine production must be more thoroughly dissected for an improved understanding of parasite-dependent and independent drivers of pathology, such as parasite and leukocyte-mediated obstruction of blood flow. An improved understanding of the local lymphoid-organizing structures which typically amplify inflammation in specific tissues, but do not appear to be present in the brain in this infection, will inform future attempts to control neuro-immunopathology.

Chapter 3: Role of coagulation and inflammation in cerebral malaria

CHAPTER 3.1: COAGULATION ACTIVITY IN MALARIA

Ischemia has been proposed to represent a significant contributor to brain pathology in malaria [34, 47, 96]. Vascular obstruction, caused either by sequestered parasite or the congestion of activated leukocytes, could inhibit the perfusion and subsequent oxygenation of tissues downstream of the blockage, resulting in neural tissue hypoxia and dysfunction. However, due to the rapid resolution of coma and lack of long-term neurological sequelae seen in most CM cases, many investigators remain unsatisfied in regards to theories focusing on vascular congestion-mediated pathology as the primary driver of brain dysfunction. Rather, there is rising evidence of the importance of hemostatic changes in mild disease [97, 98], and an increasing focus on coagulation activity in severe malaria [99-101]. Studies have shown that the relative dysfunction in the coagulation cascade correlates with severity of malaria disease [99, 102] and parasitemia [103]. Furthermore, although increased bleeding is relatively rare in cases of severe malaria, disseminated intravascular coagulation (DIC) is associated with malaria infection in up to 10% of cases [104]. In many of the other cases, however, it has been noted that all of the symptoms of DIC (increased microparticles, platelet accumulation, apoptosis, etc.) are present except for a reduced clotting time. It is well known from studies of sepsis that organ failure can be associated with elevated coagulation and inflammation [105].

Evidence of elevated coagulation products has been demonstrated in some studies of severe malaria [106, 107], but was not a prominent feature in others [108, 109]. Similar contradictory trends have been observed in sepsis reports as well [110]. D-dimer, an important clinical marker of coagulation status, is often upregulated in severe malaria cases, but lacks in specificity as it is also known to be increased in mild disease [103,

111]. However, elevated D-dimer levels are indicative of increased fibrin turnover by plasmin, suggestive of a pro-coagulant state. One proposed explanation for the apparent discrepancy is that lower levels of coagulation proteins are indicative of functional fibrinolysis that occurs during inflammation [112]. Other potential mechanisms involve activated immune cells, such as the production of elastase from neutrophils that is known to degrade the anti-coagulation protein factor XIII [102], or the upregulation of pro-fibrinolytic proteins expressed on endothelial cells during CM [113]. Furthermore, the parasite itself expresses proteins that can degrade components of the coagulation cascade [104, 114].

Despite the abundance of evidence suggestive of increased coagulation in severe malaria infection [115], standard anticoagulation therapy using heparin has so far proved unsuccessful, even given its proven ability to disrupt rosette formation [116] and inhibit parasite growth *in vitro* [117, 118]. As an alternative, some promise has been demonstrated in an animal model of pregnancy-associated malaria using low-molecular weight heparin (LMWH), which is more specific than unfractionated heparin and has decreased hemorrhagic side effects [119]. Studies in sepsis have also demonstrated significant interactions between the coagulation cascade and systemic inflammation [120, 121], suggesting more complex mechanisms are at work than are currently understood. Septic shock models using *Escherichia coli* infection demonstrate the important role that tissue factor (TF) plays in regulating the coagulopathy [122, 123], findings also recently observed in severe malaria infection [124]. There is a demonstrated link between pro-thrombotic TF and inflammatory cascades, as TF can be promoted by high levels of TNF in severe malaria infection [80, 125]. As a result, modulation of the systemic immune response and factors involved in promoting a pro-thrombotic state are likely to be key in preventing immunopathology due to excessive, vascular-localized inflammation, such as that observed in CM. Anti-coagulation therapy and approaches aimed at reversing thrombocytopenia have seen some success in the treatment of experimental sepsis [122,

123], so a logical step would be to take the same approach in the management of severe malaria infection.

CHAPTER 3.2: HYPERINFLAMMATORY EXPERIMENTAL CEREBRAL MALARIA

Histopathological studies from fatal CM cases have provided insight into the pathologic events that correlate with fatal disease [48-50]. Though more evidence is required, a recent striking study on several patients using magnetic resonance imaging (MRI) linked evidence of severe cerebral edema with death via compression of the brain stem, leading to respiratory failure [40]. Systemic TNF is sufficient for causing vascular leakage and edema; however, the causal mechanisms leading to blood-brain barrier breakdown and brain swelling in CM cases are not clear. Sequestration is also cited as a cause of vascular blockage and edema [51]; however, sequestration as a causation for edema has not been demonstrated to date. Fortunately, animal models have been developed that share significant similarities to human CM. In *Plasmodium berghei* ANKA-induced ECM infection, pathogenic mononuclear cells accumulate in cerebral blood vessels as a result of inflammatory TNF secretion and the upregulation of chemokine receptors like C-X chemokine receptor 3 (CXCR3) on T cells [126], and cell-adhesion molecules such as ICAM-1 on the vascular endothelium [127]. Other studies have shown cytotoxic CD8⁺ T cell recruitment, occurring downstream of IFN- γ , can directly damage microvascular endothelial cells and contribute to edema [128-131]. Though vascular endothelial damage in *P. berghei* ANKA infection depends on perforin and granzyme, it may be independent of direct contact [129, 130, 132].

In this dissertation, we utilized a hyperinflammatory experimental cerebral malaria (HECM) model, using the rodent malaria parasite *Plasmodium chabaudi*, to study the contributions of inflammation, independent of the effects of parasite sequestration, to neuropathology. *P. chabaudi* leads to mild malaria in wild-type (WT)

C57BL/6J mice. However, in IL-10-knockout (KO) mice, *P. chabaudi* infection leads to excessive inflammation, cerebral symptoms, and death. The severe syndrome includes significantly increased levels of the pro-inflammatory cytokines TNF and IFN- γ [133], and lethal disease characterized by cerebral pathology involving gross cerebral edema and hemorrhage [134]. Strikingly, there is no significant parasite sequestration in the brains of these mice. While a few parasites have been seen in the brain vasculature via electron microscopy [135], a thorough examination of the brain using luminescent parasites failed to show significant enrichment of parasites in the brain, but only in other organs [136].

The *P. chabaudi* lifecycle is synchronous, as is *P. falciparum* infection in humans, with schizonts disappearing from the peripheral circulation almost completely. This is beneficial to the parasite because it reduces parasite killing in the spleen. Through this process, *P. chabaudi* parasites can be found sequestered in the liver and lungs of mice in a partially ICAM-1-dependent manner [137]. However, pathological damage within each organ does not necessarily correspond to the degree of organ-specific sequestration of the parasite [136], arguing for a more prominent role for inflammation in mediating pathology. In support of this, activated immune cells and pro-inflammatory cytokines have been implicated in the mortality of IL-10 KO mice infected with *P. chabaudi*. IL-10 is required to protect animals from lethal pathology, as it regulates the pro-inflammatory cytokines IL-12 and TNF [138]. IL-10 is primarily made by CD4⁺ IFN- γ ⁺ T cells in *P. chabaudi* infection, and is downstream of IL-27 [139]. Neutralization of TNF ameliorates the severe phenotype, while administration of TGF- β antibodies exacerbates disease [133]. IL-10 KO mice lacking IFN- γ receptor signaling are also rescued from mortality, even though they exhibit higher levels of parasitemia [140]. This data demonstrate that a delicate balance of inflammatory and regulatory cytokines can control development of lethal malaria disease. This model provides an opportunity to investigate the effect of

systemic inflammation, as separate from the effect of parasite sequestration in the brain, on neurological damage during malaria infection.

RESULTS

Chapter 4: Behavioral defects and cellular neuroinflammation in hyperinflammatory experimental cerebral malaria

INTRODUCTION

Plasmodium chabaudi, a rodent malaria species, leads to uncomplicated disease in wildtype (WT) animals. However, in IL-10-deficient (IL-10 KO) mice, *P. chabaudi* infection leads to lethal disease characterized by cerebral pathology, including gross cerebral edema and hemorrhage [134], in the absence of cerebral sequestration [136]. In *P. chabaudi*, sequestration has been documented in several organs, including liver and lungs, but adherent parasite is not readily detectable in the brain vasculature [135, 136]. On the other hand, there is a strong spike of systemic, pro-inflammatory, TNF at the peak of infection that has been shown to cause the lethal pathology in this model [133]. As such, it is clear that inflammatory cytokines can promote, and anti-inflammatory cytokines protect from, malaria-related pathology in murine models [141-143]. In humans, a strong balance of the anti-inflammatory cytokine IL-10 with TNF is also known to be critical for control of parasitemia and pathology [144].

Neuroinflammation and behavioral changes have not been studied in the lethal course of disease in *P. chabaudi*-infected IL-10 KO animals. Furthermore, the type and location of immune cells in the brain are unknown in this model. Therefore, by using the SHIRPA behavioral screen, general health, neurological reflexes, and baseline behavior were assayed. Multiple deficiencies in these measures were observed in infected IL-10

KO mice compared with even the most moribund WT animals. A significant population of monocytes were found in the brains of *P. chabaudi*-infected IL-10 KO mice by flow cytometry. T cells were also found in the brain, although not at significantly higher levels than WT animals. Interestingly, the infiltration of T cells was localized primarily to blood vessels and not the brain parenchyma. This study supports the role of brain-localized inflammatory leukocytes in promoting lethal malarial pathology and behavioral changes in mice infected with *P. chabaudi*.

MATERIALS AND METHODS

MICE

C57BL/6 (WT) and B6.129P2-Il10^{tm1Cgn}/J (IL-10 KO) animals (The Jackson Laboratory, Bar Harbor, ME) were bred in The University of Texas Medical Branch (UTMB) animal care facility. Experimental animals were between 6-12 weeks of age at the time of infection. All animals were kept in specific-pathogen free housing with *ad libitum* access to food and water. General health, neurological, and behavioral analyses were performed on 16 IL-10 KO and 16 wildtype mice (female only) in UTMB's *Rodent in Vivo Assessment (RIVA)* core facility (directed by Dr. Kelly Dineley) housed within the Center for Addiction Research (directed by Dr. Kathryn Cunningham).

PARASITE AND INFECTION

Frozen stocks of *Plasmodium chabaudi chabaudi* (AS)-infected RBCs (iRBCs) (Jean Langhorne, Francis Crick Institute, London, UK) stored at -80°C were thawed and injected intraperitoneally (i.p.) into C57BL/6 mice. Parasitemia was assessed by preparing thin blood smears stained with Diff-Quik (Siemens Healthcare Diagnostics, Newark, DE) and counted using a light microscope. Parasitized blood was diluted in Krebs glucose, and normal saline to deliver 10⁵ iRBCs in 200µL i.p. Thin blood smears were collected at regular intervals to monitor for peripheral parasitemia.

ANIMAL BODY TEMPERATURE AND WEIGHT

Internal body temperature measurements were determined by subcutaneous implantation of IPTT-300 temperature transponders and read using a DAS-6007 reader system (BMDS, Seaford, DE). Animal weights were measured using an OHAUS CS 200 portable balance (OHAUS, Parsippany, NJ).

BEHAVIORAL STUDIES

Beginning on day 3 post-infection, throughout the peak of parasitemia (days 9-11), and up to day 14, all surviving animals were assessed using a modified SmithKline Beecham, Harwell, Imperial College, Royal London Hospital, phenotype assessment (SHIRPA) protocol [145]. This comprehensive behavioral assessment involves a battery of 33 semi-quantitative tests for general health and sensory function, baseline behaviors and neurological reflexes. Higher scores are given for measures showing higher functional ability. The procedures were carried out in an open testing environment away from the home cage, and took 15-20 minutes per animal daily.

Initially, observation of undisturbed behavior was conducted with the mouse in an open-bottomed viewing jar placed on top of a metal grid suspended above a piece of white paper for 3 minutes, during which Body Position, Spontaneous Activity, Respiration Rate, and Tremor were assessed. Body Position scores ranged from 0 (completely flat) to 5 (repeated vertical leaping). Spontaneous Activity scores ranged from 0 (none) to 4 (rapid/dart movement). Respiration Rate scores ranged from 0 (irregular) to 3 (hyperventilation). Tremor scores ranged from 0 (important) to 2 (none).

At the end of the observation period, the number of fecal pellets and urinary stains accumulated on the paper was recorded. Transfer arousal is measured by transferring the animal in the jar quickly to a gridded arena (3x5 grid) from ~6-8 inches in the air. The immediate reaction is recorded with scores ranging from 0 (no movement) to 6 [126]. Locomotor activity is the number of squares entered by all four feet in 30 seconds after transfer. Palpebral closure is scored from 0 (eyes closed) to 2 (eyes wide open), and piloerection is 0 (present) or 1 (absent). Gait is observed as the animal traverses the arena and is scored from 0 (incapacity) to 3 (normal). Pelvic elevation notes the height the animal's pelvis as it moves, and is scored from 0 (markedly flattened) to 3 (elevated). Similarly, tail elevation scores range from 0 (dragging) to 2 (elevated). Touch escape measures the reaction to a finger stroke, and is scored from 0 (no response) to 3 (escape response to approach). Positional passivity records the animal's response to sequential handling, with scores ranging from 0 (no struggle) to 4 (struggles when held by tail). Trunk curl is recorded as either 0 (absent) or 1 (present) and limb grasping is either 0 (absent) or 1 (present), while holding the animal by the tail. As the animal is lowered back down to the wire grid, visual placing (how early the animal reaches out for the grid) is scored from 0 (none) to 4 (early extension at 25mm). As the animal grips the grid, a gentle horizontal pressure is applied to assess qualitative grip strength, scored from 0 (none) to 4 (unusually strong). Body tone is assessed by compressing the sides of the animal between the thumb and index finger, and scored from 0 (flaccid) to 2 (extreme resistance). Pinna reflex is observed by ear retraction to the tip of a fine cotton swab, recorded as 0 (none) to 2 (repetitive flick). Corneal reflex is measured by lightly touching the cornea of the animal with a cotton swab and scored from 0 (none) to 2 (multiple eye

blinks). Toe pinch is assessed by gentle compression of a hind foot digit with fine forceps to observe the response, scored from 0 (none) to 4 (repeated extension and flexion). Wire maneuver is assessed by measuring the length of grasp on an inverted wire grid, scored from 0 (falls immediately) to 4 (active grip with hind legs). Skin color: 0 (blanched) to 2 (flushed); heart rate: 0 (slow) to 2 (fast); limb tone as measured by resistance to gentle fingertip pressure of the plantar surface of the hind paw, scored 0 (no resistance) to 4 (extreme resistance); abdominal tone by palpation of the abdomen, scored 0 (flaccid) to 2 (extreme resistance); lacrimation as 0 (present) or 1 (absent). A small dowel is inserted between the teeth at the side of the animal's mouth to measure salivation, recorded as 0 (wet zone entire sub-maxillary area) to 2 (none), and provoked biting, recorded as 0 (present) or 1 (absent). Righting reflex is scored from an upside-down position near the surface and observing the responding effort to upright itself upon release, scored from 0 (fails to right) to 3 (lands on feet). Contact righting reflex is assessed by placing the animal inside a plastic restrainer tube and inverting it to assess its ability to sense its position and correct, scored as 0 (absent) or 1 (present). Throughout this entire battery of tests, vocalization, urination, and general fear, irritability, or aggression were recorded as either being 0 (present) or 1 (absent). For analysis, SHIRPA data was pooled from infected IL-10 KO mice exhibiting fatal symptoms early during the acute phase of infection (<12 days post-inoculation) and synchronized to the time of death of the individual mouse. Synchronized IL-10 KO SHIRPA scores were compared to the peak of infection for C57BL/6J control animals (day 10 post-inoculation).

The results obtained using the full SHIRPA screen as described above and displayed in **Table 1** was used to design an abbreviated SHIRPA, termed “mini-SHIRPA” screen using only the behaviors that showed the greatest significance between WT and IL-10 KO mice at the peak of infection. The parameters included in the mini-SHIRPA screen are body position, spontaneous activity, palpebral closure, grip strength, gait, tail elevation, touch escape, heart rate, and righting reflex. Any mouse that scored below a 17 (out of a total score of 22) before day 9 post-infection was sacrificed by intracardiac perfusion.

FORELIMB GRIP STRENGTH

Quantitative forelimb grip strength was measured using a Chatillon DFIS-2 digital force gauge (Ametek, Largo, FL) measuring maximal grams of resistance by restraining the animal at the base of the tail and allowing it to grasp the tension bar whilst pulling back gently until the animal released its grip. Resistance was calculated in real-time and the maximal resistance achieved by each mouse was averaged. Animals were subjected to three trials (with at least 10 minutes of rest between each trial).

TAIL FLICK ANALGESIA

To test for nociceptive pain sensitivity, animals were placed on a tail flick analgesia meter (Columbus Instruments, Columbus, OH) and gently restrained. Latency to tail flick was recorded as the time (in seconds) required for the mouse to move its tail

out of the path of a heat source. Animals were subjected to three trials with no less than 20 minutes between trials.

FLOW CYTOMETRY

Mice infected with *Plasmodium chabaudi* were anesthetized with inhaled isoflurane (0.25% - 3%, to effect) or ketamine/dexmedetomidine cocktail (60-75 mg/kg K, 0.5-1.0 mg/kg D) i.p. and perfused with 20 mLs PBS via cardiac puncture. Single-cell suspensions from brains were made in PBS by pressing through a 70µm cell strainer, enriched by collecting the cells at the interface of a 30/70% Percoll overlay (Sigma-Aldrich, St. Louis, MO), and stained in PBS supplemented with 2% FBS (Sigma-Aldrich) and 0.1% sodium azide with anti-CD16/32 (2.4G2) supernatant (BioXCell). This was followed by combinations of FITC, PE, PerCP-Cy5.5, PE/cyanine 7 (Cy7), PE/Cy5, (allophycocyanin)-, or allophycocyanin/eflour780-conjugated Abs (all from eBioscience); CD4-Brilliant Violet 785 (BioLegend, San Diego, CA); Ly5.2 PE, Ly-6C FITC, TNF-PE/Cy7 (all from eBioscience), and CD11b-Biotin, followed by Streptavidin-PE/Cy5. Cells were collected on a LSRII Fortessa using FACSDiva software (BD Biosciences, San Jose, CA) and analysed in FlowJo (version 9.7, TreeStar, Ashland, OR). Cells were analysed within 1 hour of staining. For intracellular staining of IFN γ and TNF, cells were stimulated for 3 hours with PMA/Ionomycin and Brefeldin A for 2 additional hours before fixation in 2% paraformaldehyde (Sigma-Aldrich) and permeabilization using BD Perm/Wash buffer. Subsequently, cells were incubated with IFN γ -Brilliant Violet 605 (BioLegend) and TNF PE/Cy7 (eBioscience) for 40 minutes at 4°C and washed. Compensation was performed in FlowJo using single-stained splenocytes (using

CD4 in all colors). For presentation, data from three to four mice were concatenated to achieve sufficient cell numbers, from which averages and SEM were calculated.

CONFOCAL MICROSCOPY

Infected IL-10 KO and WT animals were injected with 2×10^6 Cell Trace Violet⁺ (CTV⁺) CD4 T cells i.p. 3.5 hours before sacrifice, and 40ug of DyLight488 labelled *Lycopersicon esculentum* (Tomato) Lectin i.v. 20 minutes before sacrifice without intracardiac perfusion. After 48 hours of post-fixation in 4% paraformaldehyde and 48 hours of cryo-protection in 30% sucrose, 30 μ m frozen sagittal sections of mouse brains were made using Tissue Freezing Medium (Triangle Biomedical Sciences, Durham, NC), mounted on glass slides with fluorescent mounting medium (DAKO, Carpinteria, CA), and cover slipped. Confocal images were acquired on a Fluoview 1000MPE system configured with an upright BX61 microscope (Olympus, Center Valley, PA). Images were analyzed using Olympus Fluoview FV1000-ASW 2.0 Viewer, and ImageJ image processing software.

STATISTICS

Where indicated, experiments were analyzed by one-way ANOVA, followed by Student's t-test or Wilcoxon rank-sum test or Wilcoxon signed-rank test for nonparametric data, in Prism (GraphPad, La Jolla, CA) and SigmaPlot 12.0 (Systat Software, San Jose, CA); SPSS (IBM, Armonk, NY) was used to calculate chi-squared formula: * $p \leq 0.05$, ** $p \leq 0.01$, *** $p \leq 0.001$. Error bars represent +/- SEM.

RESULTS

Chapter 4.1: IL-10 KO animals exhibit significant behavioral deficits

P. chabaudi-infected IL-10 KO mice suffered a more severe course of disease with decreased survival (females: 6/39, 15.4%; males: 9/20, 45.0%; **Figure 1A**) and significant weight and temperature loss, despite comparable parasitemia to WT animals (**Figure 1B, C**). The majority of IL-10 KO animals succumbed between days 7 and 11 post-infection. This is comparable to previous studies in *P. chabaudi*, although mortality is increased [140, 146]. While severe anemia is an important cause of death in *P. chabaudi* infection of several strains of mice [147, 148], anemia peaks in both IL-10 KO and WT mice at day 10 post-infection [146], and not during the time frame when most IL-10 KO animals are succumbing to infection (days 7-9 post-infection, **Figure 1D**). Furthermore, anemia is not an accurate predictor of mortality [133], nor is it correlated with percent parasitemia in this model [149]. In order to determine the behavioral phenotype of IL-10 KO mice infected with *P. chabaudi*, IL-10 KO and WT mice were infected with 10^5 *P. chabaudi*-infected red blood cells (iRBCs), and a comprehensive animal health and behavior assessment was performed daily. The SHIRPA, a rigorous and semi-quantitative battery of tests, has revealed significant deficits in animals with *P. berghei* ANKA-induced ECM [150]. During the acute phase of infection (5-14 days post-infection), IL-10 KO mice demonstrated significant deficiencies in many behavioral tests when compared to infection-matched WT mice. However, more results of the SHIRPA assessment became significant when analyzed at time points closer to death, even when compared to WT mice at their most severe state (10 days post-infection). This analysis is

shown in **Table 1**. Deficiencies in each SHIRPA functional domain in infected IL-10 KO mice were found, suggesting that malaria infection affects a broad array of neurological functions.

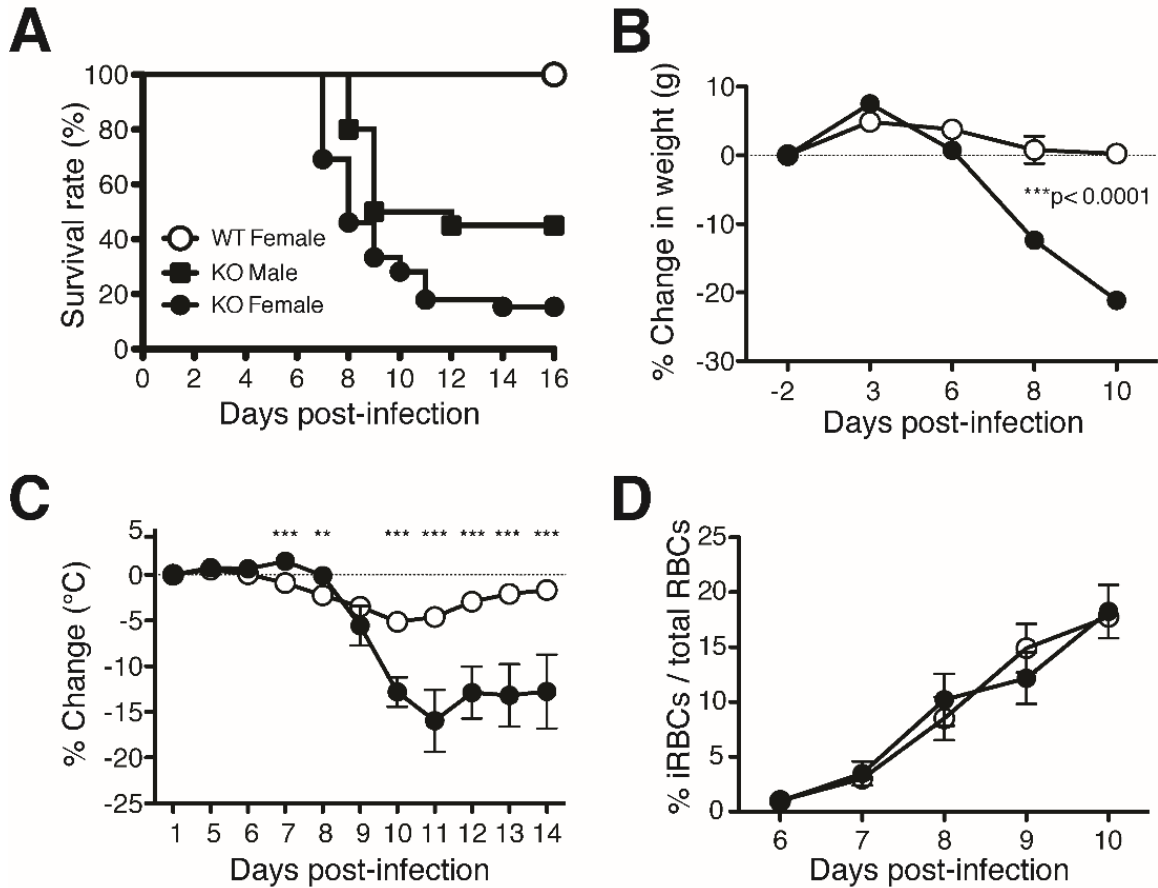


Figure 1. Female IL-10 KO animals succumb to *P. chabaudi* infection and exhibit increased malaria-related pathology. **A)** Survival of female and male IL-10 mice KO and female WT mice inoculated with 10^5 Pcc-iRBCs i.p. and followed for 16 days during the acute phase of infection. Statistical significance determined by Log-rank (Mantel-Cox) Test. **B)** Animal weights (in grams) were measured during the peak of infection via digital scale. Percent change in weight determined as compared to baseline measurement (2 days pre-inoculation). Student's t-test ***p < 0.001. **C)** Infection-matched female IL-10^{-/-} and WT animals were implanted with subdermal temperature-transmitting microchips and monitored daily throughout the peak of infection. Student's t-test **p < 0.01, ***p < 0.001. **D)** Slides of thin blood smears from the tail vein were collected and stained to measure peripheral parasitemia. Data points and error bars represent mean values and +/- SEM, respectively.

	Day 10		IL-10 KO vs. C57BL/6J								
	C57BL/6J	<120hr		<96 hr		<72 hr		<48 hr		<24 hr	
	n=16	n=4	P	n=6	P	n=5	P	n=5	P	n=8	P
Weight	17.8 (1.6)	18.2 (2.7)	NS	17.4 (1.9)	NS	16.8 (3.1)	NS	16.4 (2.3)	NS	14.7 (1.9)	<0.001*
Reflex/Sensory Function											
Visual Placing	4 (4/4)	3.5 (3/4)	NS	3 (3/4)	0.015*	3 (3/4)	0.039*	3 (3/3.5)	0.005*	3 (3/4)	0.006*
Pinna Reflex	1 (1/1)	1 (1/1)	NS	1 (1/1)	NS	1 (1/1)	NS	1 (1/1)	NS	1 (1/1)	NS
Corneal Reflex	1 (1/1)	1 (1/1)	NS	1 (1/1)	NS	1 (1/1)	NS	1 (1/1)	NS	1 (1/1)	NS
Toe Pinch	4 (4/4)	4 (4/4)	NS	4 (4/4)	NS	4 (4/4)	NS	4 (4/4)	NS	4 (4/4)	NS
Righting Reflex	3 (3/3)	3 (3/3)	NS	3 (3/3)	NS	3 (3/3)	NS	3 (2.5/3)	NS	3 (1/3)	0.018*
Cont. Right. Reflex	1 (1/1)	1 (1/1)	NS	1 (1/1)	NS	1 (1/1)	NS	1 (1/1)	NS	1 (1/1)	NS
Neuropsychiatric State											
Spontaneous Activity	2 (2/2)	2 (2/2)	NS	2 (2/2)	NS	2 (1/2)	0.012*	1 (1/2)	0.001*	1 (1/1.5)	<0.001*
Transfer Arousal	5 (5/5)	5 (4.25/5)	NS	5 (4/5)	NS	5 (4.5/5)	NS	3 (2.5/5)	0.017*	2 (2/4.5)	<0.001*
Touch Escape	2 (2/2)	2 (2/2)	NS	2 (2/2)	NS	2 (1.5/2)	NS	2 (2/2)	NS	2 (1/2)	0.005*
Posit. Passivity	4 (4/4)	4 (4/4)	NS	4 (4/4)	NS	4 (4/4)	NS	4 (4/4)	NS	4 (4/4)	NS
Provoked Biting	0 (0/0)	0 (0/0)	NS	0 (0/0)	NS	0 (0/0)	NS	0 (0/0.5)	NS	1 (0/1)	0.001*
Fear	1 (1/1)	1 (1/1)	NS	1 (1/1)	NS	1 (1/1)	NS	0 (0/1)	0.001*	0 (0/1)	<0.001*
Irritability	1 (1/1)	1 (1/1)	NS	1 (1/1)	NS	1 (1/1)	NS	1 (1/1)	NS	1 (0.5/1)	NS
Aggression	1 (1/1)	1 (1/1)	NS	1 (1/1)	NS	1 (1/1)	NS	1 (1/1)	NS	1 (1/1)	NS
Vocalization	1 (1/1)	1 (1/1)	NS	1 (1/1)	NS	1 (1/1)	NS	1 (0/1)	NS	0 (0/0.5)	0.002*
Motor Behavior											
Body Position	4 (3/4)	4 (4/4)	NS	4 (4/4)	NS	3 (3/3.5)	NS	3 (3/3.5)	NS	3 (3/3.5)	0.043*
Tremor	2 (2/2)	2 (2/2)	NS	2 (2/2)	NS	2 (2/2)	NS	2 (1/2)	0.012*	2 (1/2)	0.005*
Locom. Activity	6.2 (4.9)	8.8 (5.4)	NS	14.3 (8.2)	0.009*	8.6 (4.8)	NS	4.2 (2.8)	NS	3.7 (1.9)	NS
Pelvic Elevation	2 (2/2)	2 (2/2)	NS	2 (2/2)	NS	2 (2/2)	NS	2 (2/2)	NS	2 (1.5/2)	NS
Gait	3 (3/3)	3 (3/3)	NS	3 (3/3)	NS	3 (3/3)	NS	3 (2/3)	0.012*	3 (1.5/3)	0.005*
Tail Elevation	1 (1/1)	1 (1/1)	NS	1 (1/1)	NS	1 (1/1)	NS	1 (1/1)	NS	1 (0/1)	0.018*
Trunk Curl	1 (1/1)	1 (1/1)	NS	1 (1/1)	NS	1 (1/1)	NS	1 (1/1)	NS	1 (1/1)	NS
Limb Grasping	1 (1/1)	1 (1/1)	NS	1 (1/1)	NS	1 (1/1)	NS	1 (1/1)	NS	1 (1/1)	NS
Wire Maneuver	4 (4/4)	4 (4/4)	NS	4 (4/4)	NS	4 (4/4)	NS	4 (4/4)	NS	4 (2/4)	0.018*
Negative Geotaxis	4 (4/4)	4 (4/4)	NS	4 (4/4)	NS	4 (4/4)	NS	4 (4/4)	NS	4 (0/4)	0.018*
Autonomous Function											
Resp. Rate	3 (2/3)	2 (2/2)	0.034*	2 (2/2)	0.012*	3 (2/3)	NS	2 (2/3)	NS	2 (2/3)	NS
Feces	1.3 (1.6)	2.0 (0.8)	NS	1.0 (1.5)	NS	0.2 (0.4)	NS	0.4 (0.5)	NS	0.4 (1.0)	NS
Urine	0 (0/0)	0 (0/0)	NS	0 (0/0)	NS	0 (0/0)	NS	0 (0/0)	NS	0 (0/0)	NS
Palpebral Closure	2 (2/2)	2 (2/2)	NS	2 (2/2)	NS	2 (1.5/2)	NS	2 (1/2)	0.012*	2 (1/2)	0.005*
Piloerection	0 (0/0.75)	1 (1/1)	0.009*	1 (1/1)	0.002*	1 (0/1)	NS	0 (0/1)	NS	0 (0/1)	NS
Skin Color	1 (1/1)	1 (1/1)	NS	1 (1/1)	NS	1 (1/1)	NS	1 (1/1)	NS	1 (0/1)	NS
Heart Rate	2 (1.25/2)	1 (1/1)	0.009*	1 (1/1)	0.002*	1 (1/2)	NS	1 (1/1.5)	0.035*	1 (1/1)	0.002*
Lacrimation	1 (1/1)	1 (1/1)	NS	1 (1/1)	NS	1 (0.5/1)	NS	1 (0/1)	0.012*	1 (0/1)	0.005*
Salivation	1 (0/2)	0 (0/0.75)	NS	0.5 (0/1)	NS	1 (0/2)	NS	1 (0/2)	NS	2 (2/2)	0.015*
Temperature	36.4 (0.9)	38.5 (0.2)	0.019*	38.7 (0.3)	0.011*	37.9 (0.3)	0.031*	35.5 (3.1)	NS	33.4 (2.9)	0.021*
Muscle Tone and Strength											
Grip Strength	3 (3/3)	3 (3/3)	NS	3 (3/3)	NS	3 (3/3)	NS	3 (2.5/3)	NS	2 (1.5/3)	<0.001*
Body Tone	1 (1/1)	1 (1/1)	NS	1 (1/1)	NS	1 (1/1)	NS	1 (1/1)	NS	1 (0.5/1)	NS
Limb Tone	2 (2/2)	2 (2/2.75)	NS	2 (2/3)	NS	2 (2/3)	NS	2 (2/3)	NS	2 (2/2)	NS
Abdominal Tone	1 (1/1)	1 (1/1)	NS	1 (1/1)	NS	1 (1/1)	NS	1 (1/1)	NS	1 (1/1)	NS

Table 1. *P. chabaudi*-infected IL-10 KO mice show impaired performance in the SHIRPA assessment. Compiled from 2 independent experiments, female IL-10 KO mice (n=11) and WT mice (n=16) were inoculated with 10^5 Pcc-iRBCs i.p. and followed for 10-14 days during the acute phase of infection in which the SHIRPA comprehensive behavioral assessment was performed daily. SHIRPA data was pooled from infected IL-10^{-/-} mice exhibiting fatal symptoms early during the acute phase of infection (<12 days post-inoculation) and synchronized to the time of death of the individual mouse. Synchronized IL-10 KO SHIRPA scores were compared to the peak of infection for WT control animals (day 10 post-inoculation). Data shown are median (lower/upper quartile) or mean (+/- SD) where appropriate. Statistical significance determined by Rank Sum Test or Student's *t* test (p<0.05). Significant values are starred and displayed in bold font. Categories adapted from [150].

Locomotor activity is measured as the number of squares on a grid traversed by mice exploring a new environment, and has been used as a surrogate measure of non-specific sickness behavior in *P. berghei* ANKA infection [151]. This activity decreased similarly between groups, until day 7 post-infection, from which time on there was a non-significant trend for surviving IL-10 KO animals to move less (**Figure 2A**). A decrease in spontaneous activity was specific to the IL-10 KO group, and was reduced beginning eight days post-infection (**Figure 2B**). Furthermore, forelimb grip strength and nociceptive pain sensitivity, measures of motor and pain-sensing neural activity, in infected IL-10 KO mice became significantly different from WT mice on days 8 and 14 post-infection, respectively (**Figures 2C, D**). Evaluation of fine motor coordination revealed transient deficits in IL-10 KO mice that resolved later in the post-infection recovery period (**Figure 3**). The results obtained using the full SHIRPA screen was used to design an abbreviated SHIRPA test, termed “mini-SHIRPA”, using only the behaviors that showed the greatest significance between WT and IL-10 KO mice at the peak of infection. The expected score of a healthy, uninfected IL-10 KO or WT mouse adds up to 22, whereas an infected mouse that succumbs to infection shows a decreased score before

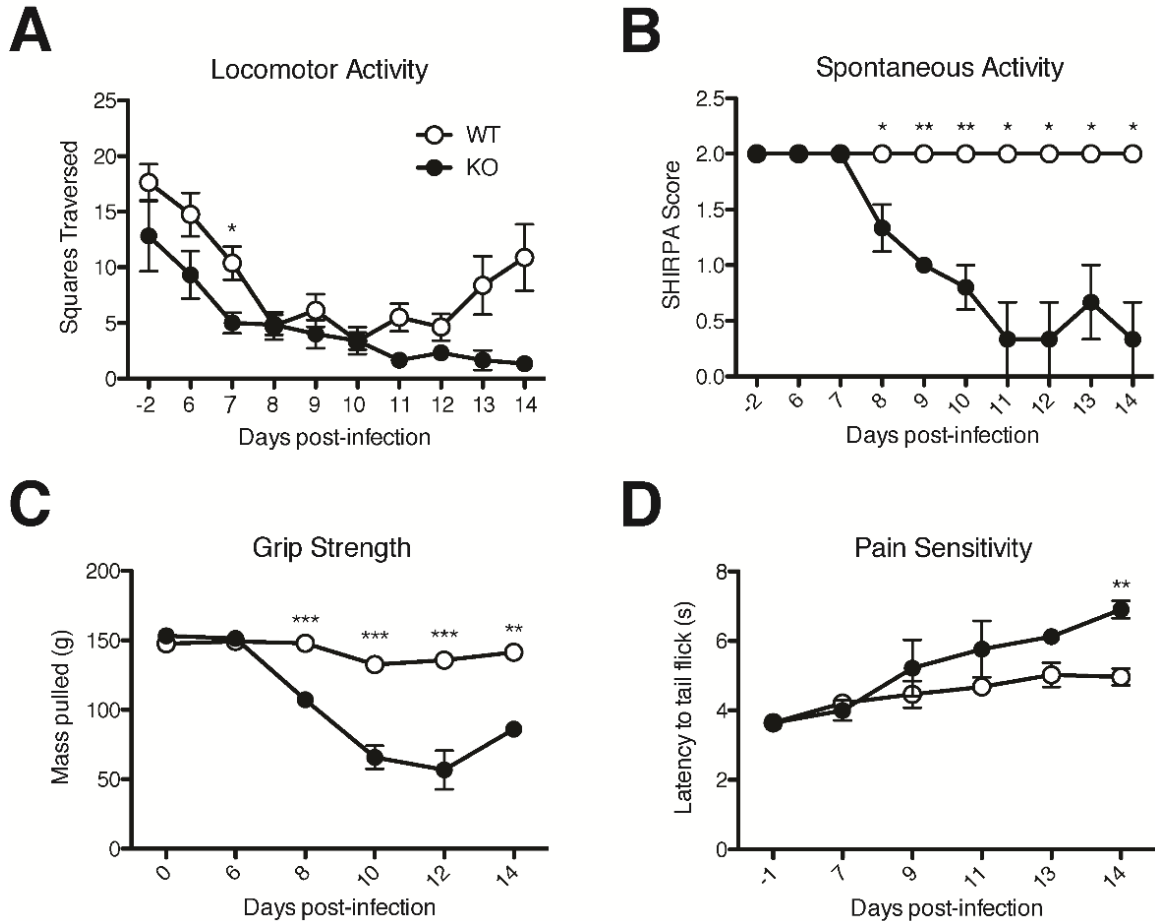


Figure 2. IL-10 KO mice exhibit impaired general health, neurological reflexes and baseline behavioral measures during *P. chabaudi* infection. As part of the comprehensive SHIRPA behavioral assessment in infection-matched IL-10 KO and C57BL/6J WT control mice, **A)** locomotor activity was measured by allowing the mice to explore a novel grid enclosure for 30 seconds. The number of squares traversed by all four feet was measured within the allotted time. **B)** Spontaneous activity was measured by observing the mouse within an enclosed environment for 2 minutes. Scores ranged from 0 (no activity, resting) to 4 (extremely vigorous, rapid/dart movement), with the baseline score being 2 (vigorous scratch, groom, moderate movement). **C)** Animal forelimb grip strength was tested using a digital force-gauging apparatus measuring maximal grams of resistance. Animals were subjected to 3 trials (with at least 10 minutes of rest between each trial). **D)** Nociceptive pain sensitivity was tested by a tail flick analgesia apparatus to measure the latency of tail removal from a nociceptive stimulus. Student's t-test (**A, C, D**) or Rank Sum Test (**B**) * $p < 0.05$, ** $p < 0.01$, *** $p < 0.001$. Data points and error bars represent mean values and \pm SEM, respectively.

death (**Figure 4A**). A score of 17 was selected as the predictive endpoint based on statistical analysis using the chi-squared test that determined any *P. chabaudi*-infected IL-10 KO mouse that scores below a 17 on the mini-SHIRPA screen before day 9 post-infection has a statistically significant chance of succumbing to infection with an odds ratio of 23.7 (95% CI: 4.0-126.0). Although 2 out of 49 mice that were predicted to die actually survived, the mini-SHIRPA screen was rapid and highly predictive of outcome, as the scores of mice that died during infection were statistically lower compared to mice that survived (**Figure 4B**). In summary, IL-10 KO mice infected with *P. chabaudi* develop behavioral and functional deficiencies across all categories of the SHIRPA assessment, suggesting damage across several brain areas, including the circuitry underlying locomotor activity, strength, and analgesia.

Chapter 4.2: Increased cerebral CD11b⁺ immune cells and microglia activation

In order to identify the cellular populations present in the brains of IL-10 KO mice infected with *Plasmodium chabaudi*, single-cell suspensions from perfused brains were prepared for flow cytometry. During the acute phase of infection (7-9 days post-infection), lymphocytes (CD45^{hi}, CD11b⁻), monocytes/macrophages (CD45^{hi}, CD11b⁺), microglia (CD45^{int}, CD11b⁺), and non-hematopoietic cells (CD45⁻, CD11b⁻) were detected. There was a significant increase in the fraction of cells in the monocyte/macrophage gate in infected animals (from 0.84% in uninfected to 1.45% in WT), with the IL-10 KO group increasing the most (2.40%, **Figure 5A**). Within the monocyte/macrophage gate, migrating “inflammatory monocytes” (CD11b⁺, Ly6C⁺, MHC-II⁺) were distinguished from the rest of the macrophage population. Migratory monocytes were increased in the brains of infected IL-10 KO animals (**Figure 5B**). CD11b⁺Ly6C⁻MHC-II⁺ macrophages, which include resident and some migratory

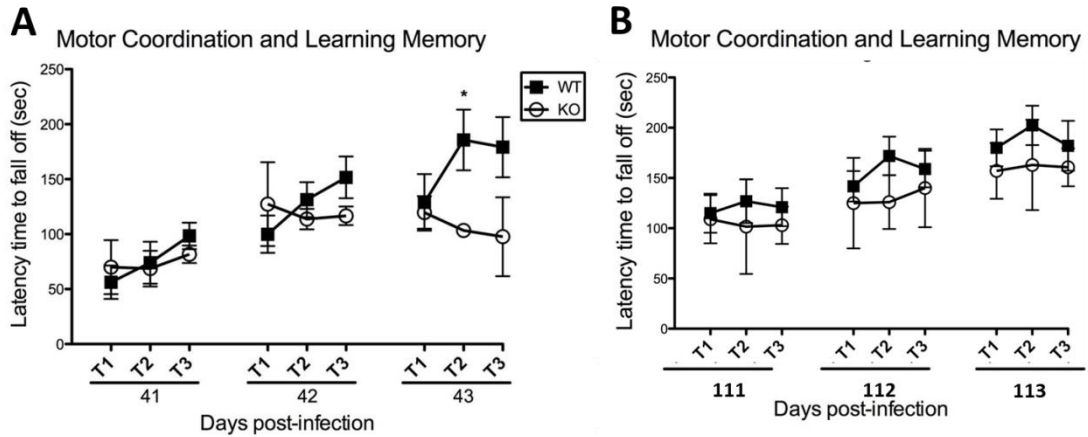


Figure 3. Motor learning, balance, and motor coordination decreased in IL-10 KO animals during the recovery phase of infection. Rotating rod examination was performed on surviving female IL-10 KO mice **A**) 41-43 days post-innoculation (n=5) and **B**) 111-113 days post-innoculation (n=3) compared to infection matched WT controls (n=8). Latency time defined as the amount of time (in seconds) for the animal to fall off the rod after initiating rotation. Experiments were performed in triplicate trials with an inter-trial interval of no less than 30 minutes for 3 consecutive days. Student's t-test *p < 0.05.

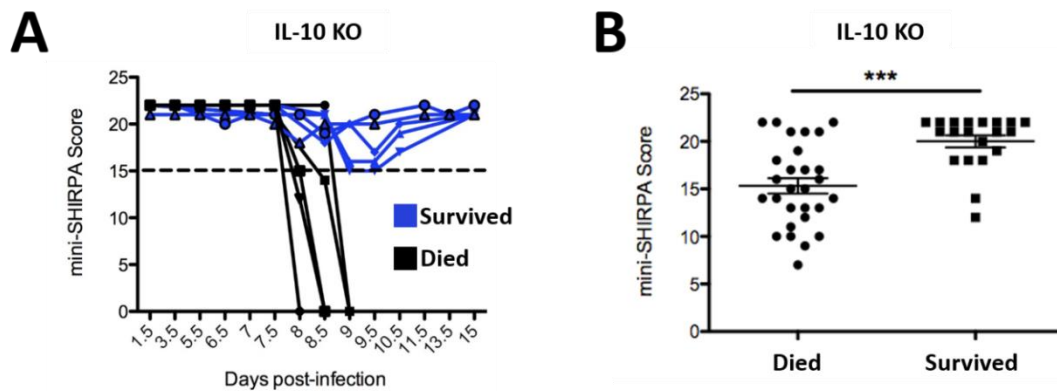


Figure 4. mini-SHIRPA screen predicts worse outcomes in *P. chabaudi*-infected IL-10 KO mice. **A**) Representative experiment showing mini-SHIRPA scores of infected male IL-10 KO mice grouped by eventual outcome (survived = blue, n= 6; died = black, n= 5). **B**) Graph showing concatenated data from multiple experiments. Infected IL-10 KO mice grouped according to eventual outcome, y-axis shows the lowest mini-SHIRPA score of individual mice before day 9 post-infection (n = 48). Wilcoxon signed rank test ***p < 0.001.

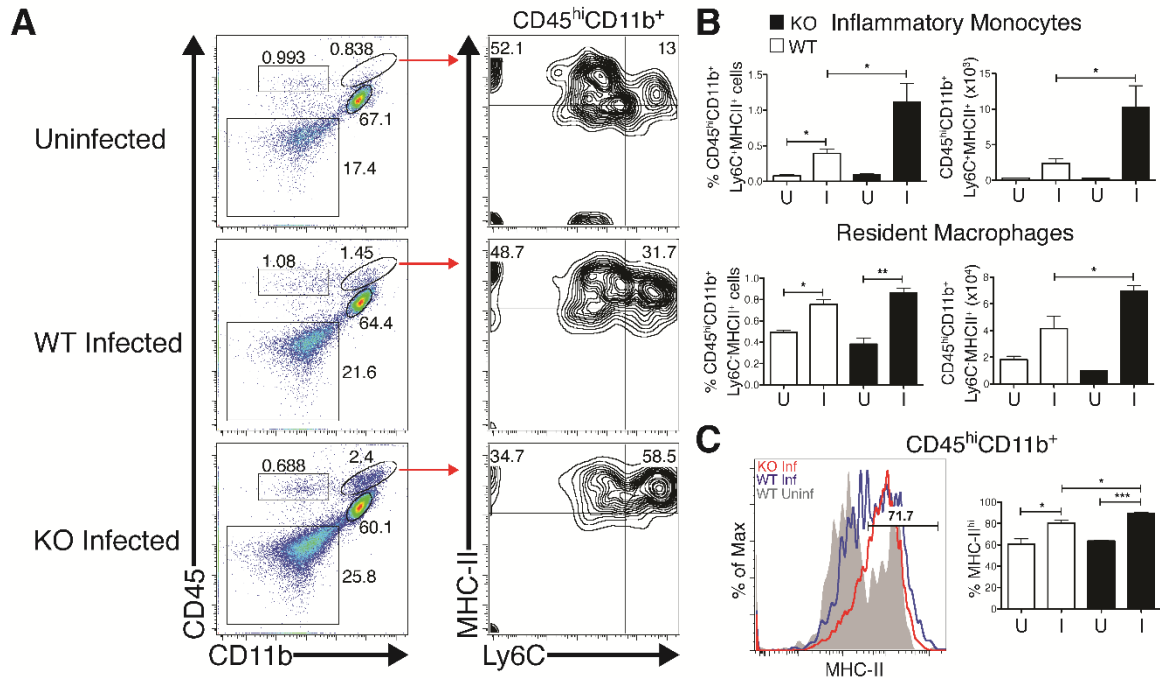


Figure 5. Brains from IL-10 KO animals show increased CD11b⁺ immune cell trafficking and MHC-II upregulation during *P. chabaudi* infection. Compiled from multiple independent experiments, cells were isolated from PBS-perfused brains of female IL-10 KO and WT mice 7-9 days post-infection **A**) Representative FACS plots showing CD11b⁺CD45^{hi} immune cells in the brain expressing Ly6C and MHC-II. **B**) Total percent and number of Ly6C⁺MHC-II⁺ tissue macrophages and of Ly6C⁺MHC-II⁺ inflammatory monocytes within the CD11b⁺CD45^{hi} gate. **C**) Histogram and % positive proportion of MHC-II expression and on CD45^{hi}CD11b⁺ immune cells. Histogram colors: Uninfected WT (Grey); day 7 and day 9 post-infection WT (Blue); day 7-9 post-infection IL-10 KO (Red). I= Infected, U= Uninfected. Student's t-test *p < 0.05, **p < 0.01, ***p < 0.001.

macrophages, were also increased in both infected WT and IL-10 KO groups. However, the numbers of Ly6C⁺ macrophages in brains of infected IL-10 KO animals were greater compared to infection-matched WT animals and uninfected controls. Furthermore, MHC-II expression was found to be upregulated on the entire CD45^{hi}CD11b⁺ monocyte/macrophage population compared to WT infected and uninfected controls, suggesting activation (**Figure 5C**). In addition, microglia (CD45^{int}, CD11b⁺) in the brains of infected IL-10 KO mice also showed increased expression of MHC-II (**Figure 6**). An increase in peripheral immune cell populations and the activation state of resident

microglia suggests cellular infiltration in the brains of IL-10 KO mice infected with *P. chabaudi*.

Chapter 4.3: IFN- γ -producing T cells in the brain

As T cells have been implicated in the pathogenesis of ECM [152-154], and the death of *P. chabaudi*-infected IL-10 KO mice [139], infiltrating CD4⁺ and CD8⁺ T cells were specifically stained within the lymphocyte gate (CD45^{hi}, CD11b⁻, Thy1 (CD90)⁺) (**Figure 7A**). Staining B cells with CD19 identified a minority of animals with B cells in the brain as well (data not shown). Some IL-10 KO animals had an increased number of CD4⁺ and CD8⁺ T cells in the brain, however it was not found to be significantly different from WT or uninfected controls (**Figure 7B**). Almost all of the T cells present within the brains of infected WT and IL-10 KO mice expressed IFN- γ . Importantly, CD4⁺ T cells in IL-10 KO mice expressed much higher levels of IFN- γ per cell than CD8⁺ T cells (**Figure 7C**). As the brains were perfused, these cells could be adherent to the vascular endothelium or infiltrating the brain parenchyma. Therefore, it is important to define their localization to determine the function that these cells may play in the pathogenesis of severe malaria.

Chapter 4.4: CD4⁺ T cells exhibit intravascular localization

To investigate the localization of potentially pathogenic CD4⁺ T cells relative to the vasculature, CellTrace Violet⁺ (CTV⁺) polyclonal CD4⁺ T cells were transferred from infection-matched (day 7 post-infection) IL-10 KO donors, and injected with Tomato lectin, which stains glycoproteins localized to the vascular endothelium. Adoptively

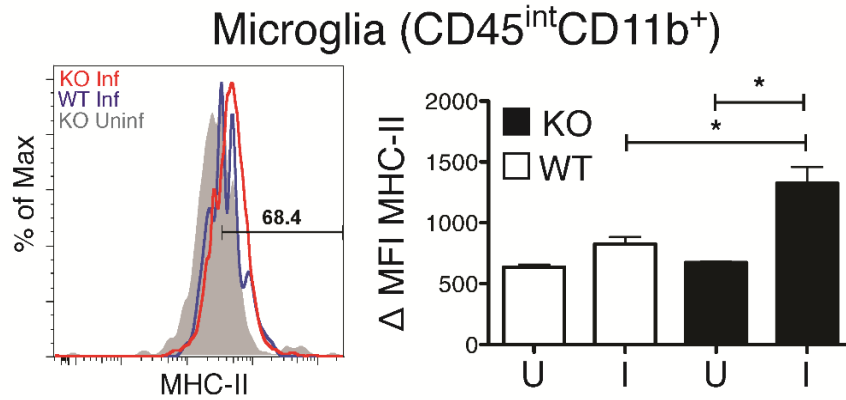


Figure 6. Brains from IL-10 KO animals show increased microglia activation during *P. chabaudi* infection. Compiled from multiple independent experiments, cells were isolated from PBS-perfused brains of female IL-10 KO and C57BL/6J WT mice 7-9 days post-infection. Mean fluorescent intensity (MFI) and histogram of MHC-II expression on resident microglia cells (CD11b⁺CD45^{int}). Histogram colors: Uninfected WT (Grey); day 7 and day 9 post-infection WT (Blue); day 7-9 post-infection IL-10 KO (Red). I= Infected, U= Uninfected. Student's t-test *p < 0.05, **p < 0.01.

transferred cells were visualized by confocal microscopy. The vast majority of T cells remained within the brain vasculature, as opposed to invading the parenchyma (**Figure 8**). Upon closer inspection, the T cells that appeared to localize to the parenchyma displayed several anomalies (multiple fluorescent staining, out of focus), that decrease their likelihood of representing true transendothelial migration. Thicker brain sections were also observed with multiphoton microscopy, confirming localization of CD4⁺ T cells in the vasculature (data not shown). Additionally, multi-organ failure was ruled out in IL-10 KO mice as there were no significantly different pathological changes found in internal organs compared to WT (**Figure 9**). In conclusion, CD4⁺ T cells that are responsible for lethal pathology in *P. chabaudi*-infected IL-10 KO mice do not infiltrate the parenchyma, but remain within the blood vessels supplying the brain.

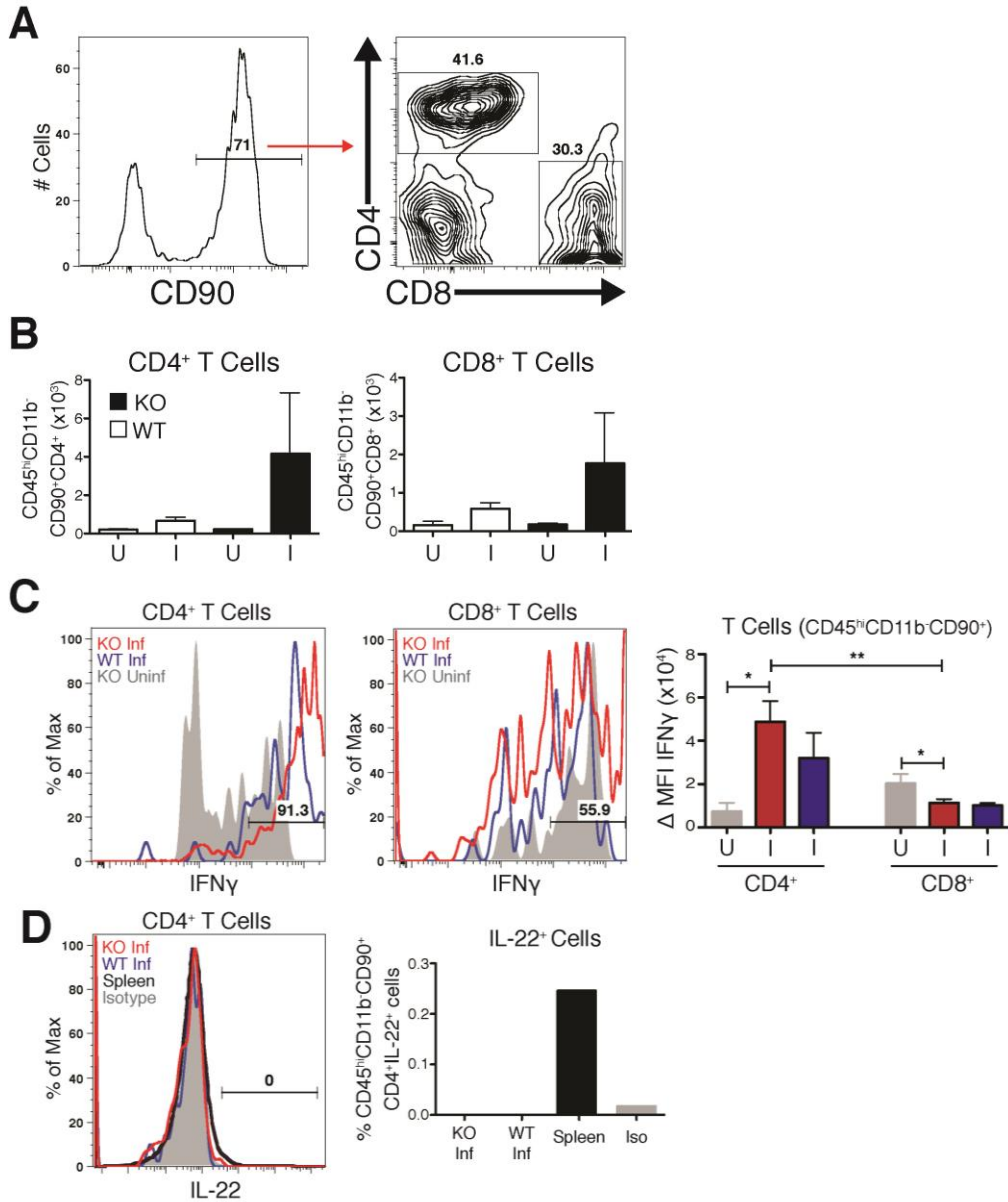


Figure 7. Mice have IFN- γ -producing T cells in the brain during *P. chabaudi* infection. Compiled from two independent experiments, cells were isolated from PBS-perfused brains of female IL-10 KO and WT mice 7-9 days post-infection. **A)** Representative FACS plots showing CD11b⁻CD45^{hi} immune cells in the brain, gated on the Thy1.2⁺ population, then CD4 and CD8a. **B)** Total cell numbers of CD4 and CD8 T cells within the CD11b⁻CD45^{hi}/Thy1.2⁺/CD4⁺ or CD11b⁻CD45^{hi}/Thy1.2⁺/CD8⁺ gate, respectively. **C)** Histograms showing the expression of IFN- γ in CD4⁺ and CD8⁺ T cells. Right panel: MFI of IFN- γ -expressing T cells in infected mice and uninfected controls. Percent positive proportion of infected IL-10^{-/-} mice shown. Histogram colors: Uninfected IL-10 KO (Grey); day 7 and day 9 post-infection WT (Blue); day 7-9 post-infection IL-10 KO (Red). I= Infected, U= Uninfected.

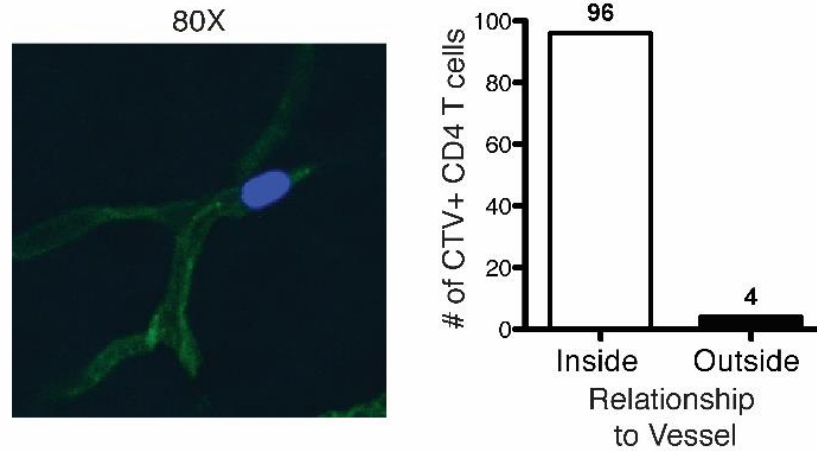


Figure 8. CD4⁺ T cells exhibit intravascular localization in IL-10 KO animals infected with *P. chabaudi*. A 30 μ m sagittal section of a female IL-10 KO brain 8 days post-inoculation with 10⁵ Pcc-iRBCs i.p. Animals were injected with 2x10⁶ CTV⁺ CD4 T cells i.p. 3.5 hours before sacrifice, and 40ug of DyLight488 labelled *Lycopersicon esculentum* (Tomato) Lectin i.v. 20 minutes before sacrifice without perfusion. Left panel: Confocal image of an adoptively transferred CTV⁺ CD4⁺ T cell located in the Lectin⁺ microvasculature of the KO brain. Right panel: Quantitation of adoptively transferred CTV⁺ CD4 T cells found inside or outside Lectin⁺ blood vessels within the KO brain. Imaging performed using a 20X objective with 4X digital zoom to visualize individual T cells within microvasculature.

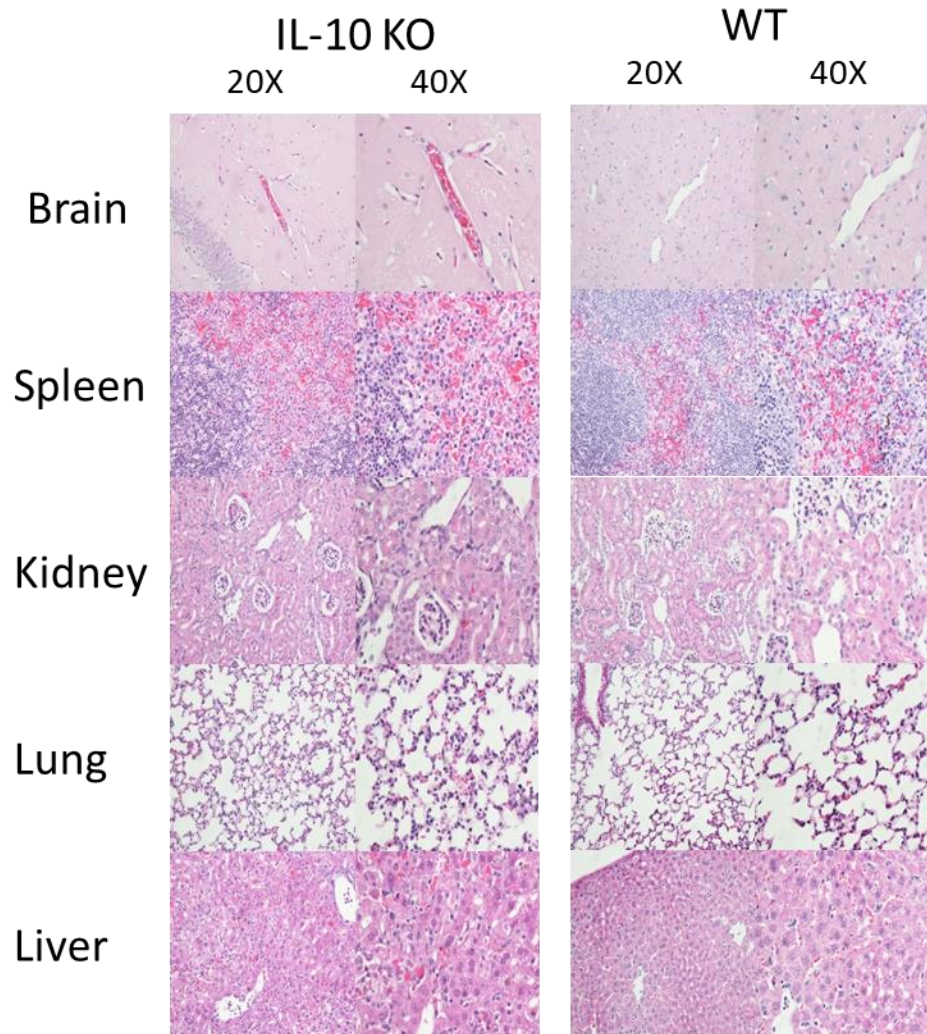


Figure 9. IL-10 KO mice do not die of multi-organ failure. Representative images from 2 independent experiments. WT and IL-10 KO mice were infected with 10^5 Pcc-iRBCs i.p. and monitored during the peak of infection. Upon severe morbidity, IL-10 KO mice were perfused with PBS and 10% Formalin via intracardiac injection. WT mice were sacrificed at the peak of infection (d10). Organs were harvested and left in 10% Formalin for 48 hours, before being paraffin-embedded, sectioned to $5\mu\text{m}$, and stained with H&E.

DISCUSSION AND CONCLUSIONS

In this study, behavioral and immunological outcomes of *P. chabaudi* infection in IL-10 KO animals were assessed. The goal was to identify the cellular immune populations associated with the neurological syndrome and the fatal phenotype [133, 140, 146]. While brain pathology has been well-documented in this model [133], behavioral assessments have not been performed to confirm that infection had severe effects on general health, neurological reflexes, and baseline behaviors in IL-10 KO mice infected with *P. chabaudi*. Trafficking immune cell populations found in the brain also had not been investigated by flow cytometry or confocal microscopy.

Behavioral studies in the *P. berghei* ANKA model have established a correlation between the deterioration in motor skills and neuromuscular function with histopathological changes associated with ECM [150, 151, 155]. Mice infected with *P. berghei* ANKA and evaluated with the SHIRPA exam showed early indications of neurological consequences via impairment in reflex and sensory functions, along with neuropsychiatric state [150]. As the disease progressed, multiple parameters became significantly different in mice suffering from ECM versus non-cerebral control mice, which also correlated with mean size of brain hemorrhage [150]. In the present study of animal behavior during *P. chabaudi* infection of IL-10 KO mice, an association of decreased function with fatal disease was observed. The main finding here was that at the peak of illness, wildtype animals performed better on virtually all behavioral tests than the IL-10 KO mice 24 hours prior to death. Thus, deficiencies in functional behavior domains may serve as early indicators of severe disease as some of these categories were decreased even earlier than 48 hours prior to death (**Table 1**). The behavioral findings in

this study are very similar to findings in *P. berghei* ANKA infection [150], suggesting brain involvement in the lethal pathology of *P. chabaudi*-infected IL-10 KO mice. Using this model, Brugat *et al.* have also shown indications of pathology in the liver and lungs, with concomitant sequestration in these organs. In addition, kidney pathology is present, however, there is no evidence of sequestration in the kidney, suggesting sequestration is not always the primary cause of organ pathology in this model [136]. Infected IL-10 KO mice show an increase in diagnostic markers of kidney damage and leukocyte trafficking to the lungs. These indications are seen in cases of multiple organ failure caused by severe malaria infection [156-158]. Liver failure is also observed in infection of the susceptible mouse strain DBA/2 [159], which is mirrored in BALB/c mice lacking expression of heme oxygenase-1 (HO-1, Hmox1 KO) [160], a free heme-catalyzing enzyme under the regulation of IL-10 that has been shown to be important in the pathogenesis of ECM and human CM [161, 162]. The role HO-1 plays in the pathogenesis of severe malaria in IL-10 KO mice infected with *P. chabaudi* has yet to be studied. While there are similarities between this model and ECM, the exact cause of death in IL-10 KO mice is unclear. Therefore, it is important that these findings demonstrate a significant peripheral immune infiltration of the central nervous system (CNS) vasculature, correlating with neurological and behavioral deficits. Given the lack of correlation of sequestration with all organ damage, and given that the mortality of infected IL-10 KO mice can be prevented with neutralization of TNF [133, 159], symptoms in this model are likely attributable to inflammation versus other features downstream of parasite biomass.

P. chabaudi infection in IL-10 KO mice results in vascular leakage and hemorrhage [134], which is also observed in *P. berghei* ANKA infection [163]. This pathological finding has been linked to the accumulation of cytotoxic CD8⁺ T cells in the cerebral microvasculature [128, 130]. The presence of microvascular hemorrhages and cerebral edema in human CM cases is correlated with adverse outcomes and death [28, 40]. The trafficking of pathogenic T cells and their involvement in mediating ECM is pertinent in our model, as it has been shown that selective deletion of IL-10 from T cells recapitulates the fatal phenotype observed in IL-10 KO mice [139]. However, it is not known at what anatomical sites these cells are lethal. Non-Treg IFN- γ ⁺ CD4⁺ T cells were identified as the primary producers of IL-10 in that study, as well as in lethal *P. yoelii* infection [164].

In order to characterize the cellular infiltrate, cell populations in the perfused brain tissue of *P. chabaudi*-infected IL-10 KO mice were identified by flow cytometry. Significant increases in macrophages (CD45⁺CD11b^{hi}) of two distinct types were observed in IL-10 KO animals compared to infection-matched WT animals. Inflammatory monocytes (CD11b⁺Ly6C⁺) were identified as well as tissue-resident (CD11b⁺Ly6C⁻) macrophages, though these are also likely to include maturing infiltrating cells [165]. A significant increase in activation of microglia was also measured, suggesting that either cytokines, or contact with other activated cell types, are affecting glial cells, which are an integral part of the brain parenchyma and act as the first line of defense in the CNS.

In this study, CD4⁺ T cells were found in perfused brains, suggesting that they are either adherent or have infiltrated into the brain parenchyma. We further show by

confocal microscopy that they are located within the brain vasculature of infected IL-10 KO mice. T cells in the brain were also shown to make IFN- γ , clearly demonstrating that pathologic lymphocytes traffic to the brain vasculature where they could contribute to the decrease in functional behavior witnessed in IL-10 KO mice infected with *P. chabaudi*. Furthermore, this suggests that infiltration of pathological immune cells may not be necessary to affect neurological function. Further supporting this interpretation, mice infected with the mild parasite *Plasmodium chabaudi adami* also transiently demonstrated behavioral defects, generalized microglial activation, and decreased neurogenesis despite the absence of gross cerebral vascular leakage [166]. Additionally, *P. chabaudi adami*-infected animals displayed elevated levels of pro-inflammatory cytokines in brain tissue during the peak of infection (day 9 post-infection), which resolved during the recovery phase (day 15 post-infection) [166]. These data, together with the present study, suggest that while relatively mild levels of inflammation may result in transiently altered behavior, a certain threshold is required to enact irreparable damage and eventual death.

Infection of IL-10 KO mice with *P. chabaudi* induces a fatal malarial disease characterized by increased mortality, severe neurological and behavioral deficits, elevated numbers of IFN- γ ⁺ T cells and macrophages adherent within the brain vasculature, and activated microglia, suggestive of elevated neuroinflammation. This study adds to the growing knowledge suggesting an integral role of inflammation in neuronal damage and downstream behavioral effects observed in malaria infection. These findings contribute to the current understanding of the etiologies of cerebral pathology and neurocognitive deficiencies in malaria infection.

Chapter 5: Thrombosis and astrocyte activation ameliorated by TNF and anticoagulation therapy in hyperinflammatory experimental cerebral malaria

INTRODUCTION

Causal mechanisms leading to brain pathology in human CM cases are multifactorial [55, 56]. Despite our incomplete understanding of the mechanisms of malaria pathogenesis, it is clear that the immune response causes much of the pathology associated with malaria infection [57]. Due to overlapping and synergistic mechanisms driving CM pathogenesis, determining the independent contributions of each pathway involved presents an ongoing challenge to investigators. The impact of parasite-specific factors, such as cerebral sequestration, has been studied in animal models of CM [58-60]. However, the interplay of inflammation with parasite-dependent factors makes it difficult to isolate the effects of organ-specific immune responses and their contribution to CM pathogenesis.

Here, we continued to utilize the HECM model to isolate the possible contributions of inflammation to severe disease from parasite sequestration. We recently defined a set of pathological behavioral phenotypes indicative of neurological and cognitive dysfunction in this model [167], distilled into the mini-SHIRPA test described in Chapter 4. The mini-SHIRPA was used here to identify animals that were moribund due to neurological inflammation, as opposed to anemia developed at later timepoints. Interestingly, despite lacking infiltration of inflammatory cells into the parenchyma, increased activation of microglia, a monocyte-related lineage derived from the yolk sac

during development, was observed in the brains of IL-10 KO mice infected with *P. chabaudi* by flow cytometry [167]. This prompted the question of how the inflammatory cells and cytokines within the vasculature could direct parenchymal activation and behavioral consequences suggestive of neuropathology.

The aim of this study was to investigate the localization of vascular leukocytes in relationship to glial cell activation in the brains of *P. chabaudi*-infected IL-10 KO mice. These studies support the contributions of cytokines, intravascular coagulation, and leukocytes confined within the brain vasculature to pathological glial cell activation in malaria infection.

MATERIALS AND METHODS

MICE

Mice were maintained according to the Materials and Methods found in Chapter 4.

PARASITE AND INFECTION

Parasite and infection of *P. chabaudi chabaudi* (AS) was carried out according to the Materials and Methods found in Chapter 4.

ANIMAL BODY TEMPERATURE AND WEIGHT

Internal body temperatures were assessed daily during infection using rounded stainless steel rectal probes and a BIO-TK8851 digital rodent model thermometer (Bioseb, Pinellas Park, FL). Probes were sanitized with Cavicide (Metrex Research Corp., Romulus, MI) between each use. Animal weights were measured according to the Materials and Methods found in Chapter 4.

ANIMAL BEHAVIOR EVALUATION

Beginning on day 5 post-infection, daily assessments were performed on all animals using an abbreviated version of the modified SmithKline Beecham, Harwell, Imperial College, Royal London Hospital, phenotype assessment (SHIRPA) protocol [145], as described in Chapter 4.

IMMUNOHISTOCHEMISTRY

Immunofluorescence of cryosections was examined after 48 hours of post-fixation of mouse brains in 4% PFA and 72 hours of cryo-protection in 30% sucrose. Fixed frozen sagittal sections (30µm) were made using Tissue Plus® Optimal Cutting Temperature Compound (Fisher Healthcare, Houston, TX) and mounted on glass slides with Fluoromount mounting medium (Novus Biologicals, Littleton, CO). Sections were incubated overnight at 4°C with primary antibodies rabbit anti-Fibrinogen (catalogue #: A0080, Agilent Technologies, Carpinteria, CA), rat (clone 2.2B10, catalogue #:13-0300, Thermo Fisher Scientific, Waltham, MA) or rabbit (catalogue #: Z0334, Agilent Technologies, Carpinteria, CA) anti-GFAP, mouse anti-CD11b biotin (clone M1/70, catalogue #: 13-0112-85, eBioscience, San Diego, CA), rat anti-CD45 biotin (clone 104, catalogue #: 13-0454-85, eBioscience, Sand Diego, CA). Secondary antibodies used were goat anti-rat AlexaFluor-488 (catalogue #:A11006, Thermo Fisher Scientific, Waltham, MA) and goat anti-rabbit AlexaFluor-568 (catalogue #:A11011, Thermo Fisher Scientific, Waltham, MA). Streptavidin-FITC (catalogue #: 11-4317-87, eBioscience, San Diego, CA) was used as a tertiary step for biotinylated antibodies. CellTrace Violet (catalogue #:C34557, Thermo Fisher Scientific, Waltham, MA)-labelled CD4 T cells were adoptively transferred into IL-10 KO mice for later co-localization with brain vasculature after i.v. perfusion with DyLight488-labelled tomato lectin (catalogue #: DL-1174, Vector Laboratories, Burlingame, CA). For detection of hypoxic cells, infected IL-10 KO and WT mice, and uninfected IL-10 KO control mice were given pimonidazole HCl i.p. 90 minutes before sacrifice and perfused with PBS and 4% PFA. 30-micrometer sagittal brain sections were stained with Zenon Alexa-fluor 488-labelled anti-

pimonidazole antibodies that detect protein-pimonidazole adducts that form during periods of low-oxygen tension (pO₂ less than 10mm Hg).

CELL AND *IN VIVO* LABELING

Some infected IL-10 KO and WT animals were injected with CTV⁺ CD4 T cells, and DyLight488 labelled *Lycopersicon esculentum* (Tomato) as described in the Materials and Methods in Chapter 4.

ANTI-TNF ANTIBODY AND ENO TREATMENT

Mice receiving anti-TNF antibody (clone XT3.11, Bio X Cell, West Lebanon, NH) were treated with 0.2µg/day for 5 days starting on day 5 post-infection (days 5-9). Untreated mice received isotype rat IgG1 as a control. Mice receiving LMWH (Lovenox, enoxaparin sodium injection, 30mg/0.3ml, Sanofi-Aventis, Bridgewater, NJ) were given 1000IU/kg i.p., twice a day (every 12 hours), starting on day 4 post-infection until day 12. Untreated mice received saline as a control.

CLARITY AND OPTICAL CLEARING

Fixed brain sections (IL-10 KO and WT) were subjected to the passive CLARITY optical clearing method [168] for large-scale labeling and imaging. In brief, mice were anaesthetized and perfused transcardially with a mixture of 4% (wt/vol) PFA, 4% (wt/vol) acrylamide, 0.05% (wt/vol) bis-acrylamide, 0.25% (wt/vol) VA044 (hydrogel

solution) in PBS. Brains were extracted and incubated in hydrogel solution at 4°C for 3 days. Solution temperature was then increased for 3 hours to 37°C to initiate polymerization. Hydrogel embedded brains were sectioned into 2mm- thick sagittal sections and placed in clearing solution (sodium borate buffer, 200 mM, pH8.5) containing 4% (wt/vol) SDS) for 3 weeks at 40°C under gentle agitation. After immunostaining, samples were optically-cleared using increasing serial concentrations (10-100%) of 2,2'-thiodiethanol (TDE) in Milli-Q water (EMD Millipore, Darmstadt, Germany) to achieve optimal refractive index matching with tissue.

MICROSCOPY

Fixed cryosections (30 µm thickness, fluorescent or confocal microscopy) or fixed, CLARITY-processed sections (2mm thickness, two-photon confocal microscopy) were imaged with a Nikon Eclipse 80i epifluorescence microscope, a Fluoview 1000MPE system configured with an upright BX61 microscope (Olympus, Center Valley, PA), or a custom Prairie Ultima IV (Prairie Technologies/Bruker, Middleton, WI) upright microscope. For two-photon microscopy, a 10X 0.3 N.A. objective (UPLFL10X, Olympus) and a 25X 1.05 N.A. super-objective (XLSLPLN25XGMP, Olympus) were used for image collection. Illumination for excitation of fluorescence was provided by a femtosecond laser (Mai Tai, SpectraPhysics, Santa Clara, CA) tuned to 800 nm. Fluorescence was collected using a 2-photon standard M filter set including filters with bandwidth 604±45nm, a filter with bandwidth 525±70nm and dichroic mirror cut off at 575nm. Samples were mounted on a 30-mm cage plate (CP06, ThorLabs, Newton, NJ) in between two #1.5 cover glass. Epifluorescence Images were acquired using a Nikon

Eclipse 80i fluorescent microscope. Images were analyzed using Image J (FIJI), Olympus Fluoview FV1000-ASW 2.0 Viewer (confocal), Imaris Image Analysis Software (confocal and two-photon microscopy; Bitplane USA, Concord, MA), and NIS Elements (confocal; Nikon Instruments, Melville, NY). Positive fibrinogen and elevated GFAP staining in each field was quantified by applying a signal intensity threshold and the % area covered was calculated via the outlined areas of positive staining that met the signal intensity threshold per field of view. The percentage of total area included was calculated using Image J software (FIJI, NIH). For quantitation of hypoxic cells, numbers of Alexa-fluor 488+ cells per section were enumerated using epifluorescence microscopy and plotted per animal using Prism software.

STATISTICS

Where indicated, groups were compared by t-test (2 groups) or one-way ANOVA (3 or more groups), followed by post-hoc Bonferroni method to identify significance between individual groups. Each point represents the average value per animal after analysis of 10 fields. Statistical analysis was performed in Prism (GraphPad, La Jolla, CA) * $p \leq 0.05$, ** $p \leq 0.01$, *** $p \leq 0.001$. Error bars represent +/- SEM.

RESULTS

Chapter 5.1: Residual fibrinogen deposition

To investigate vascular abnormalities in *P. chabaudi*-infected IL-10 KO mice, we examined sagittal sections of perfused and fixed brain tissue for evidence of vascular leakage as indicated by fibrinogen extravasation at the peak of infection (day 8 post-infection). Brains from infection-matched, disease-resistant WT mice were used as controls. Residual fibrinogen foci were identified within the vascular lumen of brain blood vessels in IL-10 KO mice despite transcardial perfusion prior to sacrifice (**Figure 10A**). Some sites of perivascular fibrinogen were also occasionally identified. Quantification of fibrin staining in the IL-10 KO mice compared to WT controls (% area of Alexa Fluor 568⁺ pixels, 10 fields/mouse), showed an increase in the area of the brain with bright fibrinogen immunoreactivity closely associated with blood vessels (red, **Figure 10A, B**). In some WT mice, we could occasionally see a low level of fibrinogen present in a minority of the brain blood vessels, but this was not statistically significant compared to uninfected mice. There was also an increase in liver fibrinogen in infected IL-10 KO, but not WT (**Figure 10C**). This could potentially be due to an increase in fibrinogen production by the IL-10 KO mouse downstream of inflammation, as fibrinogen is an acute phase response protein [169]. However, while production of fibrinogen is a risk factor for coagulation, it does not lead to clotting [170].

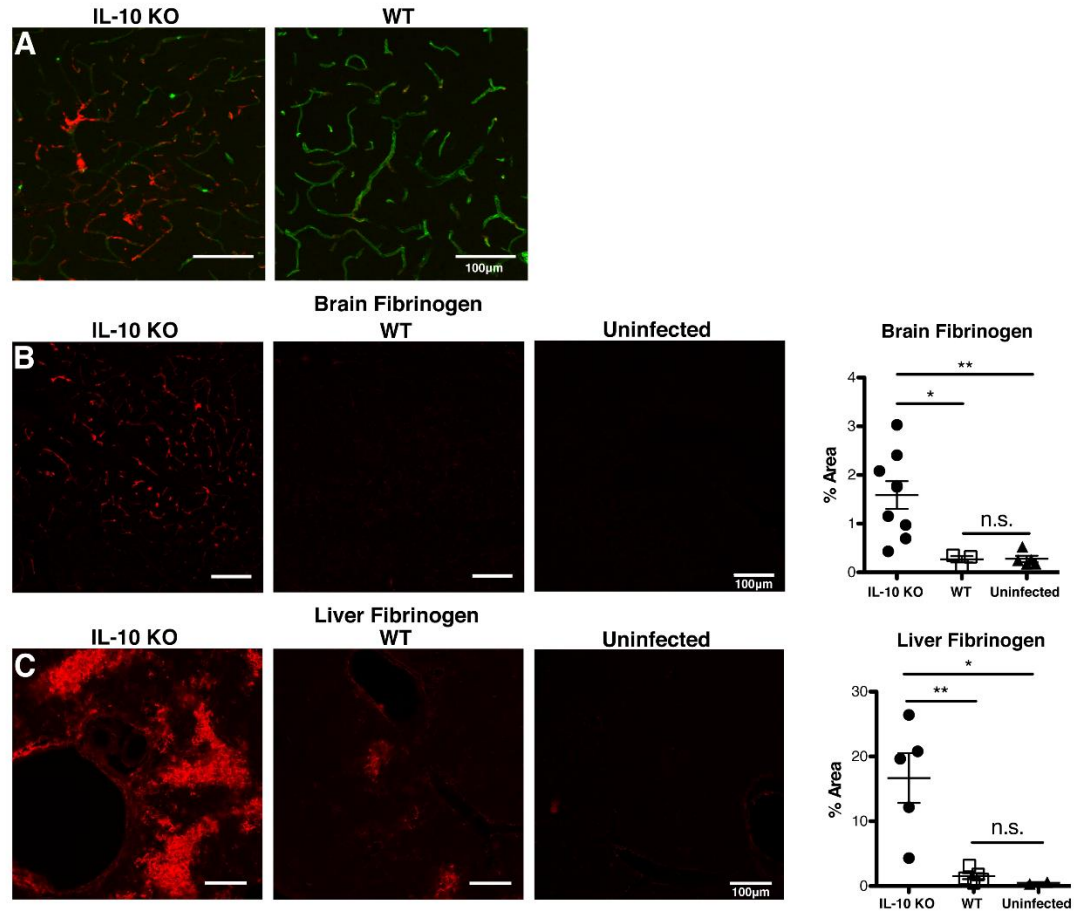


Figure 10. IL-10 KO mice have residual fibrin(ogen) deposition in and around brain vasculature, and increased liver fibrinogen. **A)** Confocal images (20X) showing immunofluorescent staining of fixed, frozen brain sections (30µm) from *P. chabaudi*-infected IL-10 KO and WT mice (day 8 p.i.). Fibrin(ogen) (red) and tomato lectin (green, vascular endothelium). **B)** Fibrin(ogen) (red) was quantified by surveying 10 fields per brain section (10X). Graph showing average % area of fibrin(ogen) positive staining above threshold in each field. **C)** Immunofluorescent staining (10X) and quantitation of fibrinogen (red) in liver from infected IL-10 KO, WT, and uninfected controls. One-way ANOVA, followed by post-hoc Bonferroni method was used to determine statistical significance. * $p < 0.05$, ** $p < 0.01$. Scale bar represents 100µm.

Chapter 5.2: Leukocyte congestion of brain vasculature

Studies of both human CM and murine ECM have documented congestion of the brain and retinal vasculature. The presence of peripheral immune cells adherent within the vasculature in mouse models of CM and in brain vessels on autopsy of CM patients [50, 171] suggest that such cells play an important role in mediating neuropathology [59]. Interestingly, we found that both large and small vessels retain intravascular fibrinogen (red, **Figure 11A**), often to the point of complete occlusion of the vascular lumen (**Figure 11B**), reminiscent of thrombosis. The coagulation cascade leads to cleavage of fibrinogen into fibrin during the formation of a clot [172]. The polyclonal antiserum used to detect fibrinogen here also detects fibrin and other fibrinolytic degradation products [173, 174]. In addition, the staining pattern resembled intravascular thrombi. Therefore, we interpret this staining pattern to represent fibrin clots. The appearance of round gaps in fibrin staining led us to hypothesize that immune cells were retained within these congested vessels. In order to identify potential immune cell populations within thrombi, we stained IL-10 KO brains using the pan-leukocyte marker CD45 (green, **Figure 11C**), and the monocyte marker CD11b (green, **Figure 11D**). Staining showed both CD45⁺ leukocytes and CD11b⁺ monocytes within areas of residual fibrinogen staining. We previously showed using flow cytometry that all of the CD11b⁺ cells within the brain were also Ly6C⁺, indicating inflammatory monocytes, in *P. chabaudi* infected IL-10 KO mice [167]. There was a large and significant increase in Ly6C^{hi} inflammatory monocytes, while a Ly6C^{int} population of resident macrophages, was not increased.

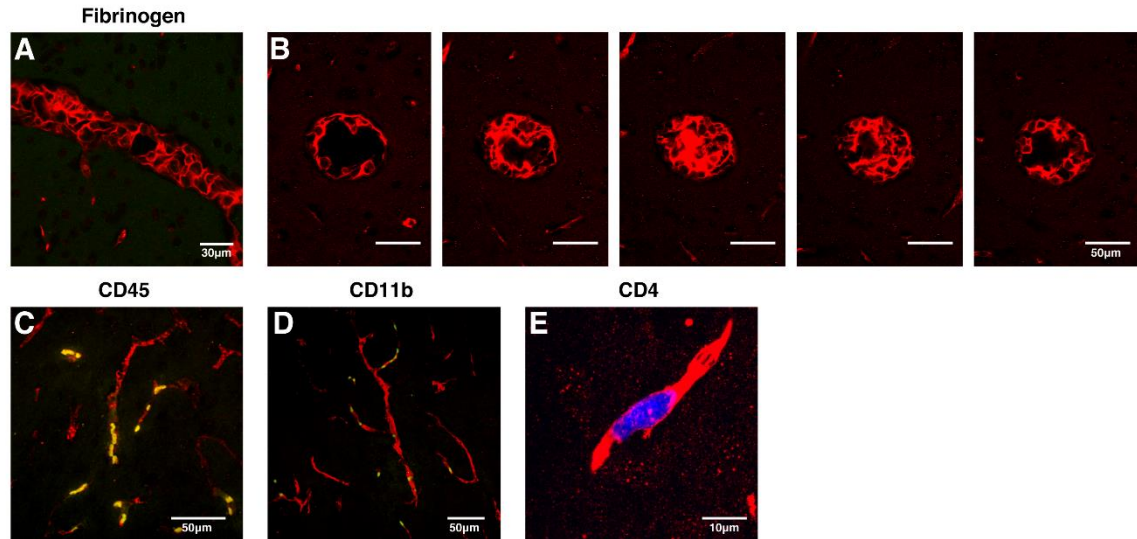


Figure 11. Vascular congestion in IL-10 KO mice with malaria includes thrombi containing monocytes and T cells. Immunofluorescent staining of fixed, frozen brain sections (30µm) from *P. chabaudi*-infected IL-10 KO mice (day 8 p.i.). **A)** Confocal images (40X) of IL-10 KO brain for fibrin(ogen) (red). **B)** Successive single-plane confocal images (40X) of a 30µm z-stack showing complete occlusion of a large vessel with residual fibrinogen (red). **C)** Immunofluorescence staining of IL-10 KO brains showing fibrin staining of blood vessels (red) and leukocytes expressing CD45 (green, 60X) and **D)** CD11b (green, 40X). **E)** CTV⁺ CD4 T cells (blue) from infected IL-10 KO mice were adoptively-transferred into infection matched IL-10 KO (d7 p.i.) recipients 3.5 hours before sacrifice. Frozen brain sections (d7 p.i.) were stained for fibrin (red). Max intensity projection of a 30µm z-stack (240X) displayed from brain tissue of IL-10 KO mice co-stained with WT control samples (n=3-4 mice per group). Scale bars represent 30µm (A), 50µm (B, C, D), or 10µm (D).

We were also interested to see if CD4 T cells, the primary producers of IL-10 in this model, were also found localized with residual fibrinogen in the vessels. Therefore, CellTrace Violet-labelled CD4 T cells from IL-10 KO mice 7 days post-infection were adoptively transferred into infection-matched IL-10 KO recipients, which underwent transcardial perfusion and brain tissue collection 3.5 hours later. Upon analysis of the localization of the transferred cells in the brain, we identified fluorescently-labelled CD4 T cells (blue) surrounded by fibrinogen (red, **Figure 11E**). Given the potential for

clusters of activated leukocytes to promote local inflammatory cytokine production, we next tested the local effect of congestion on the neuroglial cells surrounding the vasculature, namely astrocytes.

Chapter 5.3: Increased astrocyte activation

As astrocytes play an important role in maintaining the integrity of the blood-brain-barrier (BBB), including in the context of ECM [175], we analyzed the extent of astrocyte activation in IL-10 KO mice infected with *P. chabaudi*. In order to visualize extensive activation of astrocytes, we utilized CLARITY followed by optical clearing, a series of tissue processing techniques which remove relatively opaque lipids, transforming thick sagittal brain sections (2mm) to make them virtually transparent. This process diminishes excess light scattering during image acquisition by confocal or two-photon microscopy, allowing for increased imaging depth beyond that possible in native opaque tissues. The ability to obtain image stacks over the full 2mm thickness combined with image stitching allowed for image acquisition of the entire thick sagittal section. Whole brain sections stained with anti-GFAP (glial fibrillary acidic protein; upregulated on activated astrocytes) were imaged to determine the extent of astrocyte activation in susceptible IL-10 KO mice (**Figure 12A**), and resistant WT animals (**Figure 12B**). A higher GFAP signal indicating astrocyte activation was observed in the IL-10 KO brain in multiple areas including the hippocampus, thalamus, and caudate putamen. While GFAP is expressed on most astrocytes, even in uninfected animals, the level of expression is significantly lower than on activated astrocytes [176]. Interestingly, there was little GFAP signal in the cortex, a finding that is consistent with findings in human CM autopsy [50]. For unbiased comparison of astrogliosis, we focused our analysis on

the hippocampal formation (**Figure 12C, D**), as a representative region in which astrogliosis was evident. This region is amenable to being isolated from other regions by image processing due to its well-defined margin and thus allowed for comparison of GFAP^{bright} cells in the full volume of the hippocampus region in the section. As shown in high-resolution 3D micrographs, in addition to upregulation of GFAP, astrocytes in IL-10 KO mice showed distinct morphological changes (**Figure 12E**), appearing hypertrophied and possessing more processes compared to WT (**Figure 12F**). Upon quantification, we showed that the hippocampal formation stained by GFAP in infected IL-10 KO mice was significantly increased compared to WT mice (**Figure 12G**). As inflammation, or vascular damage, can lead to astrocyte activation, we next investigated whether congestion and astrocyte activation occurred in close proximity.

Chapter 5.4: Astrocyte activation clusters with fibrinogen staining

To investigate the potential connection between vascular congestion and astrocyte activation, we performed immunofluorescent staining of infected and uninfected IL-10 KO brains for fibrinogen and the astrocyte marker GFAP. In the hippocampal formation, we observed an increase in residual fibrinogen staining in the infected IL-10 KO brains compared to WT (**Figure 13**). Interestingly, the astrocytes near fibrin-staining vessels frequently showed an increase in GFAP intensity. Uninfected mice showed neither residual fibrinogen deposition, nor an increase in GFAP immunoreactivity. However, it was noted that not all areas with residual fibrinogen staining showed an increase in GFAP intensity. This could potentially be due to the kinetics of astrocyte activation upon encountering a vascular abnormality, however, further studies will need to be done to address the kinetics of these events. Having established a link between microvascular

congestion characterized by residual fibrinogen staining and astrocyte activation, we next sought to determine the role that inflammatory cytokines might play in this process.

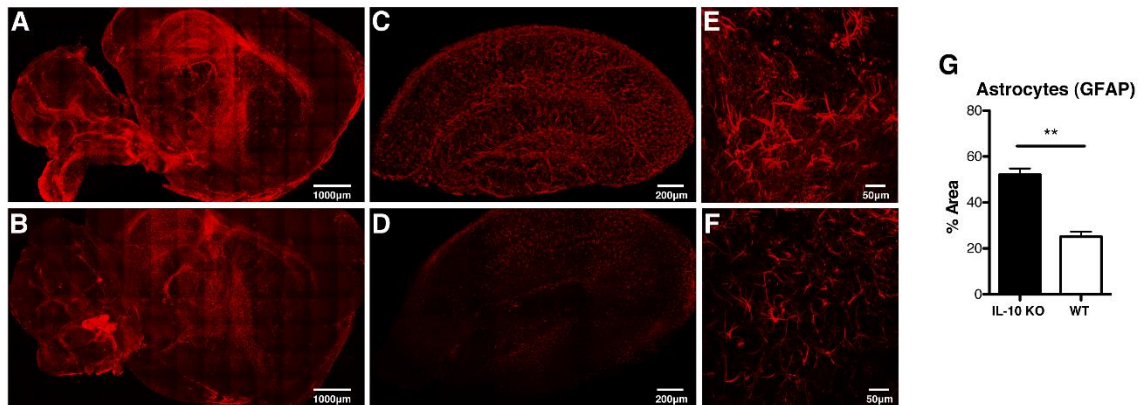


Figure 12. Increased astrocyte activation in IL-10 KO mice during *P. chabaudi* infection. Mice were infected with *P. chabaudi* and sacrificed 8 days post-infection. Thick sagittal brain sections (2mm) were CLARITY-processed, optically-cleared, stained with GFAP (red), and imaged by two-photon confocal microscopy. **A, C, E**) IL-10 KO and **B, D, F**) WT brains from the peak of *P. chabaudi* infection (d8 p.i.). **A, B**) Single fields of the entire tissue section (10X) stitched together. **C, D**) Hippocampus of thick brain section is masked for increased resolution and quantitation in **C**) IL-10 KO, and **D**) WT animals. **E, F**) Representative high resolution image (25X) of astrocytes from hippocampus showing **E**) IL-10 KO and **F**) WT control brains. **G**) Quantification of the percent area of astrocyte staining above threshold in the hippocampal formation of *P. chabaudi*-infected IL-10 KO and WT brains. Number of fields for IL-10 KO (n=15) and WT (n=9). Scale bars represent 1mm (**A, B**), 200 μ m (**C, D**) and 50 μ m (**E, F**). Student's t-test was used to determine statistical significance. **p < 0.01.

Chapter 5.5: Anti-TNF treatment prevents clotting and astrocyte activation

Immunopathology in IL-10 KO mice infected with *P. chabaudi* is generated by the hyper-inflammatory cytokine response generated in the absence of this regulatory cytokine primarily made by T cells. Neutralizing TNF, or IFN- γ receptor deficiency in IL-10 KO mice, ameliorates disease and improves survival, while neutralizing the other major regulatory cytokine, transforming growth factor- β , increases mortality [133].

Therefore, we hypothesized that brain pathology, including astrocyte activation, is driven by inflammatory cytokines. To test this, we treated IL-10 KO mice with neutralizing anti-TNF antibody for five days (days 5-9 post-infection). Behavioral symptoms were monitored using the *P. chabaudi*-specific SHIRPA health assessment that we previously described [167], and measured systemic pathology including temperature and weight loss. Infected IL-10 KO and WT mice treated with rat isotype IgG1 were used as controls. To monitor for fibrin(ogen) accumulation and astrocyte activation, mice were sacrificed at day 8 post-infection, which is at the onset of severe disease, and stained their brains for microscopic analysis. Despite IL-10 KO mice treated with anti-TNF antibody showing improved survival over the course of infection, temperature and weight loss were similar with the isotype IgG-treated IL-10 KO mice (**Figure 14**).

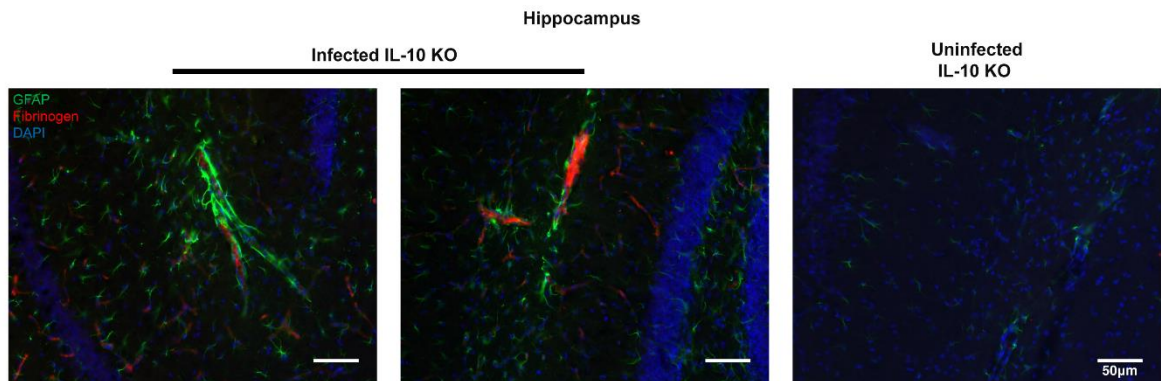


Figure 13. Activated astrocytes cluster along thrombus-containing brain vasculature. IL-10 KO mice were either infected with *P. chabaudi* and sacrificed 8 days post-infection, or used as uninfected controls. Representative epifluorescence images (20X) of the hippocampal formation in cryosections (30 μ m) from infected (d8 p.i.) IL-10 KO brains (left, middle), and uninfected IL-10 KO brains (right) immunostained for GFAP (green), fibrinogen (red), and DAPI (blue). IL-10 KO mice were co-stained with WT control samples (n=5-6 mice per group). Scale bars represent 50 μ m.

While we observed an increase in GFAP staining and increased residual fibrinogen in isotype-IgG-treated IL-10 KO animals (**Figure 15A**), we did not observe these changes in the IL-10 KO group treated with neutralizing anti-TNF antibodies (**Figure 15B**), which was similar to isotype-IgG-treated WT mice (**Figure 15C**). Immunofluorescent staining in the brain showed a significant reduction of fibrinogen accumulation upon neutralization of TNF (**Figure 15D**). Furthermore, the anti-TNF-treated IL-10 KO group showed a significant decrease in astrocyte activation (**Figure 15E**), and was protected from behavioral symptoms during treatment (**Figure 15F**). Excess production of fibrinogen in the liver was also reduced by anti-TNF treatment (**Figure 15G**), suggesting a decrease in the acute-phase reaction. Therefore, anti-TNF treatment decreased intravascular fibrin clotting and astrocyte activation, suggesting that inflammation plays a critical role in regulating vascular and parenchymal cell homeostasis within the context of malaria infection.

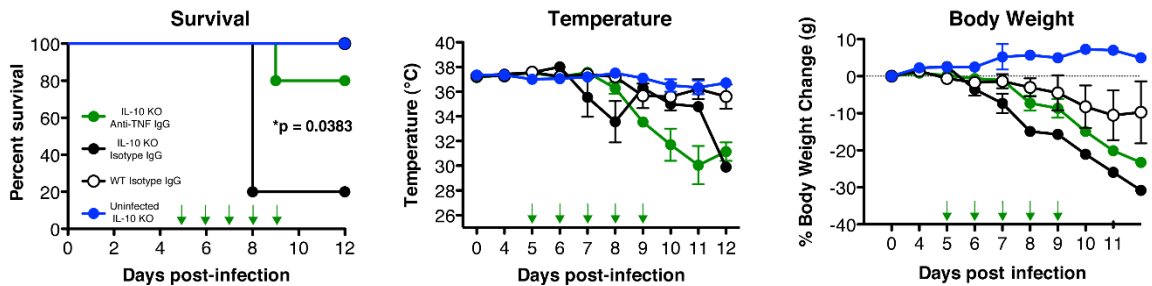


Figure 14. Anti-TNF antibody treatment improves survival of IL-10 KO mice infected with *P. chabaudi*, despite similar temperature and weight loss. Mice were infected with *P. chabaudi* and followed throughout the acute phase of infection (day 12 p.i.). One group of IL-10 KO mice was kept as uninfected controls (n=2). 2 groups of infected IL-10 KO mice (n= 5 each) received either anti-TNF IgG treatment, or isotype IgG treatment, with one group of infected WT mice (n=5) receiving isotype IgG treatment. Survival (left), internal body temperature (middle), and body weight (right) were monitored daily during the course of infection. Green arrows represent the dosing schedule of either anti-TNF IgG, or isotype control IgG. Log-rank test (Mantel-Cox) was used to determine statistical significance in the survival graph.

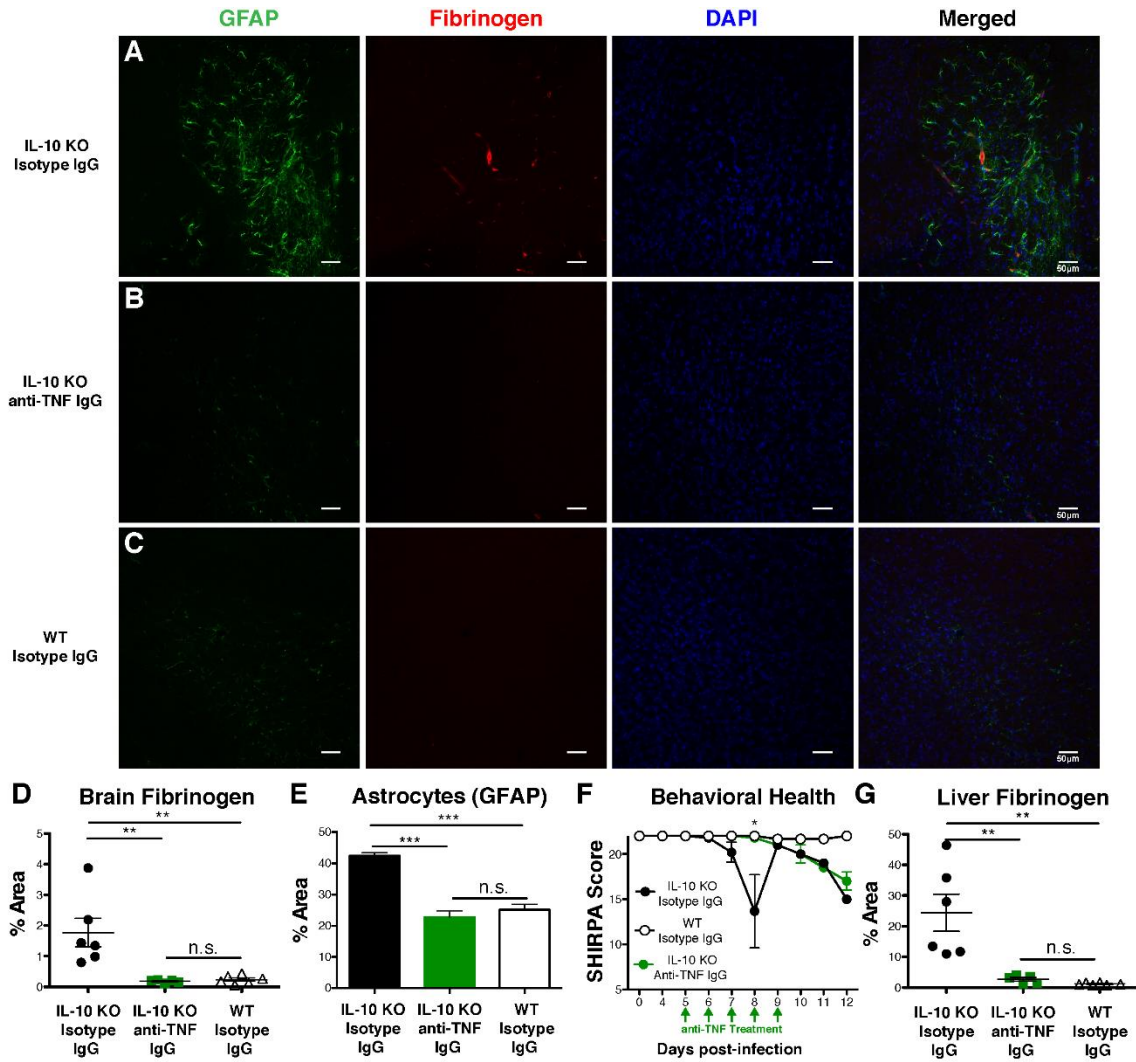


Figure 15. Anti-TNF antibody treatment prevents astrocyte activation and mortality in IL-10 KO mice during *P. chabaudi* infection. Mice were infected with *P. chabaudi* and followed throughout the acute phase of infection (day 12 p.i.), or sacrificed 8 days post-infection for immunofluorescent staining. One group of IL-10 KO mice received anti-TNF IgG treatment, while another group of IL-10 KO mice and a group of WT mice received isotype IgG as control. **A**) Representative confocal images (20X) of cryosections stained for astrocytes (GFAP; green) and fibrinogen (red) with DAPI (blue) in sagittal brain sections in anti-TNF antibody treated IL-10 KO mice, **B**) isotype-IgG-treated IL-10 KO mice, **C**) and isotype-IgG-treated WT mice. **D**) Brain fibrinogen, and **E**) GFAP staining for reactive astrocytes in the hippocampus was quantified by calculating the % area per field of immunostaining above signal threshold. Ten fields per animal was assessed, with the graph showing the mean value per animal. **F**) General behavior as measured by the abbreviated SHIRPA screen of anti-TNF antibody treated (IL-10 KO, n=5) and isotype-IgG treated (IL-10 KO, n=5; WT, n=5) mice infected with *P. chabaudi*. Green arrows represent the dosing schedule of either anti-TNF IgG, or isotype control IgG. **G**) Liver fibrinogen quantitation. Data shown is representative of 2 independent experiments. One-way ANOVA, followed by post-hoc Bonferroni method was used to determine statistical significance. * $p < 0.05$, ** $p < 0.01$, *** $p < 0.001$. Scale bars represent 50 μ m.

Chapter 5.6: Hypoxic brain cells

As one of the most prominent hypotheses regarding neurological damage in CM centers around pathology caused by hypoxia secondary to vascular congestion [96, 177], we investigated the possibility of hypoxic cells in the brain tissue of *P. chabaudi*-infected mice. Using a commercial kit that requires injection of a chemical compound (pimonidazole HCl) that selectively binds reduced thiol groups only in the presence of low oxygen tension (pO₂ less than 10mm Hg), brain tissue was collected during the peak of malaria symptoms in infected WT and IL-10 KO mice, with uninfected controls. The brain tissue was immunostained and visualized for hypoxic cells using fluorescent microscopy. Surprisingly, we found small numbers of cells that appeared neuronal in morphology (**Figure 16A**). And while they were found in small amounts across the entire tissue section, there were a significant increase in hypoxic cells in infected IL-10 KO brains compared to infected WT tissue (**Figure 16B**). While it appears that anti-TNF IgG treatment reduces the number of hypoxic cells in IL-10 KO mice infected with *P. chabaudi*, it did not reach statistical significance. The significance of this finding is uncertain, as the number of hypoxic cells found in the tissue was highly variable in IL-10 KO tissue and in relatively negligible abundance compared to the unstained neuronal cells that are presumably healthy. Additionally, there was no consistent pattern of co-localization of hypoxic cells near areas of residual fibrinogen.

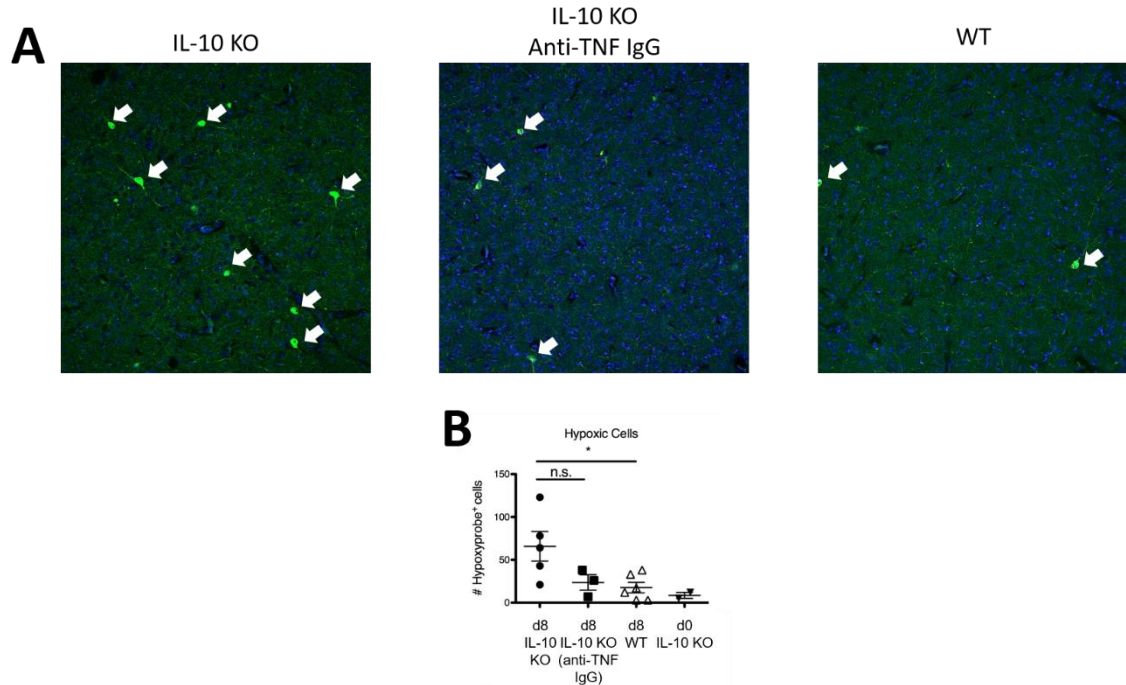


Figure 16. **IL-10 KO mice infected with *P. chabaudi* have few, but significantly increased numbers of hypoxic cells in the brain.** During *P. chabaudi* infection, mice were given pimonidazole HCl i.p. 90 minutes before sacrifice. 30-µm sagittal brain sections were immunostained with anti-pimonidazole antibodies. Numbers of Alexa-fluor 488+ cells per section were enumerated using epifluorescence microscopy and plotted per animal using Prism software. Representative 20X confocal images from each infection group displayed. One-way ANOVA, followed by post-hoc Bonferroni method was used to determine statistical significance. * $p < 0.05$.

Chapter 5.7: Enoxaparin treatment of IL-10 KO mice

Finally, in order to support our hypothesis that intravascular congestion mediated by residual fibrinogen contributes to the fatal neurological phenotype of IL-10 KO mice infected with *P. chabaudi*, we treated infected IL-10 KO mice with anti-coagulants. Unfractionated heparin treatment showed no efficacy in protecting IL-10 KO mice from fatal neuropathology (**Figure 17**). Following that study, we treated IL-10 KO mice with a low-molecular weight heparin (enoxaparin sodium, ENO) starting on day 4 post-infection, through to the end of peak illness at day 12 post-infection. Mice were treated

twice per day and monitored using the mini-SHIRPA screen (**Figure 18A**). Blood smears were also collected on day 9 post-infection to monitor parasite burden. To our surprise, ENO

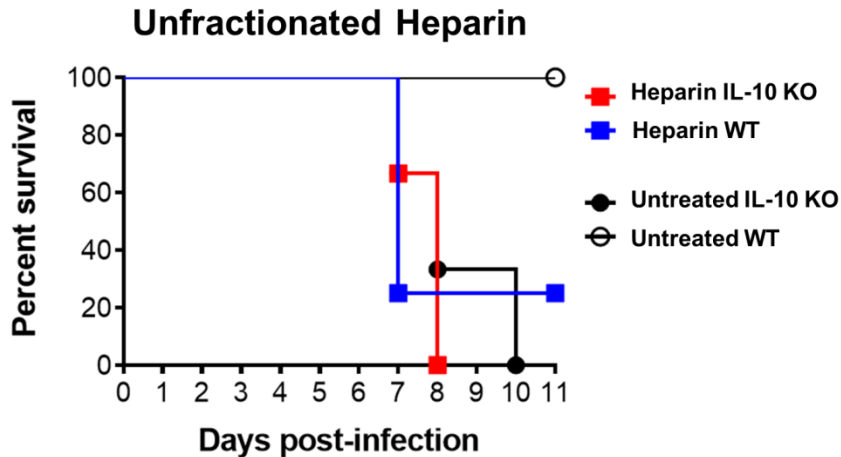


Figure 17. IL-10 KO mice are not rescued from fatal neurologic disease with unfractionated heparin treatment. Four groups of IL-10 KO or WT mice (n= 4/group) were either treated with 2,500IU/kg unfractionated heparin i.p. once a day (red/blue), or given saline (black/white) starting at day 5 post-infection until the middle of the anemic period of disease (day 11 post-infection).

treatment of IL-10 KO mice rescued them from fatal neurologic disease, with the saline-treated mice succumbing to fatal neurological disease early in the infection despite having comparable parasite burden (**Figure 18B**). However, ENO-treated IL-10 KO mice were still susceptible to severe anemia that presents after the peak of infection (day 9 post-infection), as 2 out of 4 ENO-treated mice (50%) died during this phase. The minimum mini-SHIRPA scores of individual mice before the peak of anemia were significantly lower in the saline-treated mice compared to the ENO-treated mice (**Figure 18C**). Additionally, the timecourse of behavioral symptoms shows a marked decrease in the saline-treated mice early in infection, whereas the ENO-treated mice do not begin to decline until after 10 days post-infection at the beginning of anemic symptoms.

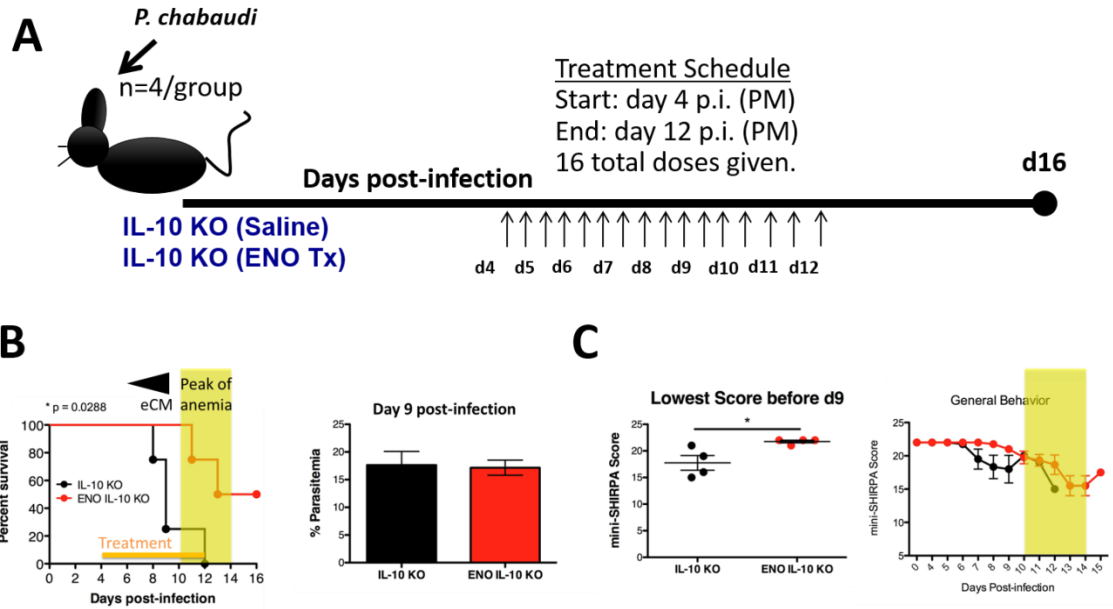


Figure 18. IL-10 KO mice are rescued from fatal neurologic disease with LMWH treatment. **A)** Two groups of IL-10 KO mice (n= 4) were either treated with 1,000IU/kg (20IU/dose) Enoxaparin Na (ENO) i.p. twice a day (12-hours apart), or given saline starting at day 4 post-infection until the middle of the anemic period of disease (day 12 post-infection). **B)** Survival was monitored daily and blood smears were collected on d9 post-infection. **C)** Behavior was monitored daily using the mini-SHIRPA score. Mice were culled at day 16 post-infection during the recovery/chronic phase of the disease.

DISCUSSION AND CONCLUSIONS

In the present study, we investigated the neuropathology of lethal *P. chabaudi* infection in IL-10 KO animals. The goal was to identify potential mechanisms driven by excessive inflammation responsible for the neurological syndrome and the fatal phenotype in IL-10 KO animals infected with *P. chabaudi* [133, 140, 146, 167]. In this model, we have demonstrated severe behavioral symptoms and leukocytes collected within the brain vasculature of mice succumbing to infection [167] in a manner similar to *P. berghei* ANKA (PbA)-infected C57BL/6 mice, the most common model of ECM [58, 150]. While cerebral pathology, including edema and hemorrhage, has been documented in this model [134], and cytokines have been shown to be essential in promoting or preventing fatal disease [133], the presence of activated leukocytes within the brain, and their contribution to brain pathology, have not been determined. Further studies to determine the specific mechanisms of leukocytes within the brain are critical, because while inflammatory cytokines are implicated by studies of host genetics and correlations of serum cytokines with poor outcomes in severe malaria [178, 179], no significant inflammatory infiltrate has been documented in human or mouse studies of the disease [50, 70, 180].

Congestion of the brain and retinal vasculature, to the extent of blocking blood flow, has been documented in human CM and is associated with poor prognoses [181, 182], although the constituents of the blockage are not certain. While parasite and erythrocyte rosettes have been identified bound to vascular endothelium and clotting factors, such as platelets and von Willebrand factor [60, 183], it is not yet clear how this alone could drive neural pathology [184]. Localized inflammatory cells are also likely to

contribute to the generation, or amplification, of neuropathology; however, several studies have shown that leukocytes are not observed in large numbers in the brain parenchyma of CM patients on autopsy [70, 180, 185]. Importantly, coagulation defects are seen in both murine ECM and in human CM infections [114, 186, 187]. DIC, the most severe abnormality, was observed in 19% of CM patients, and correlated with poor outcomes in a recent study in Malawi [188]. Other patients suffered many of the characteristic symptoms of DIC, except lacked evidence of coagulopathy. In order to understand the role of intravascular inflammatory leukocytes and coagulation in promoting neuronal malfunction, we investigated parenchymal events associated with vascular congestion by focusing on astrogliosis as a marker of potential parenchymal dysfunction.

The vascular findings in this study, suggestive of intravascular coagulation (**Figure 10**) and incomplete perfusion secondary to congestion (**Figure 11**), are striking. These abnormalities have not been described in the *P. chabaudi* model before. Yet, coagulation is of major relevance for our understanding of neuroinflammatory mechanisms in CM [170, 185, 189]. Clotting defects in both pro- and anti-coagulatory proteins have been documented in human CM [190, 191]. Recent studies show that the endothelial protein C receptor (EPCR) may link coagulation, inflammation, and *P. falciparum* sequestration by both binding the parasite and promoting inflammation and BBB breakdown [114, 192]. Systemic inflammation has also been recently shown to contribute to intravascular clotting via potential mechanisms involving neutrophils and monocyte interaction with platelets in CM [193, 194], linking inflammation and clotting,

which in turn also promotes sequestration. Studies of the intersection of the clotting cascade and inflammation point to bi-directional amplification of both pathways [170].

Macrophages and inflammatory monocytes are the best-known example of an immune effector cell regulated by IL-10 [195], although the critical cell type expressing IL-10 receptor is not yet known in this infection. The role of inflammatory monocytes in ECM is not clear, as C-C chemokine receptor type 2 KO mice still succumb to disease [196]. The role of CD4⁺ T cells, although few in number, cannot be underestimated as demonstrated by their critical regulatory role in *P. berghei* ANKA [197], and *P. chabaudi* infection of IL-10 KO [139]. Mice that express a T-cell specific deletion of the IL-10 gene do not succumb to *P. chabaudi* infection [139]. The immunoregulatory cytokines (IL-10 and TGF- β) from CD4⁺ T cells regulate many aspects of the Th1-type response (IFN- γ , TNF) that must be carefully balanced to kill the parasite, but not cause lethal immunopathology. The data presented here in an inflammation-dependent model confirms a critical role for cytokines in both clot formation and vascular pathology in the absence of the effects of local parasite enrichment.

Studies in PbA-infected ECM mice have established the importance of several of the aforementioned processes to the development of IFN γ [150, 151, 155]. PbA infection shows pathogenic immune cell accumulation in cerebral blood vessels as a result of inflammatory TNF and IP-10 secretion [198, 199], and intercellular adhesion molecule-1 (ICAM-1) on the vascular endothelium [127]. PbA infection has also been shown to induce astrocyte activation and degeneration near sites of monocyte vascular adhesion [175, 200]. However, the signals leading to the breakdown of local astrocyte barrier function in malaria have not yet been defined.

The activation of astrocytes is a well-defined feature in many neurological diseases, including CM [201, 202]. Our results demonstrate a link between excessive inflammation, intravascular cellular congestion, coagulation, astrocyte activation, and hypoxia (**Figures 12, 13, 16**). Identification of monocytes and T cells within fibrin clots suggests a new working model where systemic inflammatory cells affect regulation (as in WT mice infected with *P. chabaudi*) and/or damage (IL-10 KO mice) via their proximity within the cerebral vasculature. Critically, as sequestration has only been shown to occur in organs other than the brain in this model, contributions can be determined independent of parasite-specific factors such as sequestration. These inflammatory foci within intravascular thrombi may act as local drivers of disease in the brain (**Figure 19**). This is important because CM is resistant to anti-malarial drug treatment despite timely therapeutic support, suggesting a local positive feed-forward cycle of inflammation. A significant amount of work remains to be done in order to define the essential features originating from these structures.

Finally, in this study, we show that cellular congestion localized within intravascular thrombi, and nearby astrocyte activation, can be reversed via neutralization of TNF (**Figure 15**). Furthermore, fatal HECM is dependent on intravascular coagulation prevented by anti-coagulant treatment acting early in the coagulation cascade (**Figure 18**). Serum TNF concentration correlates with severity of human malaria [81]. However, TNF blockade has thus far proven ineffective in preventing death in childhood CM [91, 92]. Two proposed explanations for this outcome are: 1) antibody to TNF prolongs cytokine circulation within the blood stream, and 2) humans with CM present too late to prevent the inflammatory cascade [91]. Most importantly, these human clinical trials

showed that different reagents had different effects, suggesting that timing, dose or precise antigenic specificity of treatments are likely play a role. New insights into the

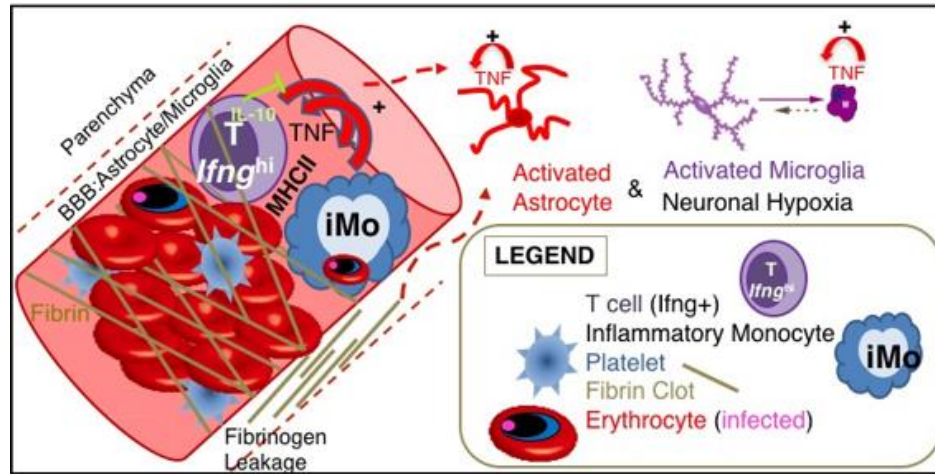


Figure 19. Model of Thrombus-Associated Lymphoid Cluster (TALC)-mediated inflammation amplification. We hypothesize that amplification of local cytokine production is necessary for inducing brain damage in infected IL-10 KO mice compared to WT. Therefore, we developed a model to explain how inflammatory cytokine production is amplified locally in the brain in the absence of direct cellular infiltration of the brain parenchyma, which is protected by microglia and astrocytes that form the blood-brain-barrier. We propose the working *hypothesis* that fibrin(ogen) deposits either within the vessels, or leaking into the perivascular space, promoting a local inflammatory cascade involving cytokine upregulation and glial cell activation. **Proposed timeline:** 1. Fibrin clots form in vessels causing mild hypoxia due to elevated pro-inflammatory cytokine circulation (TNF). 2. Clots also trap blood immune cells which interact with circulating antigen-presenting cells and activated endothelium, 3. leading to the amplification of systemic immunity within the brain microvasculature, 4. increasing the activation and production of TNF from glial cells. This contributes to poor brain function, as shown by behavioral deficiencies associated with infection of IL-10 KO.

intricate regulatory mechanisms of TNF and other important immune-mediated cytokines that may regulate the coagulation cascade will increase our chances of understanding the full range of immunopathology at play in human CM.

The studies presented in this dissertation demonstrate that leukocytes are a component of intravascular coagulation, and that these thrombi are an important mechanism of vascular congestion. We further demonstrated the proximity of reactive astrocytes to these congested vessels containing inflammatory foci mediated by fibrin deposition. The presence of activated astrocytes near the leukocyte-rich congested areas, and the orchestration of both thrombi and astrogliosis via excessive TNF production (likely, but not yet proven to be initiated by these leukocytes), indicate that the congestion within vessels is central to the neuropathology. These findings contribute to the current understanding of the etiologies of cerebral pathology and neurovascular abnormalities in malaria infection, which could inform the rationale design of future therapeutics aimed at targeting intravascular coagulation, cytokine, or cellular mediators of disease. Future investigations should aim to determine whether anti-inflammatory and anti-coagulant therapies could synergize in the treatment of human CM, and determine their efficacy in the late-stage treatment of the most severely ill and comatose patients.

REFERENCES

1. Cox FE: **History of human parasitology.** *Clin Microbiol Rev* 2002, **15**:595-612.
2. Reiter P: **From Shakespeare to Defoe: malaria in England in the Little Ice Age.** *Emerging Infectious Diseases* 2000, **6**:1-11.
3. Stitt ER, Strong RP: *Stitt's Diagnosis, prevention and treatment of tropical diseases.* Philadelphia: The Blakiston company; 1944.
4. Tu Y: **The discovery of artemisinin (qinghaosu) and gifts from Chinese medicine.** *Nat Med* 2011, **17**:1217-1220.
5. Cadbury D: *Seven Wonders of the Industrial World.* Fourth Estate; 2003.
6. Cook GC, Zumla A: *Manson's Tropical Diseases.* Saunders; 2009.
7. van den Berg H: **Global Status of DDT and Its Alternatives for Use in Vector Control to Prevent Disease.** *Environmental Health Perspectives* 2009, **117**:1656-1663.
8. Narayanasamy K, Chery L, Basu A, Duraisingh MT, Escalante A, Fowble J, Guler JL, Herricks T, Kumar A, Majumder P, et al: **Malaria Evolution in South Asia: Knowledge for Control and Elimination.** *Acta tropica* 2012, **121**:256-266.
9. Bhatt S, Weiss DJ, Cameron E, Bisanzio D, Mappin B, Dalrymple U, Battle KE, Moyes CL, Henry A, Eckhoff PA, et al: **The effect of malaria control on Plasmodium falciparum in Africa between 2000 and 2015.** *Nature* 2015, **526**:207-211.

10. WHO. **World Malaria Report 2016**. Geneva: World Health Organization; 2016. <http://www.who.int/malaria/publications/world-malaria-report-2016/report/en/>. Accessed 13 July 2017.
11. Campo B, Vandal O, Wesche DL, Burrows JN: **Killing the hypnozoite – drug discovery approaches to prevent relapse in Plasmodium vivax**. *Pathogens and Global Health* 2015, **109**:107-122.
12. Garcia JE, Puentes A, Patarroyo ME: **Developmental Biology of Sporozoite-Host Interactions in Plasmodium falciparum Malaria: Implications for Vaccine Design**. *Clinical Microbiology Reviews* 2006, **19**:686-707.
13. Stark KR, James AA: **Anticoagulants in vector arthropods**. *Parasitol Today* 1996, **12**:430-437.
14. Champagne DE: **The role of salivary vasodilators in bloodfeeding and parasite transmission**. *Parasitol Today* 1994, **10**:430-433.
15. Vanderberg JP: **Development of Infectivity by the Plasmodium berghei Sporozoite**. *The Journal of Parasitology* 1975, **61**:43-50.
16. Yamauchi LM, Coppi A, Snounou G, Sinnis P: **Plasmodium sporozoites trickle out of the injection site**. *Cellular microbiology* 2007, **9**:1215-1222.
17. Prudencio M, Rodriguez A, Mota MM: **The silent path to thousands of merozoites: the Plasmodium liver stage**. *Nat Rev Micro* 2006, **4**:849-856.
18. Josling GA, Llinas M: **Sexual development in Plasmodium parasites: knowing when it's time to commit**. *Nat Rev Micro* 2015, **13**:573-587.
19. Vaughan AM, Kappe SHI: **Malaria Parasite Liver Infection and Exoerythrocytic Biology**. *Cold Spring Harb Perspect Med* 2017, **7**.

20. Ma J, Trop S, Baer S, Rakhmanaliev E, Arany Z, Dumoulin P, Zhang H, Romano J, Coppens I, Levitsky V, Levitskaya J: **Dynamics of the major histocompatibility complex class I processing and presentation pathway in the course of malaria parasite development in human hepatocytes: implications for vaccine development.** *PLoS One* 2013, **8**:e75321.
21. Olivier M, Van Den Ham K, Shio MT, Kassa FA, Fougeray S: **Malarial Pigment Hemozoin and the Innate Inflammatory Response.** *Frontiers in Immunology* 2014, **5**:25.
22. White NJ, Chapman D, Watt G: **The effects of multiplication and synchronicity on the vascular distribution of parasites in falciparum malaria.** *Trans R Soc Trop Med Hyg* 1992, **86**:590-597.
23. Rouzine IM, McKenzie FE: **Link between immune response and parasite synchronization in malaria.** *Proceedings of the National Academy of Sciences* 2003, **100**:3473-3478.
24. Gabrieli P, Smidler A, Catteruccia F: **Engineering the control of mosquito-borne infectious diseases.** *Genome Biology* 2014, **15**:535.
25. Mace KE, Arguin PM: **Malaria Surveillance - United States, 2014.** *MMWR Surveill Summ* 2017, **66**:1-24.
26. Organization WH: **World Malaria Report 2015.** 2015.
27. Titus RG, Sherry B, Cerami A: **The involvement of TNF, IL-1 and IL-6 in the immune response to protozoan parasites.** *Parasitology Today* 1991, **7**:13-16.

28. Taylor TE, Fu WJ, Carr RA, Whitten RO, Mueller JG, Fosiko NG, Lewallen S, Liomba NG, Molyneux ME: **Differentiating the pathologies of cerebral malaria by postmortem parasite counts.** *Nat Med* 2004, **10**:143-145.
29. Newton CR, Warrell DA: **Neurological manifestations of falciparum malaria.** *Ann Neurol* 1998, **43**:695-702.
30. Newton CRJC, Hien TT, White N: **Cerebral malaria.** *Journal of Neurology, Neurosurgery & Psychiatry* 2000, **69**:433-441.
31. Beare NA, Taylor TE, Harding SP, Lewallen S, Molyneux ME: **Malarial retinopathy: a newly established diagnostic sign in severe malaria.** *Am J Trop Med Hyg* 2006, **75**:790-797.
32. Beare NA, Southern C, Chalira C, Taylor TE, Molyneux ME, Harding SP: **Prognostic significance and course of retinopathy in children with severe malaria.** *Arch Ophthalmol* 2004, **122**:1141-1147.
33. Cordoliani YS, Sarrazin JL, Felten D, Caumes E, Leveque C, Fisch A: **MR of cerebral malaria.** *AJNR Am J Neuroradiol* 1998, **19**:871-874.
34. Newton CR, Peshu N, Kendall B, Kirkham FJ, Sowunmi A, Waruiru C, Mwangi I, Murphy SA, Marsh K: **Brain swelling and ischaemia in Kenyans with cerebral malaria.** *Arch Dis Child* 1994, **70**:281-287.
35. Patankar TF, Karnad DR, Shetty PG, Desai AP, Prasad SR: **Adult cerebral malaria: prognostic importance of imaging findings and correlation with postmortem findings.** *Radiology* 2002, **224**:811-816.
36. Crawley J, Smith S, Kirkham F, Muthinji P, Waruiru C, Marsh K: **Seizures and status epilepticus in childhood cerebral malaria.** *Qjm* 1996, **89**:591-597.

37. Mishra SK, Mohanty S, Satpathy SK, Mohapatra DN: **Cerebral malaria in adults -- a description of 526 cases admitted to Ispat General Hospital in Rourkela, India.** *Ann Trop Med Parasitol* 2007, **101**:187-193.
38. Ashley EA, Dhorda M, Fairhurst RM, Amaratunga C, Lim P, Suon S, Sreng S, Anderson JM, Mao S, Sam B, et al: **Spread of artemisinin resistance in Plasmodium falciparum malaria.** *N Engl J Med* 2014, **371**:411-423.
39. Amante FH, Haque A, Stanley AC, Rivera Fde L, Randall LM, Wilson YA, Yeo G, Pieper C, Crabb BS, de Koning-Ward TF, et al: **Immune-mediated mechanisms of parasite tissue sequestration during experimental cerebral malaria.** *J Immunol* 2010, **185**:3632-3642.
40. Seydel KB, Kampondeni SD, Valim C, Potchen MJ, Milner DA, Muwalo FW, Birbeck GL, Bradley WG, Fox LL, Glover SJ, et al: **Brain swelling and death in children with cerebral malaria.** *N Engl J Med* 2015, **372**:1126-1137.
41. Mehta U, Durrheim DN, Blumberg L, Donohue S, Hansford F, Mabuza A, Kruger P, Gumede JK, Immelman E, Sanchez Canal A, et al: **Malaria deaths as sentinel events to monitor healthcare delivery and antimalarial drug safety.** *Trop Med Int Health* 2007, **12**:617-628.
42. Idro R, Jenkins NE, Newton CR: **Pathogenesis, clinical features, and neurological outcome of cerebral malaria.** *Lancet Neurol* 2005, **4**:827-840.
43. Carter JA, Ross AJ, Neville BG, Obiero E, Katana K, Mung'ala-Odera V, Lees JA, Newton CR: **Developmental impairments following severe falciparum malaria in children.** *Trop Med Int Health* 2005, **10**:3-10.

44. John CC, Bangirana P, Byarugaba J, Opoka RO, Idro R, Jurek AM, Wu B, Boivin MJ: **Cerebral malaria in children is associated with long-term cognitive impairment.** *Pediatrics* 2008, **122**:e92-99.
45. Oluwayemi IO, Brown BJ, Oyedeji OA, Oluwayemi MA: **Neurological sequelae in survivors of cerebral malaria.** *The Pan African Medical Journal* 2013, **15**:88.
46. van Hensbroek MB, Palmer A, Jaffar S, Schneider G, Kwiatkowski D: **Residual neurologic sequelae after childhood cerebral malaria.** *J Pediatr* 1997, **131**:125-129.
47. Idro R, Marsh K, John CC, Newton CRJ: **Cerebral Malaria; Mechanisms Of Brain Injury And Strategies For Improved Neuro-Cognitive Outcome.** *Pediatric research* 2010, **68**:267-274.
48. Milner DA, Jr., Whitten RO, Kamiza S, Carr R, Liomba G, Dzamalala C, Seydel KB, Molyneux ME, Taylor TE: **The systemic pathology of cerebral malaria in African children.** *Front Cell Infect Microbiol* 2014, **4**:104.
49. Manning L, Rosanas-Urgell A, Laman M, Edoni H, McLean C, Mueller I, Siba P, Davis TM: **A histopathologic study of fatal paediatric cerebral malaria caused by mixed Plasmodium falciparum/Plasmodium vivax infections.** *Malar J* 2012, **11**:107.
50. Dorovini-Zis K, Schmidt K, Huynh H, Fu W, Whitten RO, Milner D, Kamiza S, Molyneux M, Taylor TE: **The neuropathology of fatal cerebral malaria in malawian children.** *Am J Pathol* 2011, **178**:2146-2158.
51. Berendt A, Tumer G, Newbold C: **Cerebral malaria: the sequestration hypothesis.** *Parasitology Today* 1994, **10**:412-414.

52. Armah HB, Wilson NO, Sarfo BY, Powell MD, Bond VC, Anderson W, Adjei AA, Gyasi RK, Tettey Y, Wiredu EK, et al: **Cerebrospinal fluid and serum biomarkers of cerebral malaria mortality in Ghanaian children.** *Malar J* 2007, **6**:147.
53. McGuire W, Hill AV, Allsopp CE, Greenwood BM, Kwiatkowski D: **Variation in the TNF-alpha promoter region associated with susceptibility to cerebral malaria.** *Nature* 1994, **371**:508-510.
54. Ouma C, Davenport GC, Were T, Otieno MF, Hittner JB, Vulule JM, Martinson J, Ong'echa JM, Ferrell RE, Perkins DJ: **Haplotypes of IL-10 promoter variants are associated with susceptibility to severe malarial anemia and functional changes in IL-10 production.** *Human genetics* 2008, **124**:515-524.
55. Wassmer SC, Grau GER: **Severe malaria: what's new on the pathogenesis front?** *International Journal for Parasitology* 2017, **47**:145-152.
56. Grau GER, Wassmer SC: **Pathogenetic Immune Responses in Cerebral Malaria.** In *Malaria: Immune Response to Infection and Vaccination*. Edited by Mota MM, Rodriguez A. Cham: Springer International Publishing; 2017: 67-80
57. Langhorne J, Ndungu FM, Sponaas AM, Marsh K: **Immunity to malaria: more questions than answers.** *Nat Immunol* 2008, **9**:725-732.
58. Hearn J, Rayment N, Landon DN, Katz DR, de Souza JB: **Immunopathology of cerebral malaria: morphological evidence of parasite sequestration in murine brain microvasculature.** *Infect Immun* 2000, **68**:5364-5376.

59. Nacer A, Movila A, Baer K, Mikolajczak SA, Kappe SH, Frevvert U: **Neuroimmunological blood brain barrier opening in experimental cerebral malaria.** *PLoS Pathog* 2012, **8**:e1002982.
60. Franke-Fayard B, Janse CJ, Cunha-Rodrigues M, Ramesar J, Buscher P, Que I, Lowik C, Voshol PJ, den Boer MA, van Duinen SG, et al: **Murine malaria parasite sequestration: CD36 is the major receptor, but cerebral pathology is unlinked to sequestration.** *Proc Natl Acad Sci U S A* 2005, **102**:11468-11473.
61. Berendt AR, Tumer GD, Newbold CI: **Cerebral malaria: the sequestration hypothesis.** *Parasitol Today* 1994, **10**:412-414.
62. van der Heyde HC, Nolan J, Combes V, Gramaglia I, Grau GE: **A unified hypothesis for the genesis of cerebral malaria: sequestration, inflammation and hemostasis leading to microcirculatory dysfunction.** *Trends in Parasitology* 2006, **22**:503-508.
63. Dondorp AM, Kager PA, Vreeken J, White NJ: **Abnormal blood flow and red blood cell deformability in severe malaria.** *Parasitol Today* 2000, **16**:228-232.
64. Springer AL, Smith LM, Mackay DQ, Nelson SO, Smith JD: **Functional interdependence of the DBLbeta domain and c2 region for binding of the Plasmodium falciparum variant antigen to ICAM-1.** *Mol Biochem Parasitol* 2004, **137**:55-64.
65. Sherman IW, Crandall I, Smith H: **Membrane proteins involved in the adherence of Plasmodium falciparum-infected erythrocytes to the endothelium.** *Biol Cell* 1992, **74**:161-178.

66. Claessens A, Adams Y, Ghumra A, Lindergard G, Buchan CC, Andisi C, Bull PC, Mok S, Gupta AP, Wang CW, et al: **A subset of group A-like var genes encodes the malaria parasite ligands for binding to human brain endothelial cells.** *Proc Natl Acad Sci U S A* 2012, **109**:E1772-1781.
67. Ochola LB, Siddondo BR, Ocholla H, Nkya S, Kimani EN, Williams TN, Makale JO, Liljander A, Urban BC, Bull PC, et al: **Specific receptor usage in Plasmodium falciparum cytoadherence is associated with disease outcome.** *PLoS One* 2011, **6**:e14741.
68. Marsh K, Forster D, Waruiru C, Mwangi I, Winstanley M, Marsh V, Newton C, Winstanley P, Warn P, Peshu N, et al.: **Indicators of life-threatening malaria in African children.** *N Engl J Med* 1995, **332**:1399-1404.
69. Maitland K, Newton CRJC: **Acidosis of severe falciparum malaria: heading for a shock?** *Trends in Parasitology* 2005, **21**:11-16.
70. MacPherson GG, Warrell MJ, White NJ, Looareesuwan S, Warrell DA: **Human cerebral malaria. A quantitative ultrastructural analysis of parasitized erythrocyte sequestration.** *Am J Pathol* 1985, **119**:385-401.
71. Pongponratn E, Riganti M, Punpoowong B, Aikawa M: **Microvascular sequestration of parasitized erythrocytes in human falciparum malaria: a pathological study.** *Am J Trop Med Hyg* 1991, **44**:168-175.
72. von Seidlein L, Olaosebikan R, Hendriksen IC, Lee SJ, Adedoyin OT, Agbenyega T, Nguah SB, Bojang K, Deen JL, Evans J, et al: **Predicting the clinical outcome of severe falciparum malaria in african children: findings from a large randomized trial.** *Clin Infect Dis* 2012, **54**:1080-1090.

73. Clark IA, Cowden WB: **The pathophysiology of falciparum malaria.** *Pharmacol Ther* 2003, **99**:221-260.
74. Thapa R, Patra V, Kundu R: **Plasmodium vivax cerebral malaria.** *Indian Pediatr* 2007, **44**:433-434.
75. Tanwar GS, Khatri PC, Sengar GS, Kochar A, Kochar SK, Middha S, Tanwar G, Khatri N, Pakalapati D, Garg S, et al: **Clinical profiles of 13 children with Plasmodium vivax cerebral malaria.** *Ann Trop Paediatr* 2011, **31**:351-356.
76. Maegraith B: **Pathological processes in malaria.** *Trans R Soc Trop Med Hyg* 1948, **41**:687-704.
77. Clark IA, Rockett KA: **The cytokine theory of human cerebral malaria.** *Parasitol Today* 1994, **10**:410-412.
78. Nebl T, De Veer MJ, Schofield L: **Stimulation of innate immune responses by malarial glycosylphosphatidylinositol via pattern recognition receptors.** *Parasitology* 2005, **130 Suppl**:S45-62.
79. Parroche P, Lauw FN, Goutagny N, Latz E, Monks BG, Visintin A, Halmen KA, Lamphier M, Olivier M, Bartholomeu DC, et al: **Malaria hemozoin is immunologically inert but radically enhances innate responses by presenting malaria DNA to Toll-like receptor 9.** *Proceedings of the National Academy of Sciences* 2007, **104**:1919-1924.
80. Lyke KE, Burges R, Cissoko Y, Sangare L, Dao M, Diarra I, Kone A, Harley R, Plowe CV, Doumbo OK, Sztein MB: **Serum Levels of the Proinflammatory Cytokines Interleukin-1 Beta (IL-1 β), IL-6, IL-8, IL-10, Tumor Necrosis Factor Alpha, and IL-12(p70) in Malian Children with Severe Plasmodium**

falciparum Malaria and Matched Uncomplicated Malaria or Healthy Controls. *Infection and Immunity* 2004, **72**:5630-5637.

81. Kwiatkowski D, Sambou I, Twumasi P, Greenwood BM, Hill AVS, Manogue KR, Cerami A, Castracane J, Brewster DR: **TNF concentration in fatal cerebral, non-fatal cerebral, and uncomplicated Plasmodium falciparum malaria.** *The Lancet* 1990, **336**:1201-1204.
82. Bauer PR, Van Der Heyde HC, Sun G, Specian RD, Granger DN: **Regulation of endothelial cell adhesion molecule expression in an experimental model of cerebral malaria.** *Microcirculation* 2002, **9**:463-470.
83. Engwerda CR, Mynott TL, Sawhney S, De Souza JB, Bickle QD, Kaye PM: **Locally up-regulated lymphotoxin alpha, not systemic tumor necrosis factor alpha, is the principle mediator of murine cerebral malaria.** *J Exp Med* 2002, **195**:1371-1377.
84. Schofield L, Grau GE: **Immunological processes in malaria pathogenesis.** *Nat Rev Immunol* 2005, **5**:722-735.
85. Sobolewski P, Gramaglia I, Frangos J, Intaglietta M, van der Heyde HC: **Nitric oxide bioavailability in malaria.** *Trends in Parasitology* 2005, **21**:415-422.
86. Sanni LA, Fu S, Dean RT, Bloomfield G, Stocker R, Chaudhri G, Dinauer MC, Hunt NH: **Are reactive oxygen species involved in the pathogenesis of murine cerebral malaria?** *J Infect Dis* 1999, **179**:217-222.
87. Stevenson MM, Riley EM: **Innate immunity to malaria.** *Nat Rev Immunol* 2004, **4**:169-180.

88. Sobolewski P, Gramaglia I, Frangos JA, Intaglietta M, van der Heyde HC: **Hemoglobin serves to protect Plasmodium parasites from nitric oxide and reactive oxygen species.** *J Investig Med* 2005, **53**:246-252.
89. Weiss G, Thuma PE, Biemba G, Mabeza G, Werner ER, Gordeuk VR: **Cerebrospinal fluid levels of biopterin, nitric oxide metabolites, and immune activation markers and the clinical course of human cerebral malaria.** *J Infect Dis* 1998, **177**:1064-1068.
90. Goncalves RM, Scopel KK, Bastos MS, Ferreira MU: **Cytokine balance in human malaria: does Plasmodium vivax elicit more inflammatory responses than Plasmodium falciparum?** *PLoS One* 2012, **7**:e44394.
91. van Hensbroek MB, Palmer A, Onyiorah E, Schneider G, Jaffar S, Dolan G, Memming H, Frenkel J, Enwere G, Bennett S, et al: **The effect of a monoclonal antibody to tumor necrosis factor on survival from childhood cerebral malaria.** *J Infect Dis* 1996, **174**:1091-1097.
92. Kwiatkowski D, Molyneux ME, Stephens S, Curtis N, Klein N, Pointaire P, Smit M, Allan R, Brewster DR, Grau GE, et al.: **Anti-TNF therapy inhibits fever in cerebral malaria.** *Q J Med* 1993, **86**:91-98.
93. Warrell DA, Looareesuwan S, Warrell MJ, Kasemsarn P, Intaraprasert R, Bunnag D, Harinasuta T: **Dexamethasone Proves Deleterious in Cerebral Malaria.** *New England Journal of Medicine* 1982, **306**:313-319.
94. Das BK, Mishra S, Padhi PK, Manish R, Tripathy R, Sahoo PK, Ravindran B: **Pentoxifylline adjunct improves prognosis of human cerebral malaria in adults.** *Trop Med Int Health* 2003, **8**:680-684.

95. White NJ, Turner GD, Medana IM, Dondorp AM, Day NP: **The murine cerebral malaria phenomenon.** *Trends Parasitol* 2010, **26**:11-15.
96. Cabrales P, Martins YC, Ong PK, Zanini GM, Frangos JA, Carvalho LJ: **Cerebral tissue oxygenation impairment during experimental cerebral malaria.** *Virulence* 2013, **4**:686-697.
97. Grobusch MP, Kremsner PG: **Uncomplicated malaria.** *Curr Top Microbiol Immunol* 2005, **295**:83-104.
98. Anstey NM, Jacups SP, Cain T, Pearson T, Ziesing PJ, Fisher DA, Currie BJ, Marks PJ, Maguire GP: **Pulmonary manifestations of uncomplicated falciparum and vivax malaria: cough, small airways obstruction, impaired gas transfer, and increased pulmonary phagocytic activity.** *J Infect Dis* 2002, **185**:1326-1334.
99. Hemmer CJ, Bierhaus A, von Riedesel J, Gabat S, Liliensiek B, Pitronik P, Lin J, Grauer A, Amiral J, Ziegler R, et al.: **Elevated thrombomodulin plasma levels as a result of endothelial involvement in plasmodium falciparum malaria.** *Thromb Haemost* 1994, **72**:457-464.
100. Pukrittayakamee S, White NJ, Clemens R, Chittamas S, Karges HE, Desakorn V, Looareesuwan S, Bunnag D: **Activation of the coagulation cascade in falciparum malaria.** *Trans R Soc Trop Med Hyg* 1989, **83**:762-766.
101. Hemmer CJ, Kern P, Holst FG, Radtke KP, Egbring R, Bierhaus A, Nawroth PP, Dietrich M: **Activation of the host response in human Plasmodium falciparum malaria: relation of parasitemia to tumor necrosis factor/cachectin, thrombin-antithrombin III, and protein C levels.** *Am J Med* 1991, **91**:37-44.

102. Holst FG, Hemmer CJ, Foth C, Seitz R, Egbring R, Dietrich M: **Low levels of fibrin-stabilizing factor (factor XIII) in human Plasmodium falciparum malaria: correlation with clinical severity.** *Am J Trop Med Hyg* 1999, **60**:99-104.
103. Horstmann RD, Dietrich M: **Haemostatic alterations in malaria correlate to parasitaemia.** *Blut* 1985, **51**:329-335.
104. Francischetti IMB, Seydel KB, Monteiro RQ: **Blood Coagulation, Inflammation and Malaria.** *Microcirculation (New York, NY : 1994)* 2008, **15**:81-107.
105. Slofstra SH, Spek CA, ten Cate H: **Disseminated intravascular coagulation.** *Hematol J* 2003, **4**:295-302.
106. Jaroonvesama N: **Intravascular coagulation in falciparum malaria.** *Lancet* 1972, **1**:221-223.
107. Boonpucknavig V, Boonpucknavig S, Udomsangpetch R, Nitiyanant P: **An immunofluorescence study of cerebral malaria. A correlation with histopathology.** *Arch Pathol Lab Med* 1990, **114**:1028-1034.
108. Pongponratn E, Turner GD, Day NP, Phu NH, Simpson JA, Stepniewska K, Mai NT, Viriyavejakul P, Looareesuwan S, Hien TT, et al: **An ultrastructural study of the brain in fatal Plasmodium falciparum malaria.** *Am J Trop Med Hyg* 2003, **69**:345-359.
109. Clark IA, Awburn MM, Whitten RO, Harper CG, Liomba NG, Molyneux ME, Taylor TE: **Tissue distribution of migration inhibitory factor and inducible nitric oxide synthase in falciparum malaria and sepsis in African children.** *Malar J* 2003, **2**:6.

110. Hersch M, Gnidec AA, Bersten AD, Troster M, Rutledge FS, Sibbald WJ: **Histologic and ultrastructural changes in nonpulmonary organs during early hyperdynamic sepsis.** *Surgery* 1990, **107**:397-410.
111. Mohanty D, Ghosh K, Nandwani SK, Shetty S, Phillips C, Rizvi S, Parmar BD: **Fibrinolysis, inhibitors of blood coagulation, and monocyte derived coagulant activity in acute malaria.** *Am J Hematol* 1997, **54**:23-29.
112. Dempfle CE: **Coagulopathy of sepsis.** *Thromb Haemost* 2004, **91**:213-224.
113. Fauser S, Deininger MH, Kremsner PG, Magdolen V, Luther T, Meyermann R, Schluesener HJ: **Lesion associated expression of urokinase-type plasminogen activator receptor (uPAR, CD87) in human cerebral malaria.** *J Neuroimmunol* 2000, **111**:234-240.
114. Moxon CA, Wassmer SC, Milner DA, Jr., Chisala NV, Taylor TE, Seydel KB, Molyneux ME, Faragher B, Esmon CT, Downey C, et al: **Loss of endothelial protein C receptors links coagulation and inflammation to parasite sequestration in cerebral malaria in African children.** *Blood* 2013, **122**:842-851.
115. Munir M, Tjandra H, Rampengan T, Mustadjab I, Wulur F: **Heparin in the treatment of cerebral malaria.** *Paediatrica Indonesiana* 1980, **20**:47-50.
116. Rogerson SJ, Reeder JC, al-Yaman F, Brown GV: **Sulfated glycoconjugates as disrupters of Plasmodium falciparum erythrocyte rosettes.** *Am J Trop Med Hyg* 1994, **51**:198-203.

117. Butcher GA, Parish CR, Cowden WB: **Inhibition of growth in vitro of Plasmodium falciparum by complex polysaccharides.** *Transactions of the Royal Society of Tropical Medicine and Hygiene* 1988, **82**:558-559.
118. Leitgeb AM, Blomqvist K, Cho-Ngwa F, Samje M, Nde P, Titanji V, Wahlgren M: **Low anticoagulant heparin disrupts Plasmodium falciparum rosettes in fresh clinical isolates.** *Am J Trop Med Hyg* 2011, **84**:390-396.
119. Avery JW, Smith GM, Owino SO, Sarr D, Nagy T, Mwalimu S, Matthias J, Kelly LF, Poovassery JS, Middii JD: **Maternal malaria induces a procoagulant and antifibrinolytic state that is embryotoxic but responsive to anticoagulant therapy.** *PLoS One* 2012, **7**:e31090.
120. Ruf W: **Protease-activated receptor signaling in the regulation of inflammation.** *Crit Care Med* 2004, **32**:S287-292.
121. Marshall JC: **Inflammation, coagulopathy, and the pathogenesis of multiple organ dysfunction syndrome.** *Crit Care Med* 2001, **29**:S99-106.
122. Taylor FB, Jr., Chang A, Ruf W, Morrissey JH, Hinshaw L, Catlett R, Blick K, Edgington TS: **Lethal E. coli septic shock is prevented by blocking tissue factor with monoclonal antibody.** *Circ Shock* 1991, **33**:127-134.
123. Creasey AA, Chang AC, Feigen L, Wun TC, Taylor FB, Jr., Hinshaw LB: **Tissue factor pathway inhibitor reduces mortality from Escherichia coli septic shock.** *J Clin Invest* 1993, **91**:2850-2860.
124. Francischetti IMB, Seydel KB, Monteiro RQ, Whitten RO, Erexson CR, Noronha ALL, Ostera GR, Kamiza SB, Molyneux ME, Ward JM, Taylor TE: **Plasmodium falciparum-infected erythrocytes induce Tissue Factor expression in**

- endothelial cells and support the assembly of multimolecular coagulation complexes.** *Journal of thrombosis and haemostasis : JTH* 2007, **5**:155-165.
125. Liu Y, Pelekanakis K, Woolkalis MJ: **Thrombin and tumor necrosis factor alpha synergistically stimulate tissue factor expression in human endothelial cells: regulation through c-Fos and c-Jun.** *J Biol Chem* 2004, **279**:36142-36147.
126. Campanella GS, Tager AM, El Khoury JK, Thomas SY, Abrazinski TA, Manice LA, Colvin RA, Luster AD: **Chemokine receptor CXCR3 and its ligands CXCL9 and CXCL10 are required for the development of murine cerebral malaria.** *Proceedings of the National Academy of Sciences* 2008, **105**:4814-4819.
127. Rudin W, Eugster HP, Bordmann G, Bonato J, Müller M, Yamage M, Ryffel B: **Resistance to cerebral malaria in tumor necrosis factor-alpha/beta-deficient mice is associated with a reduction of intercellular adhesion molecule-1 up-regulation and T helper type 1 response.** *The American Journal of Pathology* 1997, **150**:257-266.
128. Belnoue E, Kayibanda M, Vigario AM, Deschemin J-C, Rooijen Nv, Viguier M, Snounou G, Rénia L: **On the Pathogenic Role of Brain-Sequestered $\alpha\beta$ CD8+ T Cells in Experimental Cerebral Malaria.** *The Journal of Immunology* 2002, **169**:6369-6375.
129. Nitecheu J, Bonduelle O, Combadiere C, Tefit M, Seilhean D, Mazier D, Combadiere B: **Perforin-Dependent Brain-Infiltrating Cytotoxic CD8+ T Lymphocytes Mediate Experimental Cerebral Malaria Pathogenesis.** *The Journal of Immunology* 2003, **170**:2221-2228.

130. Potter S, Chan-Ling T, Ball HJ, Mansour H, Mitchell A, Maluish L, Hunt NH: **Perforin mediated apoptosis of cerebral microvascular endothelial cells during experimental cerebral malaria.** *International Journal for Parasitology* 2006, **36**:485-496.
131. Belnoue E, Potter SM, Rosa DS, Mauduit M, GrÜNER AC, Kayibanda M, Mitchell AJ, Hunt NH, RÉNia L: **Control of pathogenic CD8+ T cell migration to the brain by IFN- γ during experimental cerebral malaria.** *Parasite Immunology* 2008, **30**:544-553.
132. Haque A, Best SE, Unosson K, Amante FH, de Labastida F, Anstey NM, Karupiah G, Smyth MJ, Heath WR, Engwerda CR: **Granzyme B expression by CD8+ T cells is required for the development of experimental cerebral malaria.** *J Immunol* 2011, **186**:6148-6156.
133. Li C, Sanni LA, Omer F, Riley E, Langhorne J: **Pathology of *Plasmodium chabaudi chabaudi* infection and mortality in interleukin-10-deficient mice are ameliorated by anti-tumor necrosis factor alpha and exacerbated by anti-transforming growth factor beta antibodies.** *Infect Immun* 2003, **71**:4850-4856.
134. Sanni LA, Jarra W, Li C, Langhorne J: **Cerebral Edema and Cerebral Hemorrhages in Interleukin-10-Deficient Mice Infected with *Plasmodium chabaudi*.** *Infection and Immunity* 2004, **72**:3054-3058.
135. Mota MM, Jarra W, Hirst E, Patnaik PK, Holder AA: ***Plasmodium chabaudi*-Infected Erythrocytes Adhere to CD36 and Bind to Microvascular Endothelial Cells in an Organ-Specific Way.** *Infection and Immunity* 2000, **68**:4135-4144.

136. Brugat T, Cunningham D, Sodenkamp J, Coomes S, Wilson M, Spence PJ, Jarra W, Thompson J, Scudamore C, Langhorne J: **Sequestration and histopathology in Plasmodium chabaudi malaria are influenced by the immune response in an organ-specific manner.** *Cell Microbiol* 2014, **16**:687-700.
137. Cunningham DA, Lin JW, Brugat T, Jarra W, Tumwine I, Kushinga G, Ramesar J, Franke-Fayard B, Langhorne J: **ICAM-1 is a key receptor mediating cytoadherence and pathology in the Plasmodium chabaudi malaria model.** *Malar J* 2017, **16**:185.
138. Freitas do Rosario AP, Langhorne J: **T cell-derived IL-10 and its impact on the regulation of host responses during malaria.** *International Journal for Parasitology* 2012, **42**:549-555.
139. Freitas do Rosario AP, Lamb T, Spence P, Stephens R, Lang A, Roers A, Muller W, O'Garra A, Langhorne J: **IL-27 promotes IL-10 production by effector Th1 CD4+ T cells: a critical mechanism for protection from severe immunopathology during malaria infection.** *J Immunol* 2012, **188**:1178-1190.
140. Li C, Corraliza I, Langhorne J: **A Defect in Interleukin-10 Leads to Enhanced Malarial Disease in Plasmodium chabaudi chabaudi Infection in Mice.** *Infection and Immunity* 1999, **67**:4435-4442.
141. Clark IA, Chaudhri G: **Tumour necrosis factor may contribute to the anaemia of malaria by causing dyserythropoiesis and erythrophagocytosis.** *British Journal of Haematology* 1988, **70**:99-103.
142. Mastelic B, do Rosario AP, Veldhoen M, Renauld JC, Jarra W, Sponaas AM, Roetynck S, Stockinger B, Langhorne J: **IL-22 Protects Against Liver**

- Pathology and Lethality of an Experimental Blood-Stage Malaria Infection.**
Front Immunol 2012, **3**:85.
143. Findlay EG, Greig R, Stumhofer JS, Hafalla JCR, de Souza JB, Saris CJ, Hunter CA, Riley EM, Couper KN: **Essential Role for IL-27 Receptor Signaling in Prevention of Th1-Mediated Immunopathology during Malaria Infection.**
The Journal of Immunology 2010, **185**:2482-2492.
144. Luty AJ, Lell B, Schmidt-Ott R, Lehman LG, Luckner D, Greve B, Matousek P, Herbich K, Schmid D, Ulbert S, et al: **Parasite antigen-specific interleukin-10 and antibody responses predict accelerated parasite clearance in Plasmodium falciparum malaria.** *Eur Cytokine Netw* 1998, **9**:639-646.
145. Rogers DC, Fisher EM, Brown SD, Peters J, Hunter AJ, Martin JE: **Behavioral and functional analysis of mouse phenotype: SHIRPA, a proposed protocol for comprehensive phenotype assessment.** *Mamm Genome* 1997, **8**:711-713.
146. Linke A, Kühn R, Müller W, Honarvar N, Li C, Langhorne J: **Plasmodium chabaudi chabaudi: Differential Susceptibility of Gene-Targeted Mice Deficient in IL-10 to an Erythrocytic-Stage Infection.** *Experimental Parasitology* 1996, **84**:253-263.
147. Yap GS, Stevenson MM: **Plasmodium chabaudi AS: Erythropoietic responses during infection in resistant and susceptible mice.** *Experimental Parasitology* 1992, **75**:340-352.
148. Cross CE, Langhorne J: **Plasmodium chabaudi chabaudi(AS): Inflammatory Cytokines and Pathology in an Erythrocytic-Stage Infection in Mice.**
Experimental Parasitology 1998, **90**:220-229.

149. Lamb TJ, Langhorne J: **The severity of malarial anaemia in Plasmodium chabaudi infections of BALB/c mice is determined independently of the number of circulating parasites.** *Malar J* 2008, **7**:68.
150. Lackner P, Beer R, Heussler V, Goebel G, Rudzki D, Helbok R, Tannich E, Schmutzhard E: **Behavioural and histopathological alterations in mice with cerebral malaria.** *Neuropathol Appl Neurobiol* 2006, **32**:177-188.
151. Desruisseaux MS, Gulinello M, Smith DN, Lee SC, Tsuji M, Weiss LM, Spray DC, Tanowitz HB: **Cognitive dysfunction in mice infected with Plasmodium berghei strain ANKA.** *J Infect Dis* 2008, **197**:1621-1627.
152. Hermesen C, Van De Wiel T, Mommers E, Sauerwein R, Eling W: **Depletion of CD4+ or CD8+ T-cells prevents Plasmodium berghei induced cerebral malaria in end-stage disease.** *Parasitology* 1997, **114**:7-12.
153. Poh CM, Howland SW, Grotenbreg GM, Renia L: **Damage to the blood-brain barrier during experimental cerebral malaria results from synergistic effects of CD8+ T cells with different specificities.** *Infect Immun* 2014, **82**:4854-4864.
154. Villegas-Mendez A, Greig R, Shaw TN, de Souza JB, Gwyer Findlay E, Stumhofer JS, Hafalla JC, Blount DG, Hunter CA, Riley EM, Couper KN: **IFN-gamma-producing CD4+ T cells promote experimental cerebral malaria by modulating CD8+ T cell accumulation within the brain.** *J Immunol* 2012, **189**:968-979.
155. Lacerda-Queiroz N, Rodrigues DH, Vilela MC, Miranda AS, Amaral DC, Camargos ER, Carvalho LJ, Howe CL, Teixeira MM, Teixeira AL: **Inflammatory changes in the central nervous system are associated with**

- behavioral impairment in Plasmodium berghei (strain ANKA)-infected mice.**
Exp Parasitol 2010, **125**:271-278.
156. Trang TTM, Phu NH, Vinh H, Hien TT, Cuong BM, Chau TTH, Mai NTH, Waller DJ, White NJ: **Acute Renal Failure in Patients with Severe Falciparum Malaria.** *Clinical Infectious Diseases* 1992, **15**:874-880.
157. Mohan A, Sharma SK, Bollineni S: **Acute lung injury and acute respiratory distress syndrome in malaria.** *J Vector Borne Dis* 2008, **45**:179-193.
158. Krishnan A, Karnad DR: **Severe falciparum malaria: An important cause of multiple organ failure in Indian intensive care unit patients.** *Critical Care Medicine* 2003, **31**:2278-2284.
159. Seixas E, Oliveira P, Moura Nunes JF, Coutinho A: **An experimental model for fatal malaria due to TNF- α -dependent hepatic damage.** *Parasitology* 2008, **135**:683-690.
160. Seixas E, Gozzelino R, Chora Â, Ferreira A, Silva G, Larsen R, Rebelo S, Penido C, Smith NR, Coutinho A, Soares MP: **Heme oxygenase-1 affords protection against noncerebral forms of severe malaria.** *Proceedings of the National Academy of Sciences* 2009, **106**:15837-15842.
161. Pamplona A, Ferreira A, Balla J, Jeney V, Balla G, Epiphanyo S, Chora A, Rodrigues CD, Gregoire IP, Cunha-Rodrigues M, et al: **Heme oxygenase-1 and carbon monoxide suppress the pathogenesis of experimental cerebral malaria.** *Nat Med* 2007, **13**:703-710.

162. Clark IA, Awburn MM, Harper CG, Liomba NG, Molyneux ME: **Induction of HO-1 in tissue macrophages and monocytes in fatal falciparum malaria and sepsis.** *Malar J* 2003, **2**:41.
163. Neill AL, Hunt NH: **Pathology of fatal and resolving Plasmodium berghei cerebral malaria in mice.** *Parasitology* 1992, **105**:165-175.
164. Couper KN, Blount DG, Wilson MS, Hafalla JC, Belkaid Y, Kamanaka M, Flavell RA, de Souza JB, Riley EM: **IL-10 from CD4CD25Foxp3CD127 adaptive regulatory T cells modulates parasite clearance and pathology during malaria infection.** *PLoS Pathog* 2008, **4**:e1000004.
165. Sponaas A-M, Freitas do Rosario AP, Voisine C, Mastelic B, Thompson J, Koernig S, Jarra W, Renia L, Mauduit M, Potocnik AJ, Langhorne J: **Migrating monocytes recruited to the spleen play an important role in control of blood stage malaria.** *Blood* 2009, **114**:5522-5531.
166. Guha SK, Tillu R, Sood A, Patgaonkar M, Nanavaty IN, Sengupta A, Sharma S, Vaidya VA, Pathak S: **Single episode of mild murine malaria induces neuroinflammation, alters microglial profile, impairs adult neurogenesis, and causes deficits in social and anxiety-like behavior.** *Brain Behav Immun* 2014, **42**:123-137.
167. Wilson KD, Stutz SJ, Ochoa LF, Valbuena GA, Cravens PD, Dineley KT, Vargas G, Stephens R: **Behavioural and neurological symptoms accompanied by cellular neuroinflammation in IL-10-deficient mice infected with Plasmodium chabaudi.** *Malar J* 2016, **15**:428.

168. Chung K, Wallace J, Kim S-Y, Kalyanasundaram S, Andalman AS, Davidson TJ, Mirzabekov JJ, Zalocusky KA, Mattis J, Denisin AK, et al: **Structural and molecular interrogation of intact biological systems.** *Nature* 2013, **497**:332-337.
169. Bertini R, Bianchi M, Villa P, Ghezzi P: **Depression of liver drug metabolism and increase in plasma fibrinogen by interleukin 1 and tumor necrosis factor: A comparison with lymphotoxin and interferon.** *International Journal of Immunopharmacology* 1988, **10**:525-530.
170. Francischetti IM, Seydel KB, Monteiro RQ: **Blood coagulation, inflammation, and malaria.** *Microcirculation* 2008, **15**:81-107.
171. Brown H, Hien TT, Day N, Mai NT, Chuong LV, Chau TT, Loc PP, Phu NH, Bethell D, Farrar J, et al: **Evidence of blood-brain barrier dysfunction in human cerebral malaria.** *Neuropathol Appl Neurobiol* 1999, **25**:331-340.
172. Blombäck B, Hessel B, Hogg D, Therkildsen L: **A two-step fibrinogen--fibrin transition in blood coagulation.** *Nature* 1978, **275**:501-505.
173. Raut S, McEvoy F, Gaffney PJ: **Development of an ELISA for the Quantification of Fibrin in Canine Tumours.** *Thrombosis Research* 1999, **96**:11-17.
174. Clemmensen I: **Three new E-antigenic fibrinogen fractions found in a commercial plasmin preparation.** *Science Tools LKB Instr J* 1973, **20**:7-8.
175. Medana IM, Chaudhri G, Chan-Ling T, Hunt NH: **Central nervous system in cerebral malaria: 'Innocent bystander' or active participant in the induction of immunopathology?** *Immunol Cell Biol* 2001, **79**:101-120.

176. Ridet JL, Privat A, Malhotra SK, Gage FH: **Reactive astrocytes: cellular and molecular cues to biological function.** *Trends in Neurosciences* 1997, **20**:570-577.
177. Hempel C, Combes V, Hunt NH, Kurtzhals JA, Grau GE: **CNS hypoxia is more pronounced in murine cerebral than noncerebral malaria and is reversed by erythropoietin.** *Am J Pathol* 2011, **179**:1939-1950.
178. Grau GE, Piguet PF, Vassalli P, Lambert PH: **Tumor-necrosis factor and other cytokines in cerebral malaria: experimental and clinical data.** *Immunol Rev* 1989, **112**:49-70.
179. Kwiatkowski DP, Luoni G: **Host genetic factors in resistance and susceptibility to malaria.** *Parassitologia* 2006, **48**:450-467.
180. Turner GD, Morrison H, Jones M, Davis TM, Looareesuwan S, Buley ID, Gatter KC, Newbold CI, Pukritayakamee S, Nagachinta B, et al.: **An immunohistochemical study of the pathology of fatal malaria. Evidence for widespread endothelial activation and a potential role for intercellular adhesion molecule-1 in cerebral sequestration.** *Am J Pathol* 1994, **145**:1057-1069.
181. Lewallen S, Bakker H, Taylor TE, Wills BA, Courtright P, Molyneux ME: **Retinal findings predictive of outcome in cerebral malaria.** *Transactions of the Royal Society of Tropical Medicine and Hygiene* 1996, **90**:144-146.
182. Patnaik JK, Das BS, Mishra SK, Mohanty S, Satpathy SK, Mohanty D: **Vascular Clogging, Mononuclear Cell Margination, and Enhanced Vascular**

- Permeability in the Pathogenesis of Human Cerebral Malaria.** *The American Journal of Tropical Medicine and Hygiene* 1994, **51**:642-647.
183. Bridges DJ, Bunn J, van Mourik JA, Grau G, Preston RJ, Molyneux M, Combes V, O'Donnell JS, de Laat B, Craig A: **Rapid activation of endothelial cells enables Plasmodium falciparum adhesion to platelet-decorated von Willebrand factor strings.** *Blood* 2010, **115**:1472-1474.
184. O'Sullivan JM, Preston RJ, O'Regan N, O'Donnell JS: **Emerging roles for hemostatic dysfunction in malaria pathogenesis.** *Blood* 2016, **127**:2281-2288.
185. Ponsford MJ, Medana IM, Prapansilp P, Hien TT, Lee SJ, Dondorp AM, Esiri MM, Day NP, White NJ, Turner GD: **Sequestration and microvascular congestion are associated with coma in human cerebral malaria.** *J Infect Dis* 2012, **205**:663-671.
186. O'Regan N, Gegenbauer K, O'Sullivan JM, Maleki S, Brophy TM, Dalton N, Chion A, Fallon PG, Grau GE, Budde U, et al: **A novel role for von Willebrand factor in the pathogenesis of experimental cerebral malaria.** *Blood* 2016, **127**:1192-1201.
187. Sun G, Chang WL, Li J, Berney SM, Kimpel D, van der Heyde HC: **Inhibition of platelet adherence to brain microvasculature protects against severe Plasmodium berghei malaria.** *Infect Immun* 2003, **71**:6553-6561.
188. Moxon CA, Chisala NV, Mzikamanda R, MacCormick I, Harding S, Downey C, Molyneux M, Seydel KB, Taylor TE, Heyderman RS, Toh CH: **Laboratory evidence of disseminated intravascular coagulation is associated with a fatal**

- outcome in children with cerebral malaria despite an absence of clinically evident thrombosis or bleeding.** *J Thromb Haemost* 2015, **13**:1653-1664.
189. Milner DA, Whitten RO, Kamiza S, Carr R, Liomba G, Dzamalala C, Seydel KB, Molyneux ME, Taylor TE: **The systemic pathology of cerebral malaria in African children.** *Frontiers in Cellular and Infection Microbiology* 2014, **4**.
190. Borochovit D, Crosley AL, Metz J: **Disseminated intravascular coagulation with fatal haemorrhage in cerebral malaria.** *Br Med J* 1970, **2**:710.
191. Reid HA, Nkrumah FK: **Fibrin-degradation products in cerebral malaria.** *Lancet* 1972, **1**:218-221.
192. Sampath S, Brazier AJ, Avril M, Bernabeu M, Vigdorovich V, Mascarenhas A, Gomes E, Sather DN, Esmon CT, Smith JD: **Plasmodium falciparum adhesion domains linked to severe malaria differ in blockade of endothelial protein C receptor.** *Cell Microbiol* 2015, **17**:1868-1882.
193. Feintuch CM, Saidi A, Seydel K, Chen G, Goldman-Yassen A, Mita-Mendoza NK, Kim RS, Frenette PS, Taylor T, Daily JP: **Activated Neutrophils Are Associated with Pediatric Cerebral Malaria Vasculopathy in Malawian Children.** *MBio* 2016, **7**:e01300-01315.
194. Hochman SE, Madaline TF, Wassmer SC, Mbale E, Choi N, Seydel KB, Whitten RO, Varughese J, Grau GE, Kamiza S, et al: **Fatal Pediatric Cerebral Malaria Is Associated with Intravascular Monocytes and Platelets That Are Increased with HIV Coinfection.** *MBio* 2015, **6**:e01390-01315.

195. Fiorentino DF, Zlotnik A, Mosmann TR, Howard M, O'Garra A: **IL-10 inhibits cytokine production by activated macrophages.** *J Immunol* 1991, **147**:3815-3822.
196. Belnoue E, Costa FTM, Vigário AM, Voza T, Gonnet F, Landau I, van Rooijen N, Mack M, Kuziel WA, Rénia L: **Chemokine Receptor CCR2 Is Not Essential for the Development of Experimental Cerebral Malaria.** *Infection and Immunity* 2003, **71**:3648-3651.
197. Villegas-Mendez A, de Souza JB, Murungi L, Hafalla JCR, Shaw TN, Greig R, Riley EM, Couper KN: **Heterogeneous and tissue specific regulation of effector T cell responses by IFN- γ during Plasmodium berghei ANKA infection().** *Journal of immunology (Baltimore, Md : 1950)* 2011, **187**:2885-2897.
198. Nie CQ, Bernard NJ, Norman MU, Amante FH, Lundie RJ, Crabb BS, Heath WR, Engwerda CR, Hickey MJ, Schofield L, Hansen DS: **IP-10-mediated T cell homing promotes cerebral inflammation over splenic immunity to malaria infection.** *PLoS Pathog* 2009, **5**:e1000369.
199. Campanella GS, Tager AM, El Khoury JK, Thomas SY, Abrazinski TA, Manice LA, Colvin RA, Luster AD: **Chemokine receptor CXCR3 and its ligands CXCL9 and CXCL10 are required for the development of murine cerebral malaria.** *Proc Natl Acad Sci U S A* 2008, **105**:4814-4819.
200. Ampawong S, Chaisri U, Viriyavejakul P, Nontprasert A, Grau GE, Pongponratn E: **Electron microscopic features of brain edema in rodent cerebral malaria in relation to glial fibrillary acidic protein expression.** *Int J Clin Exp Pathol* 2014, **7**:2056-2067.

201. Ma N, Madigan MC, Chan-Ling T, Hunt NH: **Compromised Blood-Nerve Barrier, Astrogliosis, and Myelin Disruption in Optice Nerves During Fatal Murine Cerebral Malaria.** *Glia* 1997, **19**:135-151.
202. Medana IM, Turner GDH: **Human cerebral malaria and the blood–brain barrier.** *International Journal for Parasitology* 2006, **36**:555-568.

Vita

Kyle David Wilson

PERSONAL INFORMATION

Date of Birth: 08/08/1989

Place of Birth: Merriam, Kansas, USA

Sex: Male

PRESENTATIONS

Wilson, K.D. (2009), Site-directed Mutagenesis of Cysteines in Skp1 to Elucidate its Role in Prolyl 4-Hydroxylase-Dependent O₂-Signaling in Dictyostelium. University of Oklahoma Health Sciences Center. Presented at OUHSC, SNU Research Symposium and 2010 BBB Regional Conference.

Wilson, K.D. (2010), Neodymium Conjugation of HLA B*0702 for Use in Serum Antibody Identification and Quantitation. University of Oklahoma Health Sciences Center. Presented at OUHSC and 2011 BBB Regional Conference.

Wilson, K.D. (2015), Decreased Animal Behavior and Altered Cellular Profile in Brains of IL-10-Deficient Mice Infected with *Plasmodium chabaudi chabaudi* (AS). Gordon Research Conference on Tropical Infectious Diseases and the 2015 IHII/McLaughlin Colloquium, University of Texas Medical Branch, Galveston, TX.

Wilson, K.D. (2016), Behavioral and Neurological Symptoms accompanied by Cellular Neuroinflammation in IL-10-deficient Mice infected with *Plasmodium chabaudi*. 20th Annual Wood's Hole Immunoparasitology meeting (WHIP 2016), Marine Biological Laboratory, Wood's Hole, MA, USA.

EDUCATION

Ponca City Senior High School, Graduated May 2007; GPA: 3.8.

Southern Nazarene University, Graduated with Honors May 2011; GPA: 3.972, Summa Cum Laude

University of Texas Medical Branch, Current M.D./Ph.D. Student (5th-yr); GPA: 3.888.

AWARDS

- Freshman Chemistry Student of the Year May 2008
-Highest ranked student in General Chemistry during the 07-08 academic year.
- President's Honor Roll 2007-2010
-Maintain a 4.0 GPA each semester.
- University Marshal 2009-2010
-Assists in commencement ceremonies. Represents top students in next graduating class.
- 2nd Place at 2010 South-Central Regional BBB Conference (Poster)
2010
- Recipient of the Gene Coburn Memorial Scholarship Spring 2010
-Awarded to the male of the traditional junior class with the highest GPA.
- Attended Baylor University's Advanced Instrumentation Workshop Oct. 29-30, 2010
-Toured Baylor's Graduate School facilities in Waco, TX. Included personal contact with Baylor's graduate students and faculty and 3 separate 2-1/2 hour instrumentation sessions involving NMR, Mass Spec, HPLC, and Confocal Microscopy.
- New Student Institute Mentor August, 2010
-Assists with the incoming freshman registration and orientation activities the week before the fall semester begins.
- T32 Pre-doctoral Trainee in Emerging and Tropical Infectious Diseases 2014-2015
UTMB, Galveston, TX
- 2015 IHII/McLaughlin Colloquium Travel Award (Poster) March 2015
UTMB, Galveston, TX
- James W. McLaughlin Pre-doctoral Fellow 2015-2016
UTMB, Galveston, TX
- Attended 15th European School of Neuroimmunology Course (ESNI) June 1-4, 2015

-Held in Prague, Czech Republic. A 4-day intensive course structured around presentations on the current topics and techniques in basic neuroimmunology research. Students were invited to submit abstracts for a chance at an oral presentation. My abstract was not selected.

2016 IHII/McLaughlin Colloquium Travel Award (Poster)	April 2016
UTMB, Galveston, TX	
2016 WHIP Best Poster Award	April 2016
Marine Biological Laboratory, Wood's Hole, MA	
Jeane B. Kempner Predoctoral Scholar Award	2016-2017
UTMB, Galveston, TX	
Robert Shope PhD Endowed Scholarship	December 2016
UTMB, Galveston, TX	

PROFESSIONAL MEMBERSHIPS AND OFFICES

Alpha Epsilon Delta (AED)	Scalpel Editor/Treasurer	2009-Present
-National Pre-Health Society		
Alpha Lambda Delta (ALD)	Member	2009-Present
-National Undergraduate Honor Society		
Beta Beta Beta (BBB)	President/Member	2009-Present
-National Biological Honor Society		
-Awarded Outstanding Chapter at 2009 and 2010 District Conference.		
-Elected Regional Parliamentarian and Co-host Chapter for 2010.		
SNU Honors Program	VP of Marketing/Member	2008-2011
-Inaugurate class of the SNU Honors program.		
American Medical Association	Member	2011-Present
Texas Medical Association	Member	2011-Present

PUBLICATIONS

Hanke van der Wel, Jennifer M. Johnson, Yuechi Xu, Chamini V. Karunaratne, **Kyle D. Wilson**, Yusuf Vohra, Geert-Jan Boons, Carol M. Taylor, Brad Bendiak, Christopher M. West. (2011) *Requirements for Skp1 Processing by Cytosolic Prolyl 4(trans)-Hydroxylase and α -N-Acetylglucosaminyltransferase Enzymes Involved in O₂ Signaling in Dictyostelium*. Biochemistry. 50, 1700-1713.

Kyle D. Wilson, Sonja J. Stutz, Lorenzo F. Ochoa, Gustavo A. Valbuena, Petra D. Cravens, Kelly T. Dineley, Gracie Vargas, Robin Stephens (2016) *Behavioral and Neurological Symptoms accompanied by Cellular Neuroinflammation in IL-10-deficient Mice infected with Plasmodium chabaudi*. Malaria Journal. 15(1):428.

PUBLICATIONS (Submitted/Under Review)

Kyle D. Wilson, Lorenzo F. Ochoa, Olivia D. Solomon, Rahul Pal, Astrid E. Cardona, Gracie Vargas, Robin Stephens (2017) *Thrombosis and Astrocyte Activation Secondary to TNF in Inflammation-dependent Experimental Cerebral Malaria*. Journal of Neuroinflammation.

Permanent address: 18626 Partner's Voice Drive, Cypress, TX 77433

This dissertation was typed by Kyle David Wilson.